

EPA-650/2-74-062

July 1974

Environmental Protection Technology Series

**COKE OVEN CHARGING EMISSION  
CONTROL TEST PROGRAM-  
-VOLUME I**



Office of Research and Development  
U.S. Environmental Protection Agency  
Washington, DC 20460



# **COKE OVEN CHARGING EMISSION CONTROL TEST PROGRAM- -VOLUME I**

by

R. W. Bee, G. Erskine, R. B. Shaller,  
R. W. Spewak, A. Wallo, III, and W. L. Wheaton

The Mitre Corporation  
Westgate Research Park  
McLean, Virginia 22101

ROAP No. 21AFF-004  
Program Element No. 1AB013  
Interagency Agreement F192628-71-C-002  
Contract 68-02-0650

EPA Project Officer: R. V. Hendriks

Control Systems Laboratory  
National Environmental Research Center  
Research Triangle Park, North Carolina 27711

Prepared for

OFFICE OF RESEARCH AND DEVELOPMENT  
U.S. ENVIRONMENTAL PROTECTION AGENCY  
WASHINGTON, D.C. 20460

July 1974

This report has been reviewed by the Environmental Protection Agency and approved for publication. Approval does not signify that the contents necessarily reflect the views and policies of the Agency, nor does mention of trade names or commercial products constitute endorsement or recommendation for use.

# CONTENTS

	<u>Page</u>
Abstract	iii
List of Figures	vii
Acknowledgements	xviii
 <u>Sections</u>	
Volume I	
I Conclusions	1
Identification of Coke Oven Charging Emissions	1
Comparison of Emissions from Wilputte and AISI/EPA Charging Systems	3
Technology of Coke Oven Emissions Measurement	5
Feasibility of a Coke Oven Compliance Monitoring System	8
II Introduction	11
III Approach	13
General	13
Continuous Measurement System	13
Sensors and Probes	20
Manual Sampling	29
Optical Program	33
Field Test Program	38
IV Data Handling Procedures	48
Input Data	48
Mathematical Treatment of Data	58
V Results	81
Comparison of Continuous Measurement and Manual Gas Sampling Methods	81
Results of Particle Size Analysis	96
Statistical Evaluation of Size Distribution Data	109
Comparison of Particulate Emissions from Wilputte and AISI/EPA Car	109
Mass Emissions	111
Supplementary Analyses	117
Optical System Program Results	126
Select Project Documentation List	163



## CONTENTS (CONTINUED)

	<u>Page</u>
Volume II*	
VI Appendices	A-1
A - Volume Flow Curves and Associated Data	A-1
B - Manual Sampling	B-1
C - Computer Programming Documentation	C-1
D - Leaking Coke Oven Doors	D-1
E - Particulate Size Distribution	E-1

\* Volume II of this document is available through EPA's Control Systems Laboratory.

## FIGURES

<u>Number</u>		<u>Page</u>
1	Wilputte Larry Car Emissions Guide	15
2	Wilputte Larry Car Emissions Guide	16
3	AISI/EPA Larry Car Emissions Guide	17
4	AISI/EPA Larry Car Emissions Guide	18
5	Wilputte Emissions Guide Sensor Duct	21
6	Wilputte Stack and AISI/EPA Emissions Guide Sensor Duct	22
7	Cross-Over Bridge Shed Area	23
8	Gas Handling System	26
9	Simplified System Component Configuration	35
10	Film Format	37
11	Test Program Schedule	39
12	Daily Test Schedule Outline	41
13	Continuous Sensor Analog Voltage Print-Out	49
14	Gas Analyzer Strip Chart Data	52
15	Gas Temperature and Pressure Strip Chart Data	53
16	Final Data Print-Out in Engineering Units	55
17	Typical Volume Flow Graph Versus Charging Procedures	60
18	Coke Oven Particulate Distribution	103
19	Log Normal Plot of Ranges 1 Thru 7	104
20	Log Normal Plot of Ranges 8 Thru 13	105
21	Brink Data	108
22	Typical System Geometry	141
23	Secondary Emissions Detector Arrangement	143



# FIGURES (CONTINUED)

<u>Number</u>		<u>Page</u>
24	Emission Conditions and Calculated RQ Values	146
25	Sample Optical Data Analyses Print-Out	149
26	Test 7 Data	155
27	Test 9 Data	157
28	Test 17 Data	158
29	Test 20 Data	160
30	Test 25 Data	161
A-1	Test 0B, #2 Wilputte Guide (Volume Flow in Cu. Ft/Min.)	A-7
A-2	Test 1, #2 Wilputte Guide (Volume Flow in Cu. Ft/Min.)	A-8
A-3	Test 1A, #2 Wilputte Stack (Volume Flow in Cu. Ft/Min.)	A-9
A-4	Test 1B, #2 Wilputte Guide and Stack (Volume Flow in Cu. Ft/Min)	A-10
A-5	Test 8A, #3 Wilputte Stacks (Volume Flow in Cu. Ft/Min.)	A-11
A-6	Test 2, Actual and Standard Volume Flow	A-13
A-7	Test 3	A-15
A-8	Test 4	A-16
A-9	Test 5, Actual and Standard Volume Flow	A-17
A-10	Test 6, Actual and Standard Volume Flow	A-19
A-11	Test 7, Actual and Standard Volume Flow	A-21
A-12	Test 8, Actual and Standard Volume Flow	A-23
A-13	Test 9, Actual and Standard Volume Flow	A-25
A-14	Test 10, Actual and Standard Volume Flow	A-27
A-15	Test 11, Actual and Standard Volume Flow	A-29
A-16	Test 12, Actual and Standard Volume Flow	A-31 A-33

# FIGURES (CONTINUED)

<u>Number</u>		<u>Page</u>
A-17	Test 13, Actual and Standard Volume Flow	A-35 A-37
A-18	Test 14, Actual and Standard Volume Flow	A-39
A-19	Test 15, Actual and Standard Volume Flow	A-41
A-20	Test 16, Actual and Standard Volume Flow	A-43 A-45
A-21	Test 17, Actual and Standard Volume Flow	A-47
A-22	Test 18, Actual and Standard Volume Flow	A-49
A-23	Test 19, Actual and Standard Volume Flow	A-51 A-53
A-24	Test 20, Actual and Standard Volume Flow	A-55
A-25	Test 21, Actual and Standard Volume Flow	A-57 A-58
A-26	Test 22, Actual and Standard Volume Flow	A-61
A-27	Test 23, Actual and Standard Volume Flow	A-63
A-28	Test 24, Actual and Standard Volume Flow	A-65
A-29	Test 25, Actual and Standard Volume Flow	A-67
A-30	Test 26, Actual and Standard Volume Flow	A-69
A-31	Test 27, Actual and Standard Volume Flow	A-71 A-73
A-32	Test 28, Actual and Standard Volume Flow	A-75
B-1	The Particulate Sampling Train	B-2
B-2	The Bag Sampler	B-5
B-3	Sampling Trains	B-6
B-4	The Total Hydrocarbon Analyzer Set-Up	B-7
B-5	Mass-Particulate Sample Process	B-15
B-6	Number of Particles Sized Per Total Area Viewed Versus Particle Diameter for Sample Number 1051	B-34



# FIGURES (CONTINUED)

<u>Number</u>		<u>Page</u>
B-7	Number of Particles Sized Per Total Area Viewed Versus Particle Diameter for Sample Number 1072	B-35
B-8	Number of Particles Sized Per Total Area Viewed Versus Particle Diameter for Sample Number 1076	B-36
B-9	Number of Particles Sized Per Total Area Viewed Versus Particle Diameter for Sample Number 1109	B-37
B-10	Number of Particles Sized Per Total Area Viewed Versus Particle Diameter for Sample Number 1222	B-38
B-11	Size Distribution by Particle Diameter for Samples	B-42
B-12	Volume Percent Versus Particle Diameter for Samples	B-43
B-13	Background Curves for Andersen Cascade Impactor - Limestone at 0.25 cfm	B-66
B-14	Background Curves for Andersen Cascade Impactor - Limestone at 0.66 cfm	B-67
B-15	Background Curves for Andersen Cascade Impactor - Iron Oxide at 0.247 cfm	B-67
B-16	Background Curves for Andersen Cascade Impactor - Iron Oxide at 0.65 cfm	B-67
B-17	Calibration Curve for Large Cyclone Using Limestone	B-68
B-18	Calibration Curve for Small Cyclone	B-68
C-1	Coke Oven Charge Data Recording Overview	C-2
C-2	Coke Oven Data Processing Overview	C-3
C-3	Input Data Record Format - Program "BILL"	C-6
C-4	Output Data Record Format - Program "BILL"	C-7 C-8
C-5	Output Test Header Record Format - Program "BILL"	C-10
C-6	Functions of Computer Program "BILL"	C-12
C-7	Linear Threshold Values	C-14
C-8	Data Transfer Details	C-15

# FIGURES (CONTINUED)

<u>Number</u>		<u>Page</u>
C-9	Functions of Computer Program "ANDY"	C-16
C-10	Output Data Record Format - Program "ANDY"	C-20 C-21
C-11	Data Transfer Details	C-192
D-1	Leaking Coke Oven Doors	D-2
D-2	Instrument Layout, J & L P-4 Battery - Pittsburgh Works 1973	D-3
D-3	Cross-Sectional View of Leaking Coke Oven Door Collecting and Measurement Equipment	D-4
D-4	Collecting Hood	D-5
D-5	Installing Collecting Hood	D-5
D-6	Measurement Duct	D-7
D-7	Measurement Duct in Place on Oven	D-8
D-8	Particulate Sampling of Leaking Door Measurement Duct	D-9
E-1	Larry Car Charging Coke Oven	E-3
E-2	Carrousel Interior Exposed	E-5
E-3	Carrousel in Operational Configuration	E-6
E-4	Housing with Two Particulate Samplers	E-8
E-5	Cumulative Size Distribution - Particle Number Percent	E-14
E-6	Cumulative Size Distribution - Weight Percent	E-15
E-7	Efficiency Curves	E-17
E-8	Test 27, 150 X	E-27
E-9	Test 27, 150 X	E-27
E-10	Test 28, 150 X	E-28
E-11	Test 28, 150 X	E-28
E-12	Test 28, 150 X	E-29
E-13	Brink Data	E-35
E-14	Coulter Analysis	E-37



## TABLES

<u>Number</u>		<u>Page</u>
1	Gas Chromatograph Parameters for MITRE Gas Analyses	32
2	Summary of Coke Oven Tests	40
3	Data Acquisition System - Channel Assignment	51
4	Variables Used in Volume Flow	62
5	Variables for Gas Analysis	66
6	Constitutents Measured by the Continuous and Manual Sampling Systems	82
7	SO <sub>2</sub>	83
8	H <sub>2</sub>	84
9	CO	85
10	CO <sub>2</sub>	86
11	THC	87
12	O <sub>2</sub>	88
13	NO <sub>x</sub> Plus NH <sub>3</sub>	89
14	NO <sub>x</sub>	90
15	Emission Volumes for Wilputte Charging	94
16	Emission Volumes for AISI/EPA Charging Including Test 21	94
17	Emission Volumes for AISI/EPA Charging Excluding Test 21	95
18	Percent Reduction of Gaseous Emissions	95
19	Constituent Concentrations (Measured)	97
20	Andersen Analysis	101
21	Size Distribution Due to Coke Oven Charging	102
22	Size Range	110

# TABLES (CONTINUED)

<u>Number</u>		<u>Page</u>
23	Anisokinetic Mass Emissions (Wilputte)	112
24	Anisokinetic Mass Emissions (AISI/EPA)	113
25	Calculated Isokinetic Mass (Mass in Grams for Wilputte Car)	115
26	Calculated Isokinetic Mass (Mass in Grams for AISI/EPA CAR)	116
27	Tar Concentrations	118
28	Benzpyrene Analysis	120
29	Elemental Analyses and Supporting Coal Analyses	121
30	Coal Analysis (Ultimate and Proximate)	122
31	Conversion of Transmission Values to Ringelmann Values	147
A-1	Temperature Record for the Coke Oven Tests	A-2
A-2	Preliminary Test Temperatures	A-3
A-3	Volume Flow	A-4 A-5 A-6
B-1	Summary of Samples Taken in the Field	B-11 B-12 B-13 B-14
B-2	Mass Results - Field Data	B-17
B-3	Mass Analytical Results	B-18
B-4	Mass Concentration Results	B-19
B-5	Andersen Analysis Summary	B-21
B-6	Andersen Analysis Summary	B-22
B-7	Andersen Analysis Summary	B-23
B-8	Andersen Analysis Summary	B-24
B-9	Andersen Analysis Summary	B-25
B-10	Andersen Analysis Summary	B-26



## TABLES (CONTINUED)

<u>Number</u>		<u>Page</u>
B-11	Andersen Analysis Summary	B-27
B-12	Andersen Analysis Summary	B-28
B-13	Andersen Analysis Summary	B-29
B-14	Andersen Analysis Summary	B-30
B-15	Andersen Analysis Summary	B-31
B-16	Cross Reference Information - AISI/EPA Larry Car	B-32
B-17	Optical Size Distribution Data on Sample Number 1051	B-39
B-18	Optical Size Distribution Data on Sample Number 1072	B-39
B-19	Optical Size Distribution Data on Sample Number 1076	B-40
B-20	Optical Size Distribution Data on Sample Number 1009	B-40
B-21	Optical Size Distribution Data on Sample Number 1222	B-41
B-22	Cumulative Percent Optical Size Distribution Data	B-41
B-23	Particle Diameter Versus Cumulative Percent (By Volume)	B-45
B-24	Results of Tar Analysis	B-46
B-25	Benzpyrene Analysis	B-48
B-26	Wavelengths and Flame Gases Used in the Elemental Analysis	B-49
B-27	Sample Combinations Used in Elemental Analysis	B-51
B-28	Filter Number 1	B-52
B-29	Filter Number 2	B-52
B-30	Aluminum	B-53
B-31	Antimony	B-53
B-32	Barium	B-53
B-33	Beryllium	B-54
B-34	Cadmium	B-54
B-35	Calcium	B-55

## TABLES (CONTINUED)

<u>Number</u>		<u>Page</u>
B-36	Cobalt	B-55
B-37	Chromium	B-55
B-38	Copper	B-56
B-39	Callium	B-56
B-40	Germanium	B-56
B-41	Lead	B-57
B-42	Iron	B-57
B-43	Magnesium	B-57
B-44	Manganese	B-58
B-45	Mercury	B-58
B-46	Molybdenum	B-59
B-47	Potassium	B-59
B-48	Nickel	B-59
B-49	Selenium	B-60
B-50	Sodium	B-60
B-51	Strontium	B-50
B-52	Thallium	B-61
B-53	Titanium	B-61
B-54	Tin	B-61
B-55	Vanadium	B-62
B-56	Zinc	B-62
B-57	Coal Analysis (Ultimate and Proximate)	B-64
B-58	Sieve Analysis	B-65
B-59	H <sub>2</sub> S Analytical Results	B-70
B-60	NO <sub>x</sub> (NO <sub>2</sub> ) Analytical Results	B-71

TABLES (CONTINUED)

<u>Number</u>		<u>Page</u>
B-61	NH <sub>4</sub> Analytical Results	B-72
B-62	CN Analytical Results	B-73
B-63	Phenol Analytical Results	B-74
B-64	SO <sub>2</sub> Analytical Results	B-75
B-65	Pyridine Analytical Results	B-76
B-66	Gas Chromatograph Parameters for Gas Analysis	B-78
B-67	Calculations for Gas Analysis	B-79
B-68	O <sub>2</sub> , N <sub>2</sub> , CO <sub>2</sub> , THC, CH <sub>4</sub> , CO and H <sub>2</sub> Results	B-80
C-1	Wilputte Volume Flow/Location, NO <sub>x</sub>	C-151 C-152
C-2	AISI/EPA Volume Flow/Location, NO <sub>x</sub>	C-153
C-3	Wilputte Volume Flow/Location, CO <sub>2</sub>	C-154 C-155
C-4	AISI/EPA Volume Flow/Location, CO <sub>2</sub>	C-156
C-5	Wilputte Volume Flow/Location, NO	C-157 C-158
C-6	AISI/EPA Volume Flow/Location, NO	C-159
C-7	Wilputte Volume Flow/Location, CO	C-160 C-161
C-8	AISI/EPA Volume Flow/Location, CO	C-162
C-9	Wilputte Volume Flow/Location, THC	C-163
C-10	AISI/EPA Volume Flow/Location, THC	C-164
C-11	Miscellaneous Constants Card	C-168
C-12	Test Duct Card	C-169
C-13	Test Time Definition Card	C-170
C-14	Duct Area Card	C-171
C-15	Free Fall Velocity Card	C-172



# TABLES (CONTINUED)

<u>Number</u>		<u>Page</u>
C-16	Anisokinetic Weight Percent Card	C-173
C-17	Sample Velocity Weight Card	C-174
C-18	Input Tape Format	C-175
C-19	Data Field Format	C-177
C-20	Particulate Correction Factors, Q	C-185 C-186
C-21	Mass Loading Computations (Sample)	C-187
C-22	Data Record Structure	C-189
D-1	Test #1 - Door Leak Experiment	D-11
D-2	Test #2 - Door Leak Experiment	D-12
D-3	Test #3 - Door Leak Experiment	D-13
D-4	Test #4 - Door Leak Experiment	D-14
E-1	Deposition Efficiency for Sampler at Coke Oven	E-12
E-2	Test 22	E-13
E-3	Test 24A	E-19
E-4	Test 26A	E-20
E-5	Test 27	E-21
E-6	Test 28	E-22
E-7	Numerical Number Percent Versus Size Range	E-24
E-8	Cumulative Percent for Particles > 18 $\mu$ - Uncorrected	E-25
E-9	Cumulative Percent for Particles > 18 $\mu$ - Corrected	E-26
E-10	Test #1 - Boom	E-31
E-11	Test #2 - Boom	E-32
E-12	Test #3 - Boom	E-33
E-13	Test #4 - Emission Guide	E-34

## ACKNOWLEDGEMENTS

Numerous people contributed to this project, from early planning through execution and data reporting. A guiding influence in steering the activities within the bounds of Jones & Laughlin plant regulations, and the EPA requirements, was R. V. Hendriks, EPA Project Officer. Personnel at J & L who cooperated are too numerous to list, although T. R. Greer and E. Renninger are to be noted for their special contributions. Gases and particulates were manually sampled during the tests by Midwest Research Institute, under EPA contract. Additional analytical support was provided by R. Statnick of EPA.

This project spanned a period of nearly three years, and accordingly, a number of MITRE personnel were assigned to the project as it developed through various phases. K. Yeager and G. Erskine shared the Group Leader responsibilities, while J. Hoffman and R. B. Shaller each in turn acted as Task Leader. R. W. Bee conducted the Optics portion of the program, while A. Wallo III was responsible for sensors and gas/particulate samples with assistance from R. W. Spewak. W. L. Wheaton was responsible for the continuous monitoring instrumentation with assistance from J. Findley, J. Miller, R. Reale, and W. R. Robinson. R. C. Kuehnel assumed the data processing responsibility, and support was provided in this area by J. Morris. Additional assistance and advice was provided by A. F. Epstein, E. Jamgochian, B. A. Stokes and J. B. Truett.

## SECTION I

### CONCLUSIONS

Measurements were successfully made defining the emission characteristics of the coke oven charging operations for the P4 battery of The Jones and Laughlin Pittsburgh works. Both the old Wilputte and the production prototype AISI/EPA larry car charging operations at this battery were characterized in terms of gaseous emissions and particulates released to the atmosphere. Both continuous monitoring and manual sampling techniques were used in a specially designed test program to obtain the required information. Additionally, optical measurements were made to determine the technical feasibility of a compliance monitoring system based on optical measurements.

#### IDENTIFICATION OF COKE OVEN CHARGING EMISSIONS

Particulate mass emissions from the Wilputte Larry Car were defined from 10 charging operations. These mass emissions are reported in terms of particulates released from combinations of six major emission points. From the data on these emission points, a composite total mass emission of 815 grams per charge was derived for the Wilputte car. Mass emissions were also defined for the production prototype AISI/EPA larry car from three major emission points from four separate charging operations. A composite total mass emission figure of 120 grams per charge was derived from the data from the four charging operations.

The major gaseous pollutants emitted during charging that were measured are: total hydrocarbons, carbon dioxide, carbon monoxide, nitrogen oxides, sulfur dioxide, hydrogen sulfide, methane, ammonia, phenol, cyanide.

Based on analysis of particulate samples collected from the charging emissions, there is a possibility that carcinogenic materials may be generally present in emissions released during coke oven charging. This conclusion is based on the detectable presence of benzpyrene in the tar portion of a large number of particulate samples. Although not all chemical forms of benzpyrene have been identified as carcinogens,

benz( $\alpha$ )pyrene has been so labeled. In at least one large composite sample of collected particulate material, analytical techniques have established the presence of benz( $\alpha$ )pyrene and/or benz(e)pyrene and other known or potential carcinogens. Based on the representative nature of the sample involved, it is reasonable to assume that the same constituents will be generally found in the tar fractions of other coke oven emissions. To further characterize the quantities of materials involved, tar concentrations in particulate samples were found to range from approximately 30% to 90%, with an average of 57%. Additionally, benzpyrene analysis of the tar fractions showed concentrations ranging from 260 ppm to 18,000 ppm (1 ppm is equivalent to 1  $\mu$  gram benzpyrene/gram of tar).

An elemental analysis was undertaken to identify the trace constituents of the coal charged and the resulting emissions. The intended emphasis was the identification and quantification of hazardous elements, particularly heavy metals. The emissions analysis was performed on particulate sizing equipment catches, and was limited by the sample size, as well as available analytic techniques. These limitations resulted in a large number of instances where constituent concentrations, if they did exist, were below detectable limits. The emission constituent concentrations which were successfully measured and reported are consistent with the constituents identified in the elemental analysis of the charging coal. Some of the more important elements identified in detectable concentrations in the emitted particulate material were Cu, Fe, Pb, and Zn. Due to the variances in particulate sample sizes, it is not possible to make a generalized statement concerning constituent concentrations in the emissions. It should be pointed out, however, that no constituent concentrations in excess of what can be reasonably explained by coal constituents was identified in the particulate material. In order to obtain more definitive information on particulate constituents, much larger samples distributed as a function of particle size must be obtained and analyzed. The particle size information is important in assessing the results, since this property will determine whether the particles fall or settle out quickly (i.e., particles  $>200 \mu$ ), or behave similar to a gas in the atmosphere (i.e.,  $<3 \mu$ ).

A particle size distribution was derived based upon a composite of samples taken from emissions released by both the Wilputte and the AISI/EPA cars. The size distribution found was characterized as a bi-populate lognormal distribution; with a distinct grouping of the finer particles containing 47% of the sample weight and a distinct grouping of the larger particles containing 53% of the sample weight. The finer particle size grouping was found to have a mass mean diameter of 8.5  $\mu$  and a standard deviation of 2.5  $\mu$ ; whereas the larger particle size grouping was found to have a mass mean diameter of 235  $\mu$  and a standard deviation of 3.9  $\mu$ . It was also concluded that the tar portion of the particulate sampling was derived primarily from the small diameter portion of the particle size distribution.

As an additional baseline measurement, gaseous concentrations were determined for the longer term emissions from leaking seals on the pusher side doors of the oven. Data was collected from four separate measurements of leaking door emissions. The primary gaseous constituent found in these emissions was total hydrocarbons, for which an average emission value of .35 ACFM was found. This measured emission value for hydrocarbons translated to an average value of 1.2 pounds of hydrocarbon released over a 19 hour coking cycle per ton of coal charged to the oven. This figure of 1.2 pounds of hydrocarbon per ton of coal coked is obviously for an oven with doors leaking at a constant maximum rate. Since the majority of the doors do not leak at this rate, this emission rate should not be construed as a normal level of emissions from all oven doors.

#### COMPARISON OF EMISSIONS FROM WILPUTTE AND AISI/EPA CHARGING SYSTEMS

It was determined that the average total particulate mass emission from the Wilputte car was 815 grams per charge. The AISI/EPA car averaged 120 grams per charge, a reduction of approximately 85% from the average particulate emission level measured from the Wilputte Larry car.

The major gases emitted during charging with the Wilputte Larry car consisted of; total hydrocarbons (33.77 scf/charge), CO<sub>2</sub> (29.4 scf/charge), CO (17.49 scf/charge) and NO<sub>x</sub> (.11 scf/charge). Other gaseous constituents



that were found in the emissions included; SO<sub>2</sub> (maximum concentration of 232 ppm), H<sub>2</sub>S (maximum concentration of 42 ppm), methane (maximum concentration of 4 ppm), ammonia (maximum concentration of 130 ppm), phenol (maximum concentration of 31 ppm) and cyanide (maximum concentration of 16 ppm).

The gaseous emissions from the AISI/EPA larry car were measured for 10 separate charging operations and are compared to similar Wilputte measurements below. The major gases emitted during charging with the AISI/EPA larry car consisted of; total hydrocarbons (20.43 scf/charge), an improvement of 40% over the Wilputte emissions, CO (6.28 scf/charge), an improvement of 64%, CO<sub>2</sub> (3.82 scf/charge), an improvement of 87%, and NO<sub>x</sub> (.021 scf/charge), an improvement of 82% over Wilputte emissions. Other gases found in these emissions included; SO<sub>2</sub> (maximum concentration of 25 ppm), and methane (maximum concentration of 1.8 ppm).

The percentage reductions of the various particulate and gaseous emission constituents are not uniform primarily because of the variations in emission reactions which occur during charging operations. Examples might be the presence or absence of flame, variations in dilution prior to sampling, and changes in volume flow causing similar changes in reaction rates. It is felt, however, that a comparison based on total mass emitted is reasonable and justified.

The elemental analysis of various particulate samples showed some degree of uniformity in constituent concentrations. This would indicate that the volume of trace elements emitted during a particular charge would be directly related to total particulates emitted. Based on this premise, it is reasonable to assume that reductions in particulate emissions from the Wilputte to the AISI/EPA car connote like reductions in total volume of trace elements (particularly heavy metals) emitted.

The primary carcinogenic materials, various types of benzpyrene, display reasonably uniform concentrations in the tar fraction of particulate samples. Therefore, it is reasonable to assume that an argument similar to the above would be valid for the appraisal of reductions in total

volume of carcinogens emitted (i.e., reductions in carcinogens could be considered equivalent to reductions in total tars).

#### TECHNOLOGY OF COKE OVEN EMISSIONS MEASUREMENT

Although a number of technical problems were encountered during coke oven testing, an extensive effort was made to minimize these problems and obtain valid data.

Sixteen separate gaseous constituents were measured by either manual sampling methods or the continuous measurement instrumentation system or both. Of these sixteen gases, eight gases were analyzed by both manual methods and the continuous measurement system, and good agreement was found between the methods for four of the major gases (CO, CO<sub>2</sub>, total hydrocarbon, and O<sub>2</sub>). Comparisons between the measurement methods for two of the gases (SO<sub>2</sub> and H<sub>2</sub>S) showed significant discrepancies which were identified as being due to chemical interferents giving a "false high" reading from the continuous measurement systems. These interferents (polycyclic organic materials were suspected) preclude accurate measurement of SO<sub>2</sub> and H<sub>2</sub>S with the best current method for continuous monitoring of these constituents - ultraviolet absorption. Additional testing must be performed to identify the nature of the chemical species which interfere with this instrumentation technique before the technique can be applied to the task of monitoring coke oven emissions.

Manual sampling was used for certain components (particulates, CH<sub>4</sub>, NH<sub>3</sub>, HCN, pyridine, and phenols) because the manual sampling method was the best and/or only technique which could be applied. In other cases (CO, CO<sub>2</sub>, SO<sub>2</sub>, H<sub>2</sub>S, total hydrocarbon, H<sub>2</sub> and O<sub>2</sub>), manual sampling was used as a supplementary method for comparison with the results of the continuous measurement instrumentation. For this latter group, good agreement was found between results from manual sampling and the continuous data, except for SO<sub>2</sub> and H<sub>2</sub>S as noted above. The manual sampling data for these two constituents was judged to be the most valid obtained during the tests and is used in the comparison of emissions. Two

conclusions were developed concerning the suitability of manual sampling techniques applied to the measurement of coke oven emissions. First, the manpower required to perform the sampling was substantial when compared with that required for operation of the continuous measurement instrumentation system. Second, the time required to obtain analytical results on the samples was considerable, and therefore, the results could not be utilized for test-by-test modification of procedures (as continuous measurement results were used).

Several problems were encountered in the implementation of an emission measurement system. The first problem relates to the concept of isokinetic sampling and the difficulty of applying this concept to a highly variable emission source such as a larry car. The approach followed was to sample at a constant controlled rate close to the predicted average stack velocity and to correct the collected mass based on the actual measured velocities to a value that would have been obtained if isokinetic sampling had been followed. To do this, it was necessary to gather continuous data on the velocity and/or volume flow at the sampling point. It was concluded that this was the best approach when considered against the alternatives of continuously and manually adjusted sampling rates (to match stack velocities), and systems which automatically adjust sampling rates. Based on a review of the results obtained this appears to be a valid and successful approach.

In the measurement of the emissions released in coke oven charging, all emission points could not be measured during one charging sequence. The approach followed was to sample at several of the emission points on separate charges, and to combine these results into a composite mass representative of the total mass emissions of the charging operation. This approach to the measurement of mass emission was the best method within the time and economic constraints of the test program. After review of the data, it was concluded that there was sufficient variability in emissions from point-to-point and charge-to-charge, so as to preclude single point testing as a means of determining the total mass released during a single charge with any degree of accuracy.

The initial test objectives called for the performance of three tests per day. However, a number of factors encountered after the start of scheduled testing made the accomplishment of this goal impossible. These factors included unscheduled equipment maintenance and repair, problems in production "non-interference" scheduling of ovens within instrumentation accessibility limits, post-test instrumentation and data acquisition system turn around delays, and unexpected severe worker fatigue.

The high temperatures and open flame prevalent in the coke oven environment often caused extensive damage to various system components necessitating unscheduled repair or replacement. The unpredictable nature of these occurrences also caused problems in replacement component availability.

The instrument lines to the battery top were capable of reaching a block of 20 consecutive ovens. However, during an eight hour shift, only one pass would normally be made through the block, exclusively charging either the odd or the even numbered ovens. This reduced by a factor of 1/2 the number of available ovens in the accessible block and spaced the charges of interest approximately 45 minutes apart. It was often found necessary to delay the scheduled charging of an oven within the accessible block to allow the completion of test preparation. Such scheduled disruptions could only be tolerated on a limited basis without affecting normal production.

Assuming no obvious damage to oven top instrumentation, the necessity remained to check the continuous monitoring instrumentation and data acquisition system components for proper operation. In addition, considerable time was required when manual sampling was scheduled to turn around manual sampling equipment between consecutive tests.

Lastly, workers experienced an unusually high level of fatigue after a test period, primarily attributed to the rapid work pace necessary to limit production interference (tests were generally completed in less than 20 minutes), high ambient temperatures (100°+), and poor air quality.

The data which forms the basis for conclusions contained in this report are judged to be consistent and repeatable in the context of test requirements and the operational environment. This assessment is founded on a careful examination of basic data element test averages for volume flow, temperature, and measured constituent concentrations including particle size distribution. For example, the average volume flow values for a Wilputte stack emissions point show an average flow rate of approximately 200 cubic feet per minute over 15 individual tests, while the maximum and minimum average values for this same group of tests are approximately 290 and 130 scfm, respectively. The temperatures in the gas streams during these tests showed similar consistency with an approximate average of 600° Rankine. The corresponding maximum and minimum temperature averages were approximately 550° and 2000° Rankine (in the presence of flame). Although almost constant fluctuations were observed in volume flow, the data obtained appears consistent with all observations of the charging process.

Good agreement between the continuous monitoring system and data obtained through manual sampling is evident with the exception of H<sub>2</sub>S/SO<sub>2</sub> data. The discrepancies noted here were several orders of magnitude and were traced to chemical interferences. In addition, the concentrations measured were consistent with similar data reported by other investigators.

A number of various techniques and equipments were used to obtain particulate size information. When the various sources of data are compared using particle statistics criteria, good agreement is shown in support of the composite particle size distribution reported here. It is felt, however, that valuable information might be obtained through the additional refinement of particulate sampling techniques and devices, and thorough analysis of the resulting data.

#### FEASIBILITY OF A COKE OVEN COMPLIANCE MONITORING SYSTEM

During the conduct of this test program, consideration was given to the applicability of this measurement approach to compliance monitoring. One factor which appears to transcend most other considerations is the

unique design efforts required to implement this measurement approach. Much of the time spent in preparing for the test operation was devoted to tasks of fitting the measurement system to the particular battery and larry car being tested (i.e., installation of sampling lines, signal cable, facility modifications, field fitting of emission guides, etc.). From this it was concluded that the measurement system and the concept of using this system could not easily be applied to the task of emission measurement of a larger population of coke ovens. Rather, the concept is tailored for specific application to the particular battery and larry car being tested.

The technical feasibility of a compliance monitoring system based upon optical measurements was established, with qualifications. The optical measurement system consisted of a fluorescent light bar source and a 35 mm sequence camera. Micro-densitometer readings of the film images of the light bar were then used to give a measure of the emissions of the charging operation based on the light transmission characteristics of the emission volume.

Light transmission or its inverse, opacity, can be mathematically related to particulate material contained in the emission plume based on the portion of source light an individual particle removes from the light reaching the detector or camera. Determination of total mass emitted using this approach depends on several assumptions. It is necessary to assume that the majority of the particles are larger than  $3\ \mu$  in diameter so as to avoid problems caused by Mie scattering. It must be assumed that the particle size distribution is constant over time and that the distribution can be described accurately by its geometric mass mean radius value. In order to make the final total mass calculation, the emission plume remains constant over short periods (5 seconds in this calculation) such that total mass emitted can be related to vertical plume rise.

Technical and economic constraints precluded a charge-by-charge comparison of the particulates measured by direct means, with estimates of mass emission as determined by the optical measurement system.



Instead, a comparison was made for six separate charging operations (four Wilputte and two AISI/EPA), between the measured flow of gaseous emissions (scf/second at one second intervals) and the particulate mass rate across the length of the light bar as calculated from micro-densitometer readings using the appropriate algorithms (measured as grams particulate/meter vertical distance at five second intervals). In such a comparison, evidence of a correlation between optical measurements and the mass loading in the emission plume would appear as similarities in the trends of each measurement (i.e., comparison of peaks, and increasing and decreasing trends of the curves). In general, these trends and relationships were found, and are reviewed in detail in the body of the report.

Although reasonable correlation was found, problems encountered in accurately characterizing the particulate characteristics and the variability of the size distribution caused serious doubt concerning the ability of the system to accurately and consistently measure total mass emitted for compliance purposes. An alternative approach was developed and discussed in the body of this report. This approach involves the use of the basic system elements to implement a refinement of Ringelmann technique accounting for duration and volume of an emissions plume.

## SECTION II

### INTRODUCTION

The atmospheric environmental problems associated with coke manufacturing are a serious concern to the industry and to anyone in the near vicinity of a coke plant. The American Iron and Steel Institute (AISI) has made studies over a number of years addressing the environmental health problems associated with coke oven emissions. The results of these early studies led most steel companies to initiate programs related to control of coke oven emissions. One particular aspect of the emissions control program was improved charging techniques - a subject receiving increasing attention from AISI and the industry. As a result of this common interest, AISI and Jones & Laughlin Steel Corporation signed an agreement in March 1969 whereby J & L would manage the AISI coke oven charging program. In June 1970, AISI signed an agreement with the Air Pollution Control Office (later designated Office of Research and Development) of the Environmental Protection Agency under which half the cost of the program would be born by EPA.

The AISI coke oven charging program was to culminate in a prototype of a new larry car that would result in smokeless charges and have an environmentally controlled cab for the safety and comfort of the operator. In order to determine the improvement in atmospheric emissions due to the new prototype larry, EPA engaged the services of The MITRE Corporation in April 1971 to conduct a test and evaluation program. The overall objectives of the test program as agreed to by EPA and The MITRE Corporation were as follows:

- quantify the atmospheric pollutants resulting from the charging operation in the coking process,
- provide a comparative evaluation of the pollution abatement system (AISI/EPA larry car versus existing Wilputte Larry Car),
- determine the feasibility of a compliance monitoring system concept based upon optical measurements.

By July 1971, construction of the new car was started on the south end of the P4 battery at the J & L Pittsburgh Works. In December 1971, the new car first operated under power.

During this period, effort under the MITRE contract consisted of the design and fabrication of emission guides to fit around the drop sleeves of each larry car so as to channel emissions that would be normally vented to the atmosphere; the design and installation of a van mounted continuous monitoring instrumentation system for monitoring these emissions; the preparation of manual sampling and analytical specifications; and the design and fabrication of equipment for the optical measurement program.

In September 1972, MITRE performed two days of preliminary testing at J & L to determine the feasibility of using certain sensors and to determine gross flow parameters. Additional preliminary tests were performed in May 1973, and full tests on the oven began in June 1973 and concluded at the end of August. Data reduction and report production efforts were then initiated in September of 1973 and were completed with the submission of this final project report in March 1974.

As an adjunct to the test activities carried on at the J & L facility, observations of two new charging cars with features similar to the J & L car were scheduled at two other coking operations in March and April of 1974. The purpose of these observations was to collect data on the operation of these cars including production data, reliability data, and a qualitative assessment of emissions from the charge through visual observations. Observations were scheduled at the Weirton, West Virginia and Granite City, Illinois plants of The National Steel Corporation. However, due to operational problems and program schedules, observations at Granite City were indefinitely postponed.

Observations carried out at the Weirton Steel Division of The National Steel Corporation provided much additional information useful in any assessment of improvements and new technology currently in use at operating coke plants. The data obtained during these observations has been compiled and is published under separate cover.

## SECTION III

### APPROACH

#### GENERAL

In order to compare the improvement in atmospheric emissions resulting from the use of the new AISI larry car, the MITRE approach was to channel all emissions from around the drop sleeves and Wilputte stacks through ductwork of defined cross-sections for flow and particulate measurement and gas quantification. These data were then integrated to obtain a typical grain loading and gas mass flow during a charge by each type larry car and, in turn, a measurable change due to the new design. This section describes the Emissions Guides used for channeling emissions from around the drop sleeves, the sensors and probes used on the oven, and the instrument van where continuous gas analyses were performed and where data were recorded. Manual gas and particulate samples were obtained, and this sub-program is also described in this section.

A study was conducted to establish the feasibility of determining or inferring the mass loading of particulate matter during a charge by means of an optical (camera) system. This experiment is also described in this section.

Finally, the test program, schedule, and operating procedures used in the field measurement program are described.

#### CONTINUOUS MEASUREMENT SYSTEM

This system was designed to allow a continuous (one reading per second) measurement of flow and selected gases. The various components required to satisfy this requirement are described in this section.

#### Emissions Guides

These are structures that were designed and fabricated to fit around the drop sleeves of the larry cars and channel the emissions that are usually vented to the atmosphere. The guides for each larry car are different because the configuration of the drop sleeves is different. In both cases, heavy emissions escape following normal charging when the drop

sleeve is raised up from the charging port on the oven floor. Consequently, the guides were designed so that moving parts would not leak emissions and still resist the heat of the gases and any local flames.

Wilputte Larry Car Emissions Guides - The duct which contained the emissions from the Wilputte car and provided a controlled measurement location was configured in the form of an annulus extending from the oven top upward around the drop sleeve assembly. The inner wall of the annulus was sealed to the bottom of the drop sleeve by means of a flexible fire retardant skirting. The outer wall of the annulus was located 7" outside the inner wall and extended from the top of the oven around the drop sleeve assembly. The outer sleeve was sealed to the top of the oven by the weight of the guide resting on its lower edge. As can be seen in Figure 1 and 2, the annulus is elliptical in shape and smaller at the bottom than at the top. This configuration provided an expanding volume in the vertical direction which allowed the hot emissions to rise and expand with minimal interference. Portions of the guide were blocked off by deflectors, allowing measurements to be made in one well-defined measurement duct. In order to provide a smooth emissions flow within the measurement area, vortex breakers were placed inside the duct at an appropriate distance from the sampling area. The breakers, in the form of wide mesh screens, appeared to improve the flow characteristics in the measurement ducts. The design of the guide was such that emission suppression or inducement was minimized.

In addition to emissions from the vicinity of the drop sleeves, emissions escaping from the three stacks on the Wilputte car were monitored. Guides for these emissions were merely cylindrical "stovepipe" extensions on the stacks.

AISI/EPA Larry Car Emissions Guide - This system consisted of two hoods connected by a flexible flameproof section for each of the three drop sleeve assemblies (Figures 3 and 4). The inner hood was designed to surround the drop sleeve and contain the emissions when the sleeve is in the lowered position. The hood was sealed at the top to the center

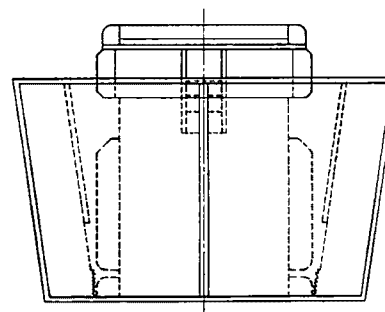
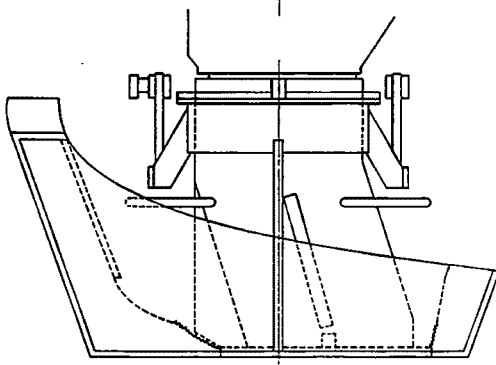
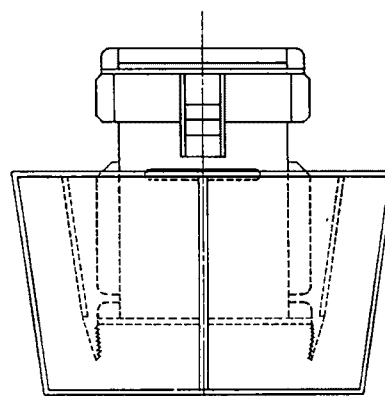
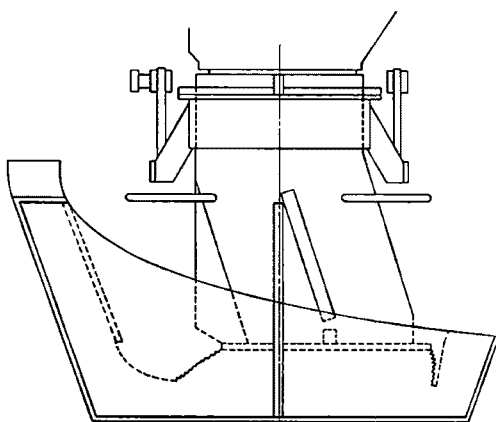
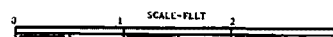
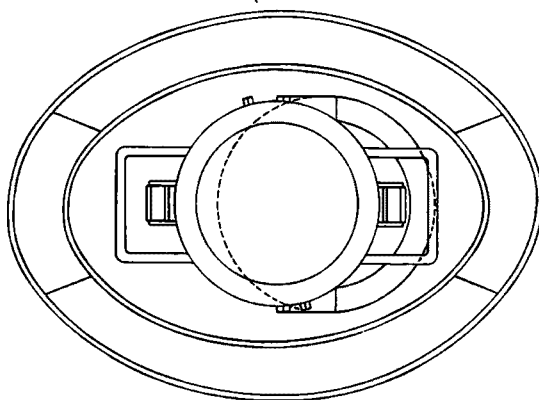


**FIGURE 1  
WILPUTTE LARRY CAR  
EMISSIONS GUIDE**



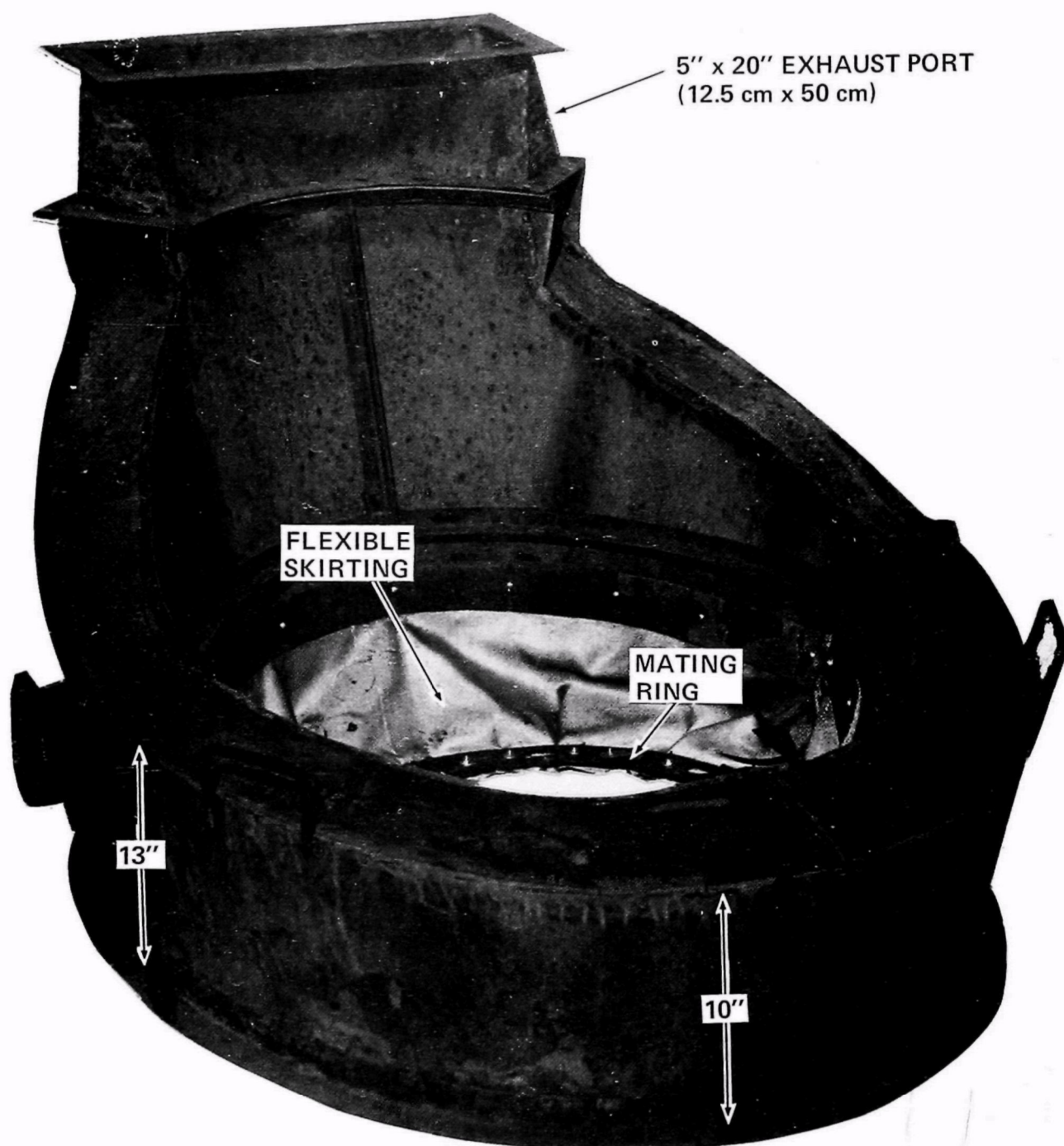
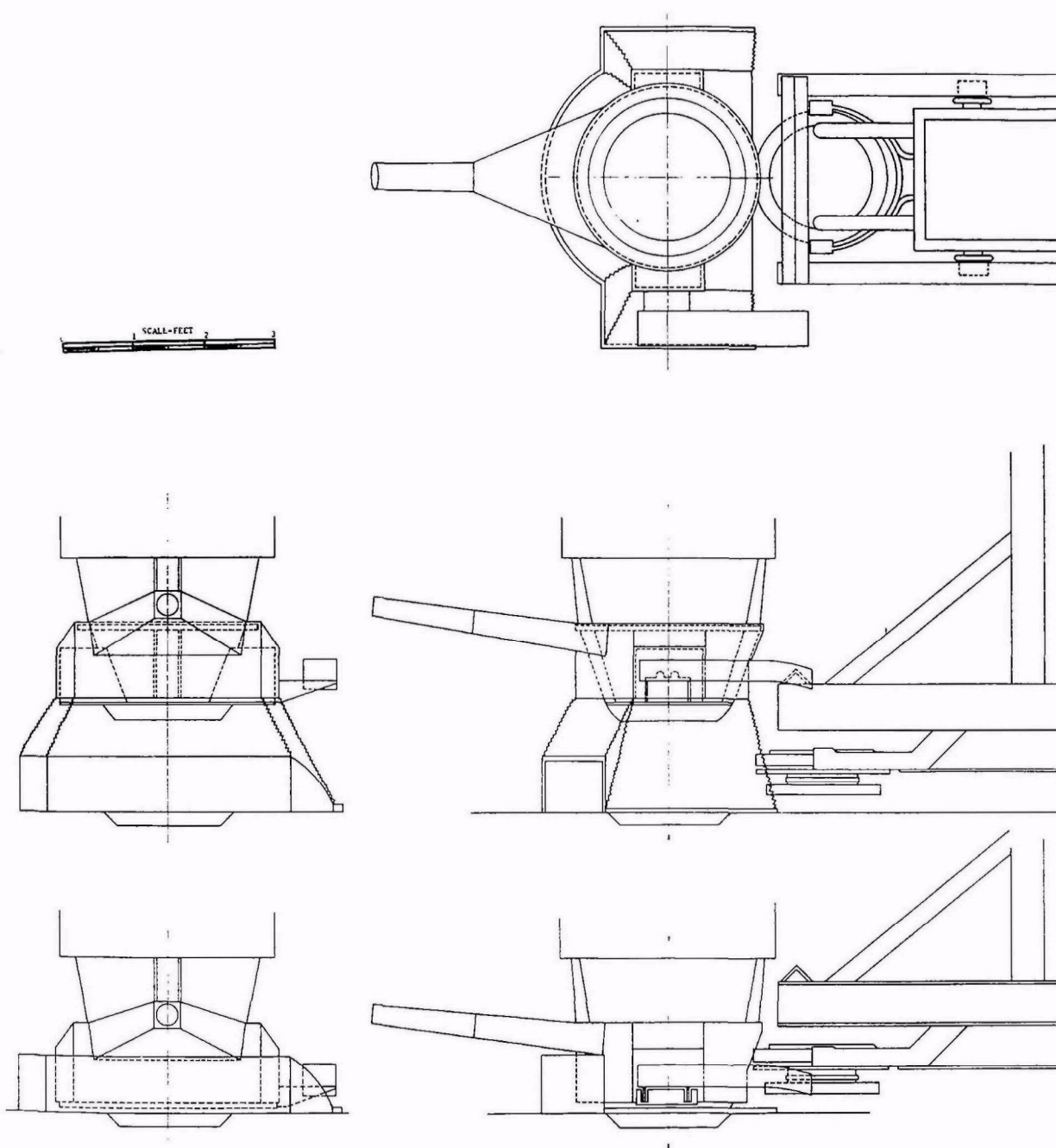


FIGURE 2  
WILPUTTE LARRY CAR EMISSIONS GUIDE



**FIGURE 3**  
**AISI/EPA LARRY CAR**  
**EMISSIONS GUIDE**

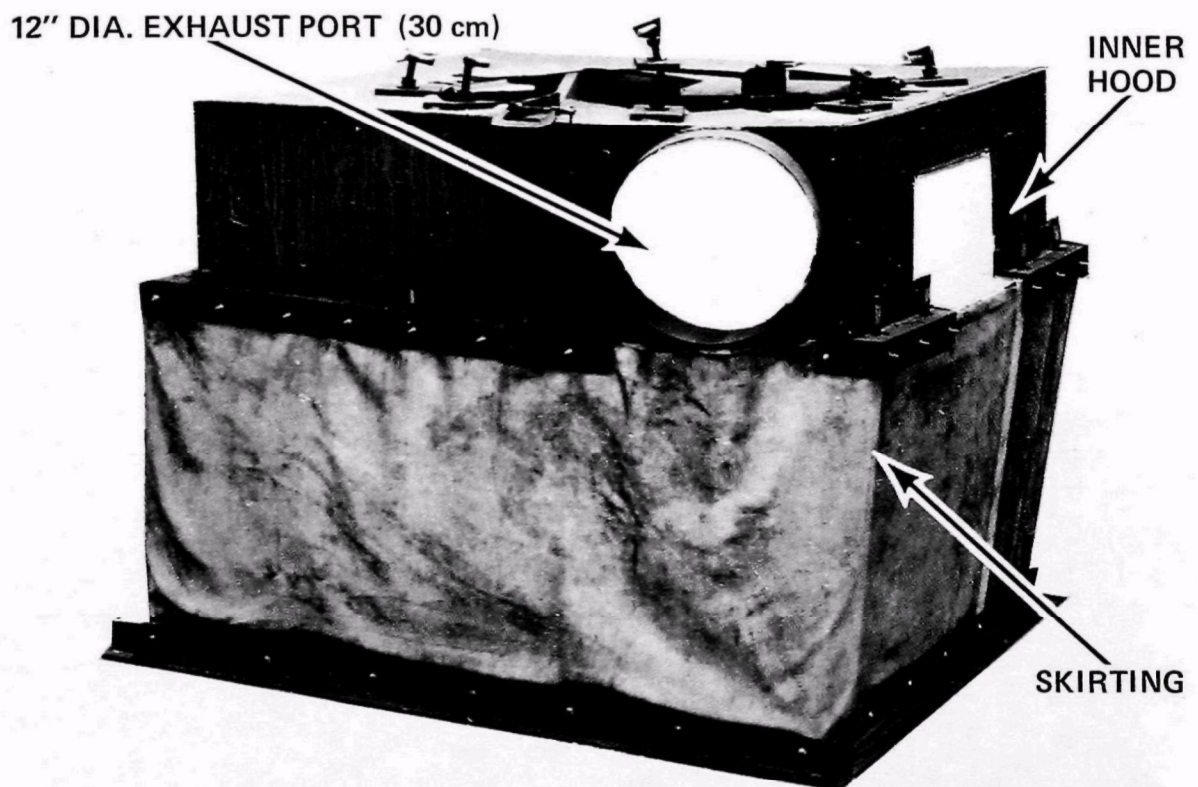


FIGURE 4  
AISI/EPA LARRY CAR EMISSIONS GUIDE

flange on the drop sleeve assembly and extended downward and completely around the drop sleeve assembly to a point slightly above the oven surface.

A flexible woven fabric was attached to the lower edge of the inner hood and extended downward to contact the oven top along a line completely surrounding the lowered drop sleeve. The flexible wall was held in contact with the oven top by the weight of the angle iron fabric frame that rested on the oven floor. The hood was designed to minimize the internal empty volume while still allowing the movement of contained emissions to a single measurement duct located at the top and forward side (away from the lid lifting mechanism) of the inner hood. The measurement duct extended some distance to obtain a smooth flow of emissions, thus providing a region in which accurate measurements could be made. The small hood volume optimized the entrapment of emissions experienced during the portion of the charging cycle when the drop sleeve is lowered. Vortex breakers were placed at the beginning of the measurement duct.

At the completion of the charging cycle, the drop sleeves were raised and the lid mechanisms replaced the charging port covers. During this period, the outer hood, sitting on the oven surface and connected to the inner hood by the lower end of the fabric wall, confined the emissions and guided them upward to the measurement duct on the inner hood. In order to allow normal operation of the lid lifter mechanism, the rear portion of the outer hood was left open from the lower edge of the inner sleeve to the oven surface. The lid lifter mechanism then passed through this opening and replaced the charging port cover in the normal manner. A partial seal of this opening was achieved by a flexible fabric skirt attached to the back of the inner hood above the lid lifting mechanism and directly behind the lid lifter magnet assembly. The inner portion of the hood was balanced so as to allow the drop sleeve to be raised or lowered while the hood was in place.

## SENSORS AND PROBES

Flow measurements and sampling require sensors and equipment located at the emissions guides and stacks. Other hardware was required on the oven to obtain the needed data. The mechanical, electrical, and electronic equipment located on the oven is described below.

Metal plates were fabricated and permanently attached to the sides of the ducts of the emissions guides, and the sensor heads were mounted on these plates in such a fashion that they extended into the flow of emissions from the ducts. This design allowed for all delicate sensors and circuitry to be handled separately from the emissions guides for ease of cleaning and maintaining, as well as for protection against rough handling. Equipment that was mounted on the plates consisted of: pitot tubes for gas velocity determination, thermocouples for temperature determination, probes for collecting gaseous emissions, filter bases for collecting particulates, and heaters for maintaining the temperature of the gas and particulate probes. Photographs of the sensor ducts are shown in Figures 5 and 6.

Sensors and sampling probes were connected to additional equipment located off the oven floor in or near the small shed on the pipe bridge opposite Oven 3-5 (see Figure 7). These connections were made through wires and heated tubing that either transmitted electrical signals, differential pressure, or gas samples. These wires and tubing were made up into bundles, termed cables, and run from the emissions guides and stacks via overhead booms and towers to the pipe bridge area.

Two booms were used in the testing area and were attached to the pipe bridge shed: one closest to the coal bin supported cables for testing the emissions guides of the Wilputte car and the one farthest from the coal bin supported cables for testing either the Wilputte stacks or the AISI/EPA emissions guides.

The small shed at the end of the pipe bridge cross-over main opposite Oven 3-5 housed equipment required to convert temperature and pressure probe outputs into electronic signals, and also served as the location

## SENSORS AND PROBES

Flow measurements and sampling require sensors and equipment located at the emissions guides and stacks. Other hardware was required on the oven to obtain the needed data. The mechanical, electrical, and electronic equipment located on the oven is described below.

Metal plates were fabricated and permanently attached to the sides of the ducts of the emissions guides, and the sensor heads were mounted on these plates in such a fashion that they extended into the flow of emissions from the ducts. This design allowed for all delicate sensors and circuitry to be handled separately from the emissions guides for ease of cleaning and maintaining, as well as for protection against rough handling. Equipment that was mounted on the plates consisted of: pitot tubes for gas velocity determination, thermocouples for temperature determination, probes for collecting gaseous emissions, filter bases for collecting particulates, and heaters for maintaining the temperature of the gas and particulate probes. Photographs of the sensor ducts are shown in Figures 5 and 6.

Sensors and sampling probes were connected to additional equipment located off the oven floor in or near the small shed on the pipe bridge opposite Oven 3-5 (see Figure 7). These connections were made through wires and heated tubing that either transmitted electrical signals, differential pressure, or gas samples. These wires and tubing were made up into bundles, termed cables, and run from the emissions guides and stacks via overhead booms and towers to the pipe bridge area.

Two booms were used in the testing area and were attached to the pipe bridge shed: one closest to the coal bin supported cables for testing the emissions guides of the Wilputte car and the one farthest from the coal bin supported cables for testing either the Wilputte stacks or the AISI/EPA emissions guides.

The small shed at the end of the pipe bridge cross-over main opposite Oven 3-5 housed equipment required to convert temperature and pressure probe outputs into electronic signals, and also served as the location



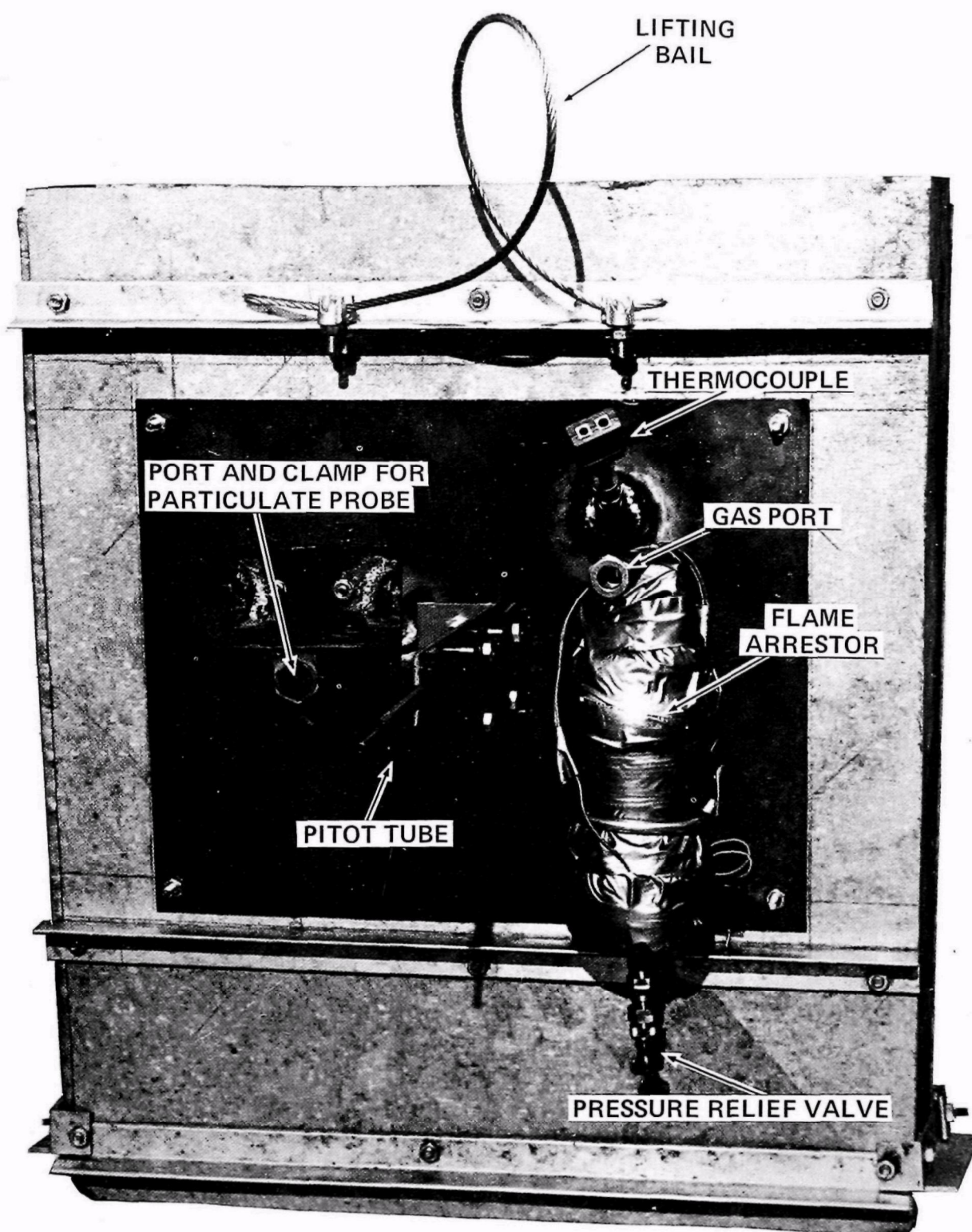


FIGURE 5  
WILPUTTE EMISSION GUIDE  
SENSOR DUCT



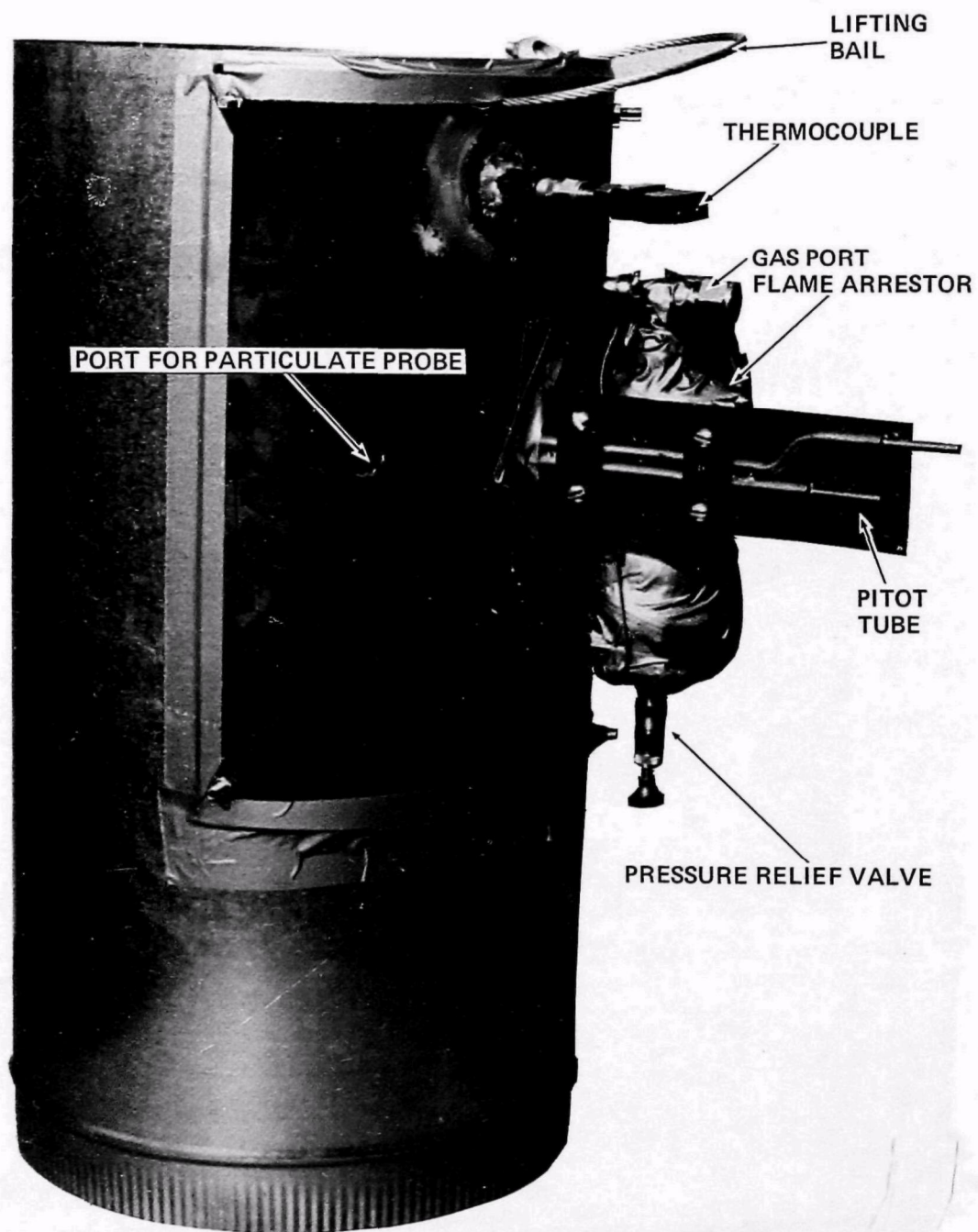


FIGURE 6  
WILPUTTE STACK AND AISI/EPA EMISSION GUIDE SENSOR DUCT

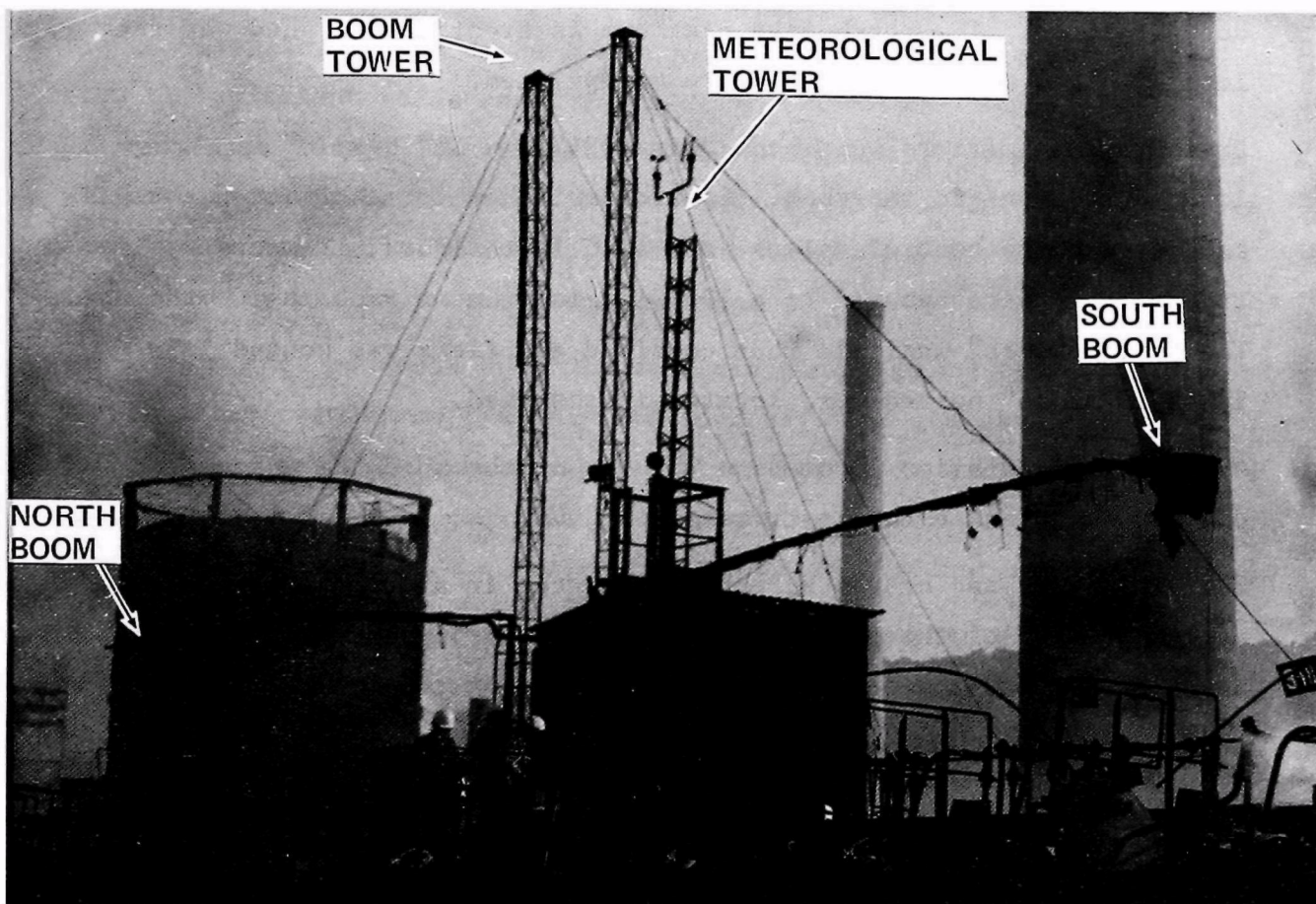


FIGURE 7  
CROSS-OVER BRIDGE SHED AREA

for combining gas samples from all measuring points into a "common duct" for manual sampling and further transmission to the instrument van. The shed also served as a central location for communications via citizen band radio between the test director, instrument van, and the optics balcony, and was also the power distribution point for the heated probes and gas lines. The porch-like platform in front of the shed was the location from which the booms were manipulated.

Pressure transmitters were housed in a 24" w x 30" h x 18" metal box, located adjacent to the shed. Control switches for activating the gas and particulate control valves were also in this box. Temperature transmitters were secured to a 19" wide instrument rack inside the shed. The "common duct" manifold that combined gas flows was housed in a 12" x 12" x 36" heated box, located in the shed.

A meteorology station located on the top of the shed had associated electronic boxes in the instrumentation van.

Cables, wires, and heated tubing were placed in a cable trough located across the top of the pipe bridge where they dropped down to ground level to the instrumentation van at the base of the bridge tower.

#### Instrument Van

Gas collected at the sensor ducts and the output of the temperature and pressure sensors was processed by electro-chemical-mechanical instrumentation and the results recorded for subsequent analysis. The processing center was a 36' van filled with seven racks of electronic equipment to perform these functions and was located at the base of the pipe bridge tower as shown in Figure 7. Three specific functions were performed in the van: gas analysis, determining physical properties in the vicinity of the measurement points, and data recording. Instrumentation used is briefly described here, and a more detailed description can be found in the Test Plan, MITRE WP-10434 and in MTR 6566, "A Continuous Monitoring System for Coke Oven Emissions Due to Charging."

## Gas Analysis System

The continuous gas measurement system consists of a number of specific gas analyzers of two basic types: raw gas analyzers which accept a gas sample as it comes from the emissions guides, and conditioned gas analyzers which require preconditioning in the form of gas drying and cooling.

The gas sampling system draws a representative sample of emitted gas from the emissions guide and the Wilputte stack (when testing the Wilputte Larry Car). The gases from the emissions guide probes and the Wilputte stack probes are combined at the common duct in the pipe bridge shed. All components in contact with the sample gas are held at elevated temperature to prevent condensation.

The common duct consists of a plenum containing a mixed representative sample of emission from the selected sources. The gas sample for the wet chemical analysis (manual sampling) equipment is extracted from this plenum. The remaining gas flowing through the common duct is fed through heated sample lines to the analyzers located in the instrumentation van.

Upon entering the instrumentation van, the gas flows through a heated manifold, from which a sample is extracted for the raw gas analyzers. The remaining gas flows through a refrigerated condenser where it is cooled and condensables are removed. The dried, cooled gas is then pumped under slightly positive pressure to the conditioned gas analyzers. A pressure regulator and bypass was provided to minimize the gas transit time. A schematic diagram of this system is shown in Figure 8.

### Raw Gas Analyzers

A number of the gas analyzers operate on the gas sample under stack conditions. The gaseous constituents monitored in this manner include:  $\text{SO}_2$ ,  $\text{H}_2\text{S}$ , THC, NO,  $\text{NO}_x$  and  $\text{H}_2\text{O}$  vapor. Each instrument incorporated an independently heated sample handling system for controlling the flow through each analyzer.

The  $\text{H}_2\text{S}$  analyzer is a dual gas instrument, manufactured by Peerless Instrument Company and operated on the principal of ultraviolet absorption.

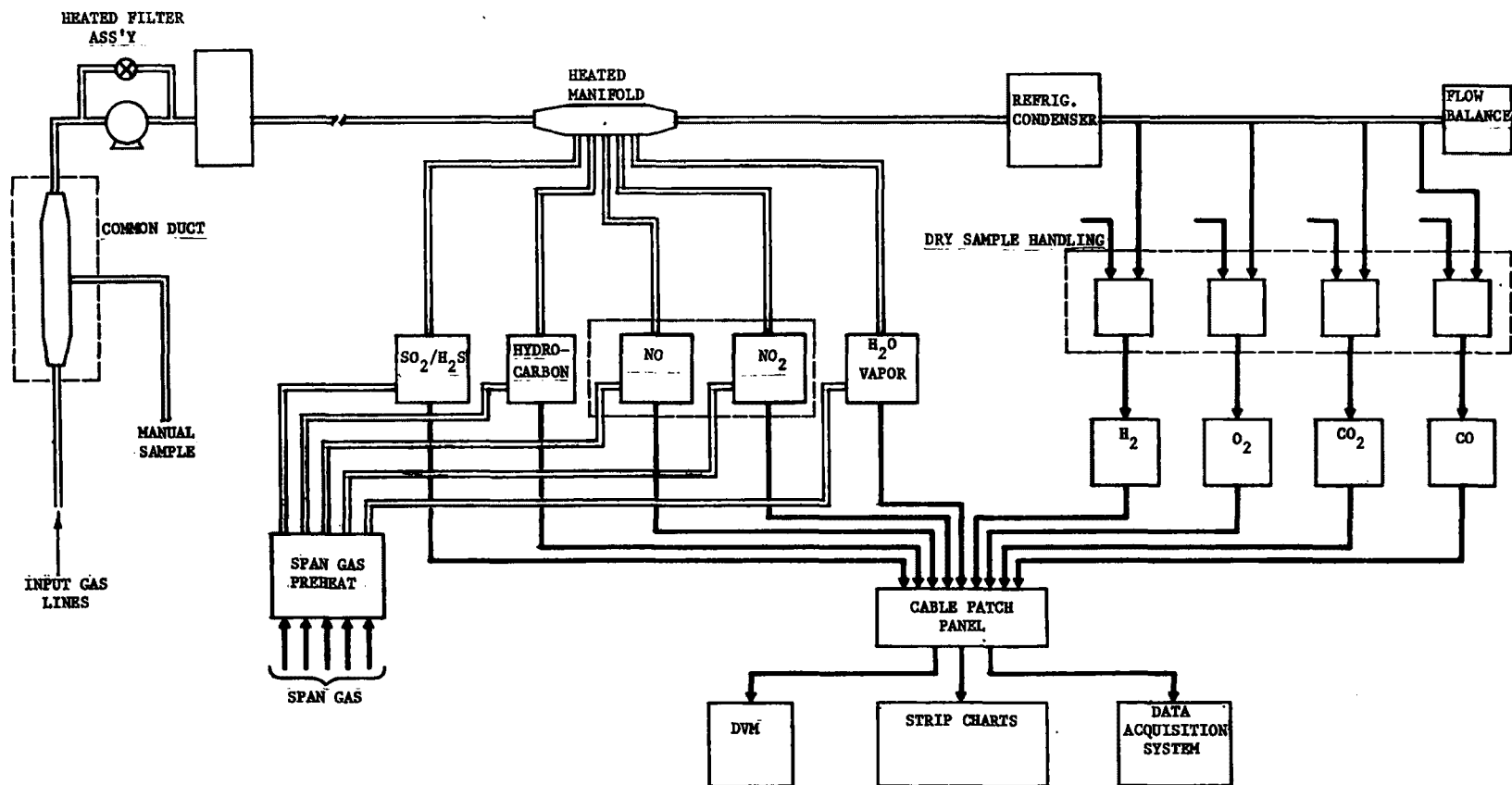


FIGURE 8  
GAS HANDLING SYSTEM

The band selected for  $\text{H}_2\text{S}$  has an  $\text{SO}_2$  interference factor, but since the analyzer was also measuring  $\text{SO}_2$  on a continuous basis, a correction circuit was employed which subtracted out the  $\text{SO}_2$  interference, providing a true output of  $\text{H}_2\text{S}$ . The analyzer incorporates three ranges providing 3,000, 300, and 100 ppm by volume full-scale.

The THC (Total Hydrocarbons) analyzer operates on the flame ionization principle whereby the gas sample is burned in an ionization chamber using a mixture of zero air and pure  $\text{H}_2$  as fuel. The combustion process produces free ions, which are detected by an ion detector. The detector produces a current whose magnitude is a function of the number of ions reaching the collector; therefore, the detector current is a function of the total hydrocarbon content of the gas sample. The analyzer utilizes an input gas dilution system to eliminate interference caused by the  $\text{H}_2$  present in the sample gas.

The analyzer for Nitrous Oxide is a chemiluminescent device. In the reaction



light ( $\lambda \approx .6\text{--}3\mu$ ) is emitted when electronically excited  $\text{NO}_2$  molecules revert to their ground state, and the intensity is proportional to the  $\text{NO}$  concentration.

The analyzer for Nitric Oxide is similar to that for  $\text{NO}$ , but includes a hot catalyst for the reduction of  $\text{NO}_2$  to  $\text{NO}$ . The resulting measurement is  $\text{NO}_x$  ( $\text{NO} + \text{NO}_2$ ). The quantity of  $\text{NO}$  is subtracted electronically, from the  $\text{NO}_x$  value, producing an output in terms of  $\text{NO}_2$  concentration.

The Water Vapor analyzer is a MSA Lira 200 HR Non-Dispersive Infra Red (NDIR) instrument. It has a dual range configuration with 10% and 50% moisture full-scale ranges.

#### Conditioned Gas Analyzers

These gas analyzers are supplied with a cooled, dried sample gas stream. A refrigerated condenser with a stainless steel condensation chamber is employed to pump the dried gas through the analyzers. A dry gas sample

handling system was employed for each analyzer, providing flow monitoring, throttling control, and calibration gas insertion. Those gases monitored are:  $H_2$ ,  $O_2$ , CO, and  $CO_2$ .

The analyzer for Hydrogen is a Beckman 7C Thermal Conductivity Analyzer. The analyzer for Oxygen is a Beckman Model 742, utilizing a polarographic oxygen sensor.

The analyzer for Carbon Monoxide is a MSA d11A 202, non-dispersive infrared instrument. The instrument is a three-range device, operating at 3%, .3%, and .03% by volume full scale.

The analyzer for Carbon Dioxide is a MSA LIRA 202 non-dispersive infrared instrument. The instrument is a four range device, operating at 10%, 3%, 1%, and .3% by volume full scale.

#### Physical Properties Measurement System

The physical properties of the gas effluent emitted at each source were monitored. These properties include temperature, static pressure, and differential pressure, and are used to compute the volume flow of the emission and in processing the data to convert the gas measurements to STP.

Temperature measurements were monitored by using Type K (Chromel-Alumel) thermocouples in conjunction with Leeds and Northrup Model 1992 temperature transmitters in a temperature range of 0-2,200°F. The temperature transmitter has a response of 1 millivolt/2°F.

The differential pressure measurements were made using a series of "S" Type pitot tubes, connected to CGS Datametrics Model 536 Barocel pressure transducers. The range of differential pressure is 0-10.0" W. C. with resolution of .0005" W. C.

Meteorological parameters were monitored on a continuous basis. These parameters include ambient temperature, humidity, barometric pressure, wind speed, and wind direction.

## Data Recording

The data produced by the gas analyzers and the physical property measurement instruments were recorded, in IBM-360 compatible format, on magnetic tape. Selected parameters were recorded in analog form on a series of strip chart recorders. In addition, each parameter could be monitored, independently, by a digital volt meter.

The data acquisition system was manufactured by Data Graphics Corporation, to MITRE specifications. The system provides 70 analog input channel capability, time of day clock, and manual data input. The analog-to-digital converter provides an accuracy and resolution of .005% of full scale and is capable of operating at a data rate of 200 conversions/second.

Selected data parameters were graphically recorded on strip charts. The recorders, manufactured by the MFE Corporation, are multi-channel devices using rectilinear heat writing and providing 29 channels of recording capability.

## MANUAL SAMPLING

The sampling of gas and particulate by manual methods was done to complement the continuous monitoring and optical portions of the program. Samples were obtained at the same measurement points on the emissions guides and Wilputte stacks as the emissions were channeled during normal charging and simultaneously with the continuous measurement tests. A brief summary of this part of the test program follows below, with a more detailed description found in MITRE WP-10179, "Manual Sampling and Analytical Requirements for the Coke Oven Charging Emissions Test Program," 16 February 1973, and MTR-6288, "Manual Sampling System for the Coke Oven Charging Emissions Test Program," December 1972.

## Gas Sampling System

Gases drawn through the probes of the sensor duct and into the overhead boom cables to the pipe bridge were mixed in the "Common Duct" manifold. The probes, cables, and common duct were maintained at elevated temperatures to prevent condensation of hydrocarbons and other tars. The



heated common duct manifold was used as the source for the manual gas samples, and a heated tube extended from this common duct to a heated box containing four Teflon bags. During the test of a normal charge, the four bags were sequentially filled with the gases from the common duct. The heated box containing the four bagged samples was removed to the portable lab where each sample was preprocessed and partially analyzed on site to minimize the possibility of degradation of any constituents. The preprocessing was as follows:

- Samples containing  $N_2$ ,  $H_2$ ,  $O_2$ ,  $CO$ ,  $CO_2$ , and  $CH_4$  were transferred to glass containers for later analysis.
- $SO_2$  was absorbed using an impinger and held for later analysis.
- $NO_x$  was analyzed on site.
- THC was analyzed on site.
- $NH_3$  was absorbed by an impinger for later analysis.
- HCN was absorbed by an impinger train for later analysis.
- $H_2S$  was absorbed by an impinger train for later analysis.
- Specific hydrocarbons (pyridine and phenols) were placed in trains for later analysis.

Later analysis of the samples was performed in the Kansas City Laboratories of Midwest Research Institute by prescribed techniques.

### Analytical Methods

In this section, the analytical methods are described for the determination of gaseous concentrations in the manual sampling program.

CO, THC, Methane - A Varian Aerograph Gas Chromatograph, Model 1420-10, equipped with a 5 ml. gas sample loop and a high sensitive thermal conductivity detector, was used throughout for this work. These gas determinations were made in the field lab due to the unstable nature of the gases. The sample loop system was evacuated to as low a pressure possible with a Welch Duo-Seal vacuum pump. For calculation purposes, this pressure drop was considered to be atmospheric pressure. The sample was

passed into the sample loop and the sample pressure measured. Using a molecular sieve 5A column, the gases were separated under the instrument conditions listed in Table 1.

O<sub>2</sub>, N<sub>2</sub>, CO<sub>2</sub> and H<sub>2</sub> - These gas concentrations were determined in the identical method as just described, except that the analyses were performed at the MRI laboratory in Kansas City at the completion of the field work.

H<sub>2</sub>S - ASTM D 2725-70, "Methylene Blue Method;" exceptions to method - Neutral CdSO<sub>4</sub> solution (140 g/liter) used in place of zinc acetate absorbing solution.

NO<sub>x</sub> - Federal Register Method 7 (Volume 37, Number 247), "Determination of Nitrogen Oxide Emissions from Stationary Sources."

NH<sub>3</sub> - Analytical Chemistry 39, 971 (1967), "Catalyzed Berthelot Reaction."

CN - ASTM D 2036-72, Method C. Colorimetric (chloramine-T/Pyridine-Barbituric Acid).

Phenol - ASTM D 1783-70. Aminoantipyrine-Ferricyanide Method.

SO<sub>2</sub> - Federal Register Method 6 (Volume 36, Number 247), "Determination of Sulfur Dioxide Emissions from Stationary Sources."

Pyridine - Gas Chromatographic Analysis. Instrument - MicroTek Gas Chromatograph, Model 220, equipped with a flame ionization detector. Column - 5% Theed on Chromasorb G, 80/100 Mesh, 9' x 1/4" Cu. Column Temperature - Isothermal at 85°C. Carrier Gas - N<sub>2</sub>. Carrier Gas Flow Rate - 20 ml/min.

#### Particulate Sampling System

Particulate sampling was done at each emissions guide and Wilputte stack. The sampling nozzles were located in the measurement ducts parallel to the expected flow directions. Each nozzle was connected directly to a heated cyclone and filter or an Andersen Sampler. This sampling system further consisted of a modified EPA particulate sampling train employing quasi-isokinetic sampling.

TABLE 1

GAS CHROMATOGRAPH PARAMETERS FOR MITRE GAS ANALYSES

Gas	O <sub>2</sub>	N <sub>2</sub>	CO <sub>2</sub>	H <sub>2</sub>
Column	(a)	(a)	(a)	(b)
Column Temperature, °C	60	60	250	25
Detector Temperature, °C	195	195	195	140
Carrier Gas	He	He	He	N <sub>2</sub>
Carrier Gas Flow Rate, ml/min	100	100	100	60
Bridge Current, ma	200	200	200	150

(a) Molecular Sieve 5A, 5 ft x 1/8 in., s.s.

(b) Molecular Sieve 5A, 15 ft x 1/8 in. s.s.

The samples were analyzed for mass loading, size distribution, and elemental analysis. The weight of each sample was correlated with the volume of the gas sampled from the stream to determine the anisokinetic particulate concentration to which theoretical corrections were applied to produce a calculated isokinetic concentration. Samples, obtained from the Andersen impactor and captured on the MITRE designed carousel sampler (see MITRE WP-10480), as well as those collected by the Brink impactor, were used for size analysis. Methods used were aerodynamic classification and optical microscopy. The particulate samples obtained were analyzed for the following elements:

Al	Cu	Mo	Se
As	Fe	Na	Sn
Ba	Ga	Ni	Sr
Be	Ge	P	Ti
Ca	Hg	Pb	Tl
Cd	K	S	V
Co	Mg	Si	Zn
Cr	Mn	Sb	U

#### Coal Sampling System

Coal Samples were obtained while testing both larry cars. Analyses performed on these samples were size distribution, elemental, proximate, and ultimate.

#### OPTICAL PROGRAM

One objective of the MITRE test program was to investigate the feasibility of developing simple monitoring systems and techniques and to define an inexpensive compliance monitoring system for evaluating emission sources with similar characteristics.

The proposed system of monitoring was to cause minimal interference with the normal operation of this coke plant and was to be adaptable to various plant configurations and conditions. Optical techniques have been successfully applied in numerous situations involving a requirement to monitor emissions to determine pollution and air quality. Because of this previous use, because it did not interfere with coke production and

would be adaptable, and because it could be operated in parallel with the continuous monitoring system, an optical monitoring system was designed to satisfy this requirement.

The three essential elements in any optical measuring system are:

- a source of radiant energy (the sun, light bulbs, lasers, etc.) or a target which reflects radiant energy,
- energy collection and focusing devices (lenses, mirrors),
- energy detectors (the eye, photoelectric cells, photographic film, etc.) plus amplification, display, and recording devices.

The basic type of light source which best satisfied the system requirements is the fluorescent tube. In order to achieve the desired vertical width for the light source, a parabolic reflector was placed behind two standard 1500 MA 96" parallel fluorescent tubes which achieved desired intensity as well. The tubes and reflector were housed in a "light bar" which had a diffuser lens mounted in front of the unit to provide a more uniform light output. The bar was mounted 25 feet above the oven floor on the south end of the battery (see Figure 9). The main section extended across the entire width of the oven, and "wing sections" extended outward and downward.

The collecting, focusing, and detecting device selected is a modified 35 mm sequence camera capable of providing a frame rate of one frame per second. The camera was mounted on the first balcony of the coal in on the oven and was equipped with a 200 mm lens such that the light bin completely filled the field of view. The camera was also equipped with a time-of-day clock which recorded time on each frame. Additionally, a near-field light (18" fluorescent lamp) was positioned in front of the camera balcony for orienting the camera after each setup.

During operation of the optical system, sequential photographs were taken of the light bar as the emissions plume from the larry car crossed the path between the camera and the bar. Each frame of the film contains an image of the large linear light source (light bar). In recording the

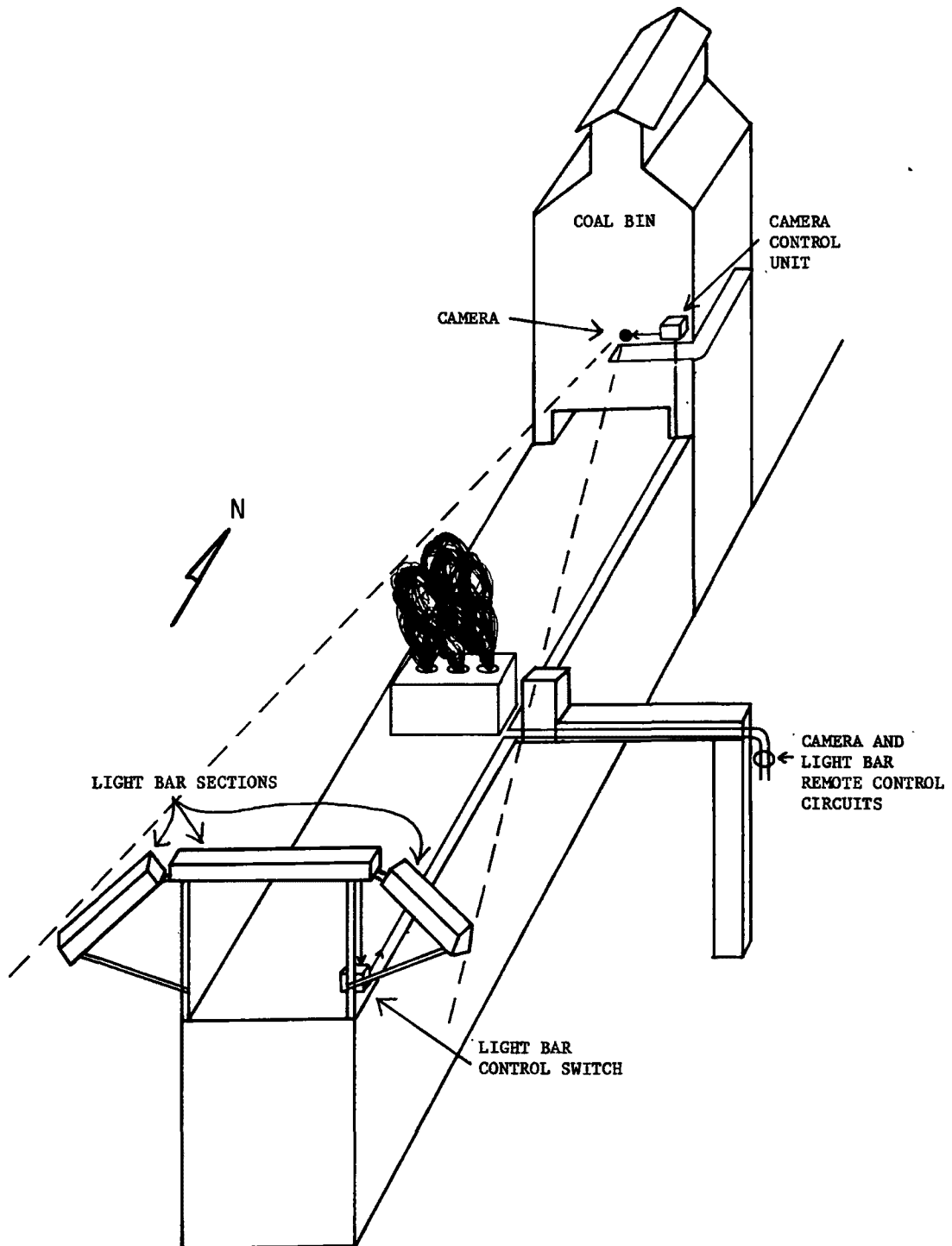


FIGURE 9  
SIMPLIFIED SYSTEM COMPONENT CONFIGURATION

image of the light bar, the film detected any diminishment of light bar brightness caused by particulate or aerosol material in the light path. This diminishment was recorded as a decrease in density of the light bar image on the film. By properly choosing the exposure values for the film and accurately processing the exposed film, the amount of light diminishment was determined using a micro-densitometer to analyze image density changes of the individual frames.

Each frame contains three light bar segments as shown in Figure 10. Each segment has two distinct areas. The bottom or black (this drawing represents a negative film frame) area represents the surface of the light source. The top or white area is a flat surface of the light bar that was painted flat black to reduce any reflected light coming from this area. All three segments are identical in construction. The light source image appears  $\sim 350\mu$  high on the film frame. The flat black area appears  $\sim 400\mu$  high and adjoins the lighted area directly above or to the outside of it. Micro-densitometer analysis of both light and dark areas of each of the three segments of the light source image can be accomplished in the following manner.

The micro-densitometer was adjusted so as to have a  $50 \times 195\mu$  aperture. A single scan was made across each area (lighted and black individually) of each of the three light bar segments. During the scan, a specified number of data points were recorded. A total of 539 data points evenly spaced were taken across the lighted and the black areas of the longer or horizontal bar section. The data obtained on each scan was placed on magnetic tape in the form of a binary density scale reading for each data point. Each scan sequence was further annotated on the magnetic tape with header information including sequence number, test number, type of frame and frame number information.

This brief summary of the optical program has been condensed from MITRE WP-10149, "Design of an Optical Emissions Measurement System for Coke Oven Monitoring," by R. W. Bee, December 14, 1972, and MTR 6596, "Optical Emissions Measurement Program Development."

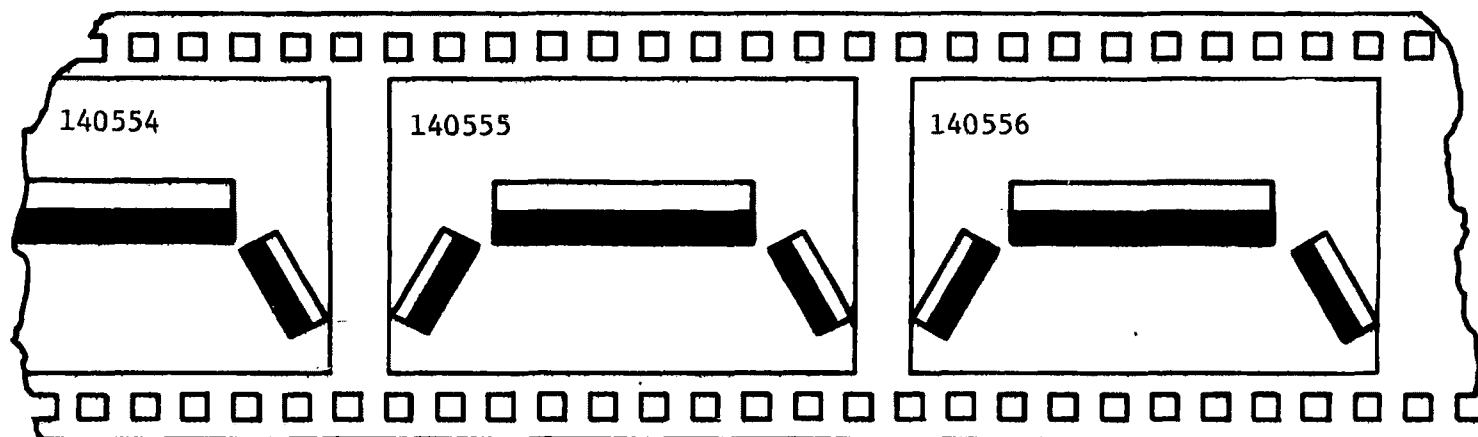


FIGURE 10  
FILM FORMAT



## FIELD TEST PROGRAM

Scheduling the tests on the battery in a reasonable sequence required coordination of many activities. First, the installation and site modifications to the new AISI/EPA larry car had to be completed; second, the procurement of critical equipment by EPA was required; third, the development and verification of the instrumentation by MITRE was necessary; and, finally, the EPA/AISI commitment to be completed at an early date was to be honored. A further requirement, to avoid interfering with J & L coke production, was also incorporated into the schedule. The system to measure the number of required parameters at the number of required measurement points, verify the measurement, convert the data to electrical signal and record these data for later processing required a large amount of equipment and an extensive amount of time for installation and checkout. Preliminary testing and data verification were also required and field tests, preliminary analysis, and dismantling had to be considered. These activities covered a five-to-six month period, during which five to six weeks of field system tests were conducted. The overall program schedule is shown graphically in Figure 11, and the final summary of the tests actually performed is provided in Table 2.

Only those ovens in the immediate vicinity of the pipe bridge and within reach of the overhead cable booms were monitored during the tests. Since an average time of approximately 15 minutes per oven was required between chargings, 11 ovens in the vicinity of the pipe bridge were normally charged during a four-hour period in any one daylight shift. MITRE avoided interfering with the charging schedule, and advantage was taken of the standard charging sequence and the normal shutdown at shift changes and noon to establish a tentative test routing. Based on this information, and experience on the battery, a Test Plan Outline for one day's activities was followed as shown in Figure 12.

### Test Procedure

Various sampling techniques were employed during the time period when the larry car charged coal into the oven. These techniques and systems,

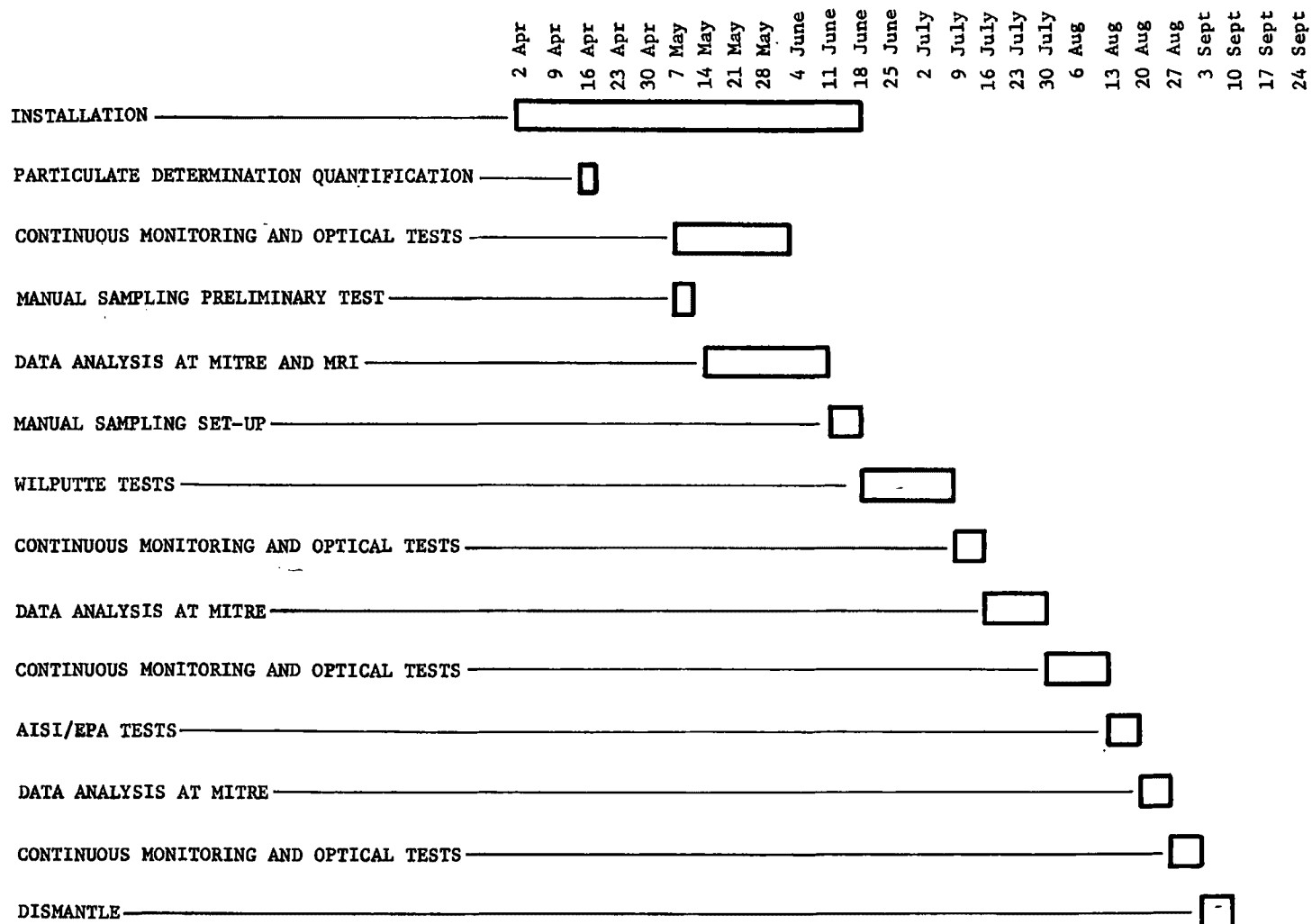


FIGURE 11  
TEST PROGRAM SCHEDULE

**TABLE 2**  
**SUMMARY OF COKE OVEN TESTS**

Date	MITRE Number	MRI Number	Oven	Time	Points Monitored	Remarks
May 7	0A		3-12		#2 Wilputte Guide	Flow data only - no mag. tape
9	0B		3-13		#2 Wilputte Guide	Flow data only - no mag. tape
10	1		3-7	7:30	#2 Wilputte Guide	Preliminary test for MRI - bad flame out
30	1A		3-5	4:45	#2 Wilputte Stack	Flow data only - no mag. tape
31	1B		3-7	10:30	#2 Wilputte Guide & Stack	Flow data only - no mag. tape
June 18			3-6	4:00		No test - boom cables shorted
19	2	W1	3-3	5:30	3 Wilputte Guides	MRI activated manually - bent boom
20						Larry car breakdown - no test
21	3	W2	3-8	1:00	#2 Wilputte Guide & Stack	Diff. press. pitot plugged
22	4	W3	3-3	11:15	#1 Wilputte Guide & Stack	Diff. press. pitot plugged
25	5	W4	3-6	5:00	#2 Wilputte Guide & Stack	
26	6	W5	3-10	12:00	#3 Wilputte Guide & Stack	
27			3-11	2:00		J & L cancelled test
28	7	W6	3-8	4:00	3 Wilputte Stacks	
29	8	W7	3-8	12:00	3 Wilputte Stacks	
July 2	8A	W8	3-6	5:20	3 Wilputte Stacks	No mag. tape - no gas sampled
3	9	W9	3-10	12:00	3 Wilputte Stacks	
4	10	W10	3-11	4:00	3 Wilputte Guides	
5	11	W11	3-8	4:00	3 Wilputte Guides	Gas leaks
11	12		3-9	3:00	3 Wilputte Guides	
12	13		3-15	10:00	#2 Wilputte Stack & Guide	
12	14		3-6	4:20	#1 Wilputte Stack & Guide	Guide gas probe plugged
Aug. 6	15		3-6	1:30	#1 & #2 AISI/EPA Guide	
7	16		3-4	12:00	3 AISI/EPA Guides	#2 probe & thermocouple data N.G.
8	17		3-4	12:00	3 AISI/EPA Guides	Early part of test not recorded
8	DL-1		2-27	2:30	Leaking Door	
9	DL-2		2-27	11:00	Leaking Door	
9	18		3-3	4:00	3 AISI/EPA Guides	#3 sensor burned out
13	19	K1	3-5	11:30	3 AISI/EPA Guides	
13	DL-3		2-26	1:00	Leaking Door	
14	20	K2	3-4	11:30	3 AISI/EPA Guides	
15	21	K3	3-3	12:00	3 AISI/EPA Guides	Bad seal on #3 drop sleeve
15	22		3-11	4:00	#2 Wilputte Stack	
16	DL-4	DL-1	2-23	2:00	Leaking Door	
16	DL-4A	DK-2	2-23	3:30	Leaking Door	
16	23	W12	3-12	4:00	#2 Wilputte Stack	
17	24	K4	3-3	2:00	3 AISI/EPA Guides	Low flow - fans burned out
17	24A		3-11	5:00	#2 Wilputte Stack	MITRE Carrousel Particulate Sampler
22	25		3-1	12:00	3 AISI/EPA Guides	Bad fire on #3
22	26		3-9	3:00	#2 Wilputte Stack	Poor gas data
22	26A		3-13	5:00	#2 Wilputte Stack	No gas data obtained
23	27		2-23	12:30	#2 AISI/EPA Guide	
23	28		3-4	3:00	#2 Wilputte Stack	
23	28A		3-10	5:00	Coke Side Door	Particulate sample during push
24	28B		3-10	9:00	Ascension Pipe	Particulate filter

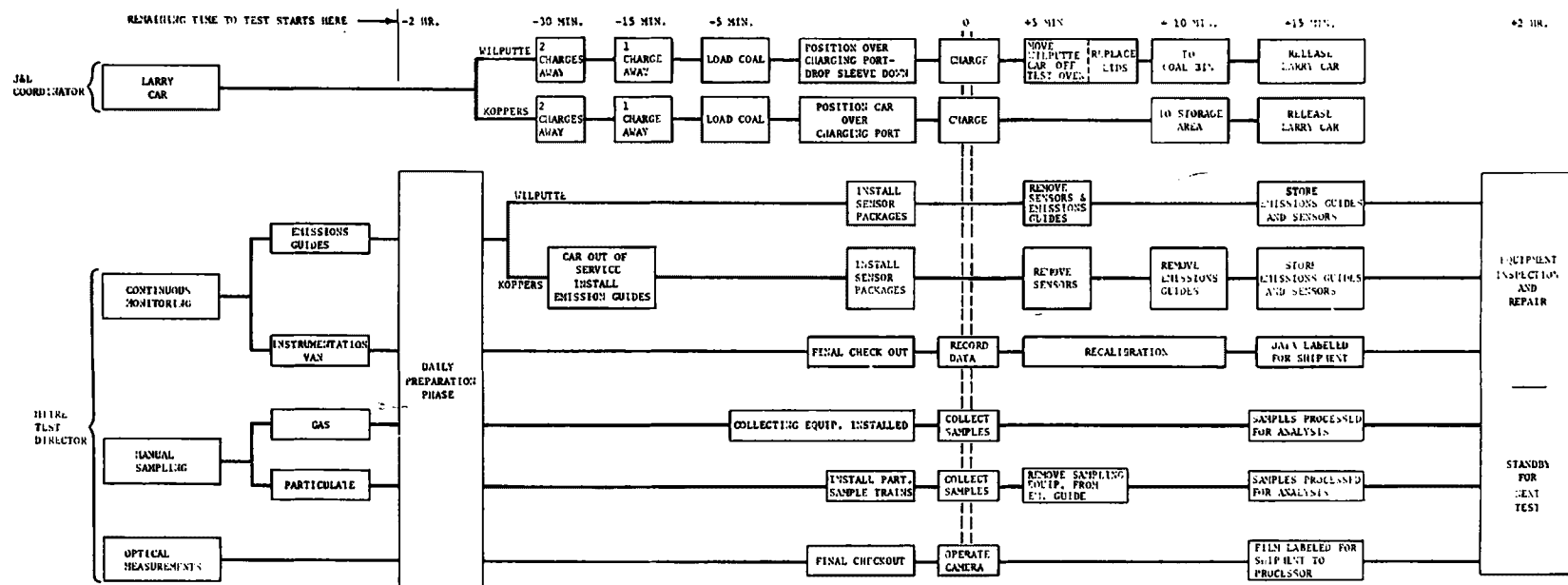


FIGURE 12  
DAILY TEST SCHEDULE OUTLINE

the continuous gas sampling system, the manual gas sampling system, the particulate sampling system, and the optical system are described in this section.

### Continuous Sampling

The MITRE Test Director obtained from J & L a list of ovens to be charged during the test day. Based on this data, a schedule was prepared which showed tentative times that the "MITRE dedicated" ovens were to be charged. Based on this schedule, the step-by-step actions for the tests were scheduled.

Two hours prior to the test, all heaters and gas samplers were turned on. One hour prior to the test, all other equipment was turned on.

Gas sample analyzers were calibrated per manufacturer's instructions and placed in a "standby" mode. Temperature and pressure sensors were tested for response, and all flow lines were checked for pressure leaks.

Emissions guides for the Wilputte car were temporarily stored beside the railing along the coke side of the battery near the oven to be tested. The sensor ducts were made ready for the test and hung on the boom. An aluminum ladder was stored in a convenient location.

During installation of test equipment on the battery, the Wilputte larry car was modified by installing the following equipment:

- Stack sensor modification rings
- Drop sleeve modification rings.

The AISI/EPA car required no modification.

Initial plans to test all stacks and emissions guides of the Wilputte larry car at one time were reduced in scope due to the time required to install equipment prior to charging, the time allowed by J & L for testing the car, and the excess exposure of personnel to heat and smoke during a prolonged period. This plan reduced to testing either the three emissions guides, the three stacks, or one emissions guide and

its corresponding stack. Testing the AISI/EPA car was done by monitoring all three emissions guides at one time. The step-by-step procedure for each of these three test situation is given below.

In testing with the Wilputte Emissions Guides, the larry car proceeded to the coal bin in the usual fashion, was loaded with coal, and was then disengaged, moved to the charging port and the drop sleeve was lowered to the top of the oven. At this point, the charging cycle was halted, and two men installed the emissions guide on the pusher side drop sleeve and then proceeded to install the center emissions guide and the coke side emissions guide. A third man then detached the sensor ducts from the boom and attached them to the emissions guides. After coordinating the quenching sequence of the coke car, to assure that excess steam was not emitted during the charging, the Test Director communicated via citizen band radio with the camera operator, the manual sampling crew chief, the boom operator, and the instrumentation van operator; and when all parties were in a state of readiness, he or the lead man on the oven floor commenced a ten point countdown to instruct the larry man to start the charge. This countdown was broadcast to all parties associated with the test so that the exact starting time for the charge was known. The charging cycle was resumed at this point, and the oven was charged in the usual fashion. The larry man reported to the lead MITRE man on the oven floor when this charge was complete. This completion time was relayed via radio to all test personnel. After all coal had been deposited in the oven, the drop sleeve was raised for approximately one minute, after which time personnel removed all instrument housings from the emissions guides, and the guide handlers removed the guides so that the larry could move far enough for the lid man to replace the oven lids. The larry car was then released to continue its normal charging duties. Emissions guides, sensor ducts, booms, and cables were removed from the oven floor near the test area, so that they would not interfere with the normal operation of the J & L personnel. Instrument probes, wires, and tubes were visually inspected, and emissions guides were examined. Any clogging, burning, or warping was repaired by the boom man and guide handlers prior to the next test.

### Wilputte Stack Tests

For these tests, the larry car was again positioned over the charging ports, and the drop sleeve was lowered to the oven top. The charging cycle was halted, and a ladder was raised against the pusher side hopper. The sensor duct was then removed from the boom, carried up the ladder, and installed in the stack cap. The ladder was then moved to the center hopper and the sensor duct installed in the stack cap. In a similar fashion, the sensor duct was installed on the coke side stack cap. After all the sensors were in place, the countdown was initiated and charging proceeded as for the emissions guide tests. At the conclusion of the charge, the larry car was backed off the oven enough to allow replacing the lids. After the lids were replaced, the ladder was used to climb up on the larry to remove the sensor housings. After the larry had been released, all equipment was inspected and repaired in preparation for the next test.

The emissions guides for the AISI/EPA larry car consists of two parts: the rigid inner hood and flexible outer skirting. The inner hood was installed while the car was stored at the south end of the battery and the drop sleeve lowered to the floor. The outer hood was placed around the charging ports of the oven to be tested while the larry was off the floor. The larry car proceeded to the coal bin for coal after the inner hood had been attached and the drop sleeve raised. The car then proceeded to the oven to be tested, was positioned over the ports, and was then placed in a standby mode while testing equipment was attached. The outer flexible skirting was then attached to the inner rigid hood. The sensor ducts were then inserted into the openings in the inner hood and firmly attached so that raising and lowering the drop sleeves would not cause them to disengage. The countdown and charging then proceeded as for the previously described tests. At the completion of the charge, the larry car operator signaled the Test Director, who broadcasted this information to all parties involved. The emissions guides were constructed so as to remain in place while the lids were automatically replaced. After replacement of the lids, the outer skirt

was then removed, the larry car was returned to storage at the south end of the battery, and the inner hoods were removed.

After the last test of the day, the emissions guides were stored at the south end of the battery, well out of the way of normal activities, and the booms were securely tied back.

### Optical Measurements

At the beginning of each test day, initial setup of optical equipment was necessary. This involved the transport of the camera and camera control unit from its storage place in the office van to the balcony of the coal bin. During inclement weather, installation of a protective hood or shelter on the balcony was accomplished prior to movement of the equipment. Also, prior to transport of the camera, film was placed in the camera and camera mechanical operation was checked. The first step in initial assembly of the system was to attach the camera body to the camera mount on the balcony rail. Next, the lens was mounted on the camera and preliminary alignment of the camera was accomplished. Next, the camera control unit was set up and connecting cables were installed. The A.C. power supply for the camera and control was connected and power applied to the system. The camera was then checked on manual pulse operation and the presence of automatic exposure pulses was confirmed. Next, the correlation data display was synchronized with the data acquisition system by using the manual set button of the display and the intercommunications circuit to the van. After synchronization, the display was allowed to run continuously during the test day. Next, fine alignment and focusing of the camera was accomplished. This step required the illumination of the light bar which normally remained on night and day during a test week. The lens opening was set and the camera frame rate switch and shutter speed adjustment checked for proper settings.

The camera was then ready for the first test. The procedure described above required 30 minutes and was started at least 45 minutes prior to the expected test time to allow proper coordination and temperature stabilization of all equipments involved. At this point, a written



record of equipment configurations and settings was made for the test record. When all equipment had been checked and configuration data recorded, a cloth cover was placed over the camera and lens to protect it from particulates and moisture in the air.

While the larry car was moving into position for the charge, the camera cover was removed, and a final visual check of the equipment was made. Ten to twelve exposures would be taken during this time to obtain a clear background base reference for the test.

Camera operation was initiated at the conclusion of the countdown by the Test Director. Exposure continued for five minutes or until only four feet of film remained on the supply roll. At this point, the camera was stopped to provide a section of unexposed film on which exposure calibration could be performed.

After the test, the connecting wires to the camera were disconnected, and the lens was removed and stored in its carrying case. The camera was next removed from its mount and placed in its carrying case and transported to the van dark room where the film was removed and placed in a storage container along with one copy of the test configuration data sheet. The container was then placed under refrigeration to await shipment to the processor.

Next, the camera was inspected and cleaned, if necessary, in preparation for the next test. When another test was contemplated for the day, a fresh roll of film was threaded into the camera and the proper mechanical operation checked. If it was the last test of the day, the camera was placed in its storage container and left in the van until the next test day. After the camera had been checked, cleaned, and stored in the van after the last test, the camera control unit and associated components were removed from the balcony and stored in the van.

#### Manual Gas Sampling

Prior to the test-charging operation, manual sampling personnel set up the gaseous sampling system on the pipe bridge. The heated lines from the sampling trains and common duct to the heated manifold were connected

and preheated to operating temperature. All components of the system (pumps, lines, connectors, solenoid valves, and heaters) were tested to see that they were in operating condition.

Once pre-test activity was completed, the manifold line was connected to the common duct. The sequential sampling system was then manually turned on at the conclusion of the start countdown for charging.

Once turned on, the sequential sampling system was manually controlled by predetermined time intervals. The sequential sampling trains then collected grab samples at selected intervals. When the charge was complete, the manual sampling personnel stopped the sequential cycle as the last grab sample bag was filled.

### Particulate Sampling

Prior to the test, sampling nozzles and filter assemblies were mounted on the sensor ducts. The impinger trains, pumps, and regulators were mounted on the instrument carts and prepared for operation, and were set up along the coke side of the battery near the oven to be charged. The lines from the filter to the impingers were connected. All quick disconnect connectors were checked to see if they were in operating order. The lines were checked for leaks and/or breaks, as well as preheating to proper temperature.

As each emissions guide was brought into place and the sensor duct connected, the manual sampling team brought the assigned instrument cart up to the guide and connected the input heated lines of the impingers to the filter assembly. This procedure was followed for each emissions guide and was performed consecutively as the guides were set up.

After the test was completed, the lines between the impingers and the valves were disconnected. At the same time the line between the filter and impinger was disconnected from the sensor ducts. The instrument carts were then moved to the coke side of the oven. Once the emissions guides or stack sensors were removed, the filter, lines, and nozzles were cleaned.

## SECTION IV

### DATA HANDLING PROCEDURES

Data obtained during the field portion of the program were consolidated at MITRE headquarters, where it was subjected to critical quality control, corrected for travel time delays, and analyzed by computer methods. The results of the analyses were then presented in terms of pollutants emitted from the two larry cars being tested. This section describes the steps taken to develop these larry car emissions characteristics.

#### INPUT DATA

Test data were obtained from the Continuous Monitoring, Manual Sampling and Optics Programs. With minor exceptions, all data required extensive analysis at a location other than the test site before meaningful information could be derived. The original data, in its various forms, is discussed here.

#### Continuous Monitoring Data

The continuous monitoring data were obtained every second from the sensors during the tests and were recorded on magnetic tape and strip charts. The data consisted of gas analysis, flow sensor output, meteorological parameters and certain control and status information. To utilize the magnetic taped data, a program was prepared for reading the tape and printing the data in a form that could be read and evaluated. In the output of this program, the units defining the data are in voltage form. The print-out from this program was inspected to prove that the basic data, as produced by the sensors, was recorded on the tape accurately. The second-by-second variations in output voltages can be observed on the print-out, and the absence of data becomes readily apparent.

An example of one of these print-out sheets is shown in Figure 13, which shows data from Test 13, for the center Wilputte stack and guide. The first line on the print-out is a data-time group [year, month, day, hour (EST) and minute]. The second line consists of headings for the data



columns further down the page. The time is in seconds to the second decimal place, therefore, the first two digits are the only significant ones for this analysis. The third line is also a heading line for the columns, indicating channel number and voltage levels. The remaining lines are data channel numbers and their respective voltage levels, ranging from 0-1.638/volts, with the channel assignments as given in Table 3.

The channel assignments given in Table 3 were made before experience was gained on the oven and several significant field modifications were performed. Of most significance is the fact that a maximum of only three measurement points were monitored at one time as opposed to the nine as originally planned. Many temperature and pressure channels were, therefore, not used. A threshold system to start and stop gas flow was found to be impractical and, therefore, those channels were also not used. These channels continued to record on the data acquisition system, but the values shown on the print-outs are noise recorded on the unused channels, and were ignored in later work with the data.

Another source of continuous monitoring data was the strip charts. All gas analyzer data and all flow related data (pitot pressure and temperature) were recorded on strip charts as well as on magnetic tape. Examples of this data are given in Figures 14 and 15, which show outputs from four gas analyzers and four channels of output data for AP and T for Test 13. The print-outs described above were compared on a channel-by-channel basis with the strip charts and corrections made to reconcile any differences. In those cases where the data acquisition channel was determined to be faulty, the data were then taken from the strip charts and punched on IBM cards for insertion in the analyses program.

As a next step, the output of gas analyzers (located in the instrument van) was correlated with the thermocouple and pitot tube output (located on the oven floor). The time difference between these two readings is due to the travel time of the gas to pass through the tubing to the analyzers and the process time in the analyzers. (During the Field Test Program, sample gases were inserted in the lines on the oven and the time

TABLE 3

## DATA ACQUISITION SYSTEM - CHANNEL ASSIGNMENT

<u>Channel No.</u>	<u>Constituent</u>	<u>Channel No.</u>	<u>Constituent</u>
00	H <sub>2</sub> O	26	St.P
01	SO <sub>2</sub>	27	ΔP
02	H <sub>2</sub> S	28	T
03	NO	29	St.P
04	NO <sub>x</sub>	30	ΔP2
05	THC	31	T.2
06	H <sub>2</sub>	32	St.P
07	O <sub>2</sub>	33	ΔP3
08	CO	34	T3
09	CO <sub>2</sub>	35	St.P
10	Wind Speed	36	ΔP
11	Wind Direction	37	T
12	Relative Humidity	38	ΔP
13	Ambient Air Temp.	39	T
14	Barometric Pressure	40	ΔP
15	Volume Flow	41	ΔP
16	Threshold Sum	42	T6
17	" #1	43	T
18	" #2	44	ΔP
19	" #3	45	ΔP9
20	" #4	46	T
21	" #5	47	T
22	" #6	48	Manual Sampling Control
23	" #7	49	Threshold Status
24	" #8	53	Gas Temp. Input in Van
25	" #9		







at which the analyzer responded was noted. This was done for all gases analyzed, and the delay varied from 16 to 30 seconds.)

After the specific "gas channels" had been time-shifted, the data were then ready to be converted from voltages to engineering units. This was done by applying the manufacturers calibration data (which was periodically checked at the site) and observed effects, adding the proper units and reformatting the print-out page into groups of rows and printing increments of 15 seconds on a page. The actual corrections and calibration factors applied are not included in this report, but have been published separately as MITRE Working Paper WP-10445, "Conversion and Correction Factors for Coke Oven Emissions Data."

The resulting print-out for part of Test 13 is shown in Figure 16. Here the columns are better separated and identified for the 15 seconds of data. The first two columns along the left hand side are channel identifying number and identifying constituent. The first ten rows are either percent or parts per million of the indicated gas. The next twelve rows (four used in Figure 16) are allocated for pitot tube pressure and associated measurement duct temperatures in inches of water and degrees Fahrenheit; actual channel assignment for each measurement point is also given in MITRE WP-10445, "Conversion and Correction Factors for Coke Oven Emissions Data." The next four lines (Ch. 10 through 14) are meteorological data: wind speed in miles per hour, wind direction in degrees from true north, ambient temperature in Fahrenheit and barometric pressure in inches of mercury. Thresholds 1 and 2 (Ch. 17 and 18) were not used. Channels 19 through 24 indicate points on the larry car that were being monitored; Emissions Guide (EG) on the Pusher Side (P), Middle (M) and Coke Side (C), and Stacks (ST) on the Pusher, Middle and Coke Sides (P, M, C). Channel 48 indicates when manual gas samples were being drawn.

The magnetic tape that produced this final print-out was then used as the starting point for the final data analysis. A complete listing of the data was sent to the Environmental Protection Agency, Office of Research and Development, National Environmental Research Center, Control Systems Laboratory.

**CVEN 3-15**

POINTS MONITORED

## #2 WILPUTTE STACK & GUIDE

REMARKS

33	.01" WC	0.140	0.129	0.089	0.065	0.081	0.066	0.065	0.065	0.084	0.129	0.072	0.046	-0.275	-0.330	-0.025
34	DEG F	59	58	100	55	56	99	58	59	99	98	99	55	55	98	95
45	.01" WC	0.700	0.700	0.700	0.700	0.670	0.670	0.670	0.670	0.560	0.560	0.560	0.560	0.450	0.450	0.450
42	DEG F	168	166	164	166	162	160	158	158	154	154	152	152	152	151	148

55

[illegible]

**FIGURE 16**  
**FINAL DATA PRINTOUT IN ENGINEERING UNITS**

100

### Manual Sampling Data

The manual samples of gas and particulate were obtained by Midwest Research Institute (MRI) under separate contract to the Environmental Protection Agency. The samples were transported to MRI's laboratory in Kansas City for final analysis, and the results were transmitted to MITRE for incorporation in the overall data study of the coke oven emissions. Particulate samples were also collected as part of the manual sampling effort, and the analyses of these samples are also incorporated in the overall study.

### Gas Samples

Results of the gas analysis were in the form of tables. Analytical results for pyridine,  $\text{SO}_2$ , cyanide, phenol,  $\text{NH}_3$ ,  $\text{NO}_x$ , and  $\text{H}_2\text{S}$  are listed on computer print-out charts. The results of the analysis for  $\text{O}_2$ ,  $\text{N}_2$ ,  $\text{CO}$ ,  $\text{CO}_2$ ,  $\text{CH}_4$ ,  $\text{H}_2$  and total hydrocarbons are listed on a hand-printed table. These print-outs and tables are provided in Appendix C of this report.

### Particulate Samples

Samples obtained at the Emissions Guides and the Stacks by MRI were analyzed at their laboratory. The data were reported in the form of computer print-outs, copies of laboratory notebook sheets and hand written mass loading tables. This data is included in Appendix B.

Particulate samples obtained by the MITRE carrousel sampler were analyzed at the MITRE Washington operations facility. This sampler, analytical procedures and a complete presentation of data has been published as MITRE Working Paper WP-10480, "Direct Impaction Particulate Collecting Carrousel." The form of these results is a series of tables and size distribution curves, which are provided in Appendix E.

### Coal Samples

Proximate analyses were performed on the four coal samples obtained. This work was done by Industrial Testing Laboratory of Kansas City under subcontract to MRI. Their findings are reported as "Certificate of Coal

Analysis", tables listing the constituents measured, and are enclosed in Appendix B.

The ultimate analysis, elemental analysis and size determination were presented as tables and are also enclosed in this appendix.

#### Optical Data

The record of light transmission from the light bar passing through the emission plume to the detector (camera) was recorded on the photographic film in the form of varying light bar image densities. The exposed film was sent to a photographic processing laboratory where a sensitometric exposure was placed on an unexposed portion of the film, and the film was developed. The sensitometric exposure provides a basis for associating an observed light bar image optical density with a value of light intensity producing the image exposure. Using the values thus obtained, it is possible to determine the value of light obscuration. This information was then used to estimate the mass loading values of the observed emission plume.

The data on optical densities of the light bar images was provided in two forms by the film processing facility. The microdensitometer electronically digitized the measured optical density value for a specific point (area of 50 by 200 microns) and placed this value in a binary number format on a magnetic tape. The microdensitometer also simultaneously produced a continuous strip chart record of measured optical density.

As stated previously, the data on the tape was contained in the form of eight place binary numbers ranging from 0 to 255. One horizontal scan across the light bar image produced 539 individual binary density records corresponding to 539 points on the scanned image. A second pass across the black surface area produced 539 more density records which correspond directly with the light bar records for purposes of comparison and mass loading calculations. A third scan containing 539 records was made for some frames as a part of an experiment to investigate the Mie scattering effect. This scan was across a short section of light source having color filters placed on the diffusion lens to approximate

monochromatic light. This unit was located on top of and at one end of the primary light bar structure.

The data tape, generated on a manually controlled data logger, was read as a binary number by a standard nine-track computer tape drive, but was not directly compatible with computational or display portions of the data processing program. Because of the format of the tape, records to be processed were combined with header information obtained from the hand-written tape log supplied with each raw data tape. The header information for each individual scan of 539 points consisted of a sequence number, test number, clock time for frame, and type of frame. This information was combined on a separate program data input tape for further processing.

A second data input consisted of two place tables in punch-card form. These tables provided necessary correlation for conversion from density values to relative exposure values (light intensity values, assuming a constant exposure time) for a particulate processing run. The table was generated by the processing laboratory using 21 density values obtained from the sensitometric exposure wedge. A computer program fitted a curve to these 21 points and produced the 300 evenly spaced (in light intensity) values of optical density in the range of the sensitometric exposure. A second table of 300 corresponding exposure values was calculated by the program from the density information. The program used to generate the exposure values is described in detail in MITRE Working Paper 1045, "Correction and Conversion Factors from Coke Oven Emissions Data."

#### MATHEMATICAL TREATMENT OF DATA

The processes of converting the data that was described above into meaningful terms such as pounds of pollutant emitted, mass loading, etc., are generally straightforward. An effort was made to perform these functions with automatic data processing hardware, although this project was a one-time effort and programming requirements are out of proportion to the amount of data processed. This was intentional so that the analytical routines developed for this project could be made available to anyone with a future similar requirement.

### Concentration and Volume Flow Variability

The pattern of emissions produced by a coke oven charging operation differs radically from a source which could be monitored by standard manual sampling techniques. As a result, real time information is required for data reduction procedures. For the brief period of time during which the charging operation lasts, differential pressure ( $\Delta P$ ), temperature (T), and constituent concentration vary erratically. Values can change from 0 to .1" H<sub>2</sub>O  $\Delta P$ , 100° to 1000°F temperature, or zero to full scale concentration in a matter of seconds. Figures 14 and 15 are strip charts showing some typical fluctuations in  $\Delta P$  and concentrations. Figure 17 shows flow with respect to time and charging procedures for a typical test.

These figures demonstrate the importance of a continuous monitoring system for measuring the type of emission fluctuation that results from a charging operation. It is obvious from Figure 17 that a manual measurement would be too insensitive for the emission guide flows and too slow for the rapid variations in the stack emissions to produce an accurate volume of emissions. An example of the effects of using real time concentration values as opposed to an average concentration value for calculating emission volume can be shown in Test 21 (see Appendix C for data). A volume of THC from Test 21 was 33 scf as calculated using real time values while the use of average concentrations and flow produced 19.2 scf (~40% error).

### Volume Flow Parameters

A program to determine volume flow and velocity of coke oven emissions was the first of the data reduction programs implemented. Both the gaseous and particulate systems depend on velocity and volume flow for final calculations of mass and/or volume.

The volume flow program uses the equation:

$$F_i(t) = (174) \chi_p A_i \sqrt{\frac{\Delta P_i(t) [T_i(t) + 460] (29.92)}{P_i(t) \cdot G_k}} \quad (2)$$

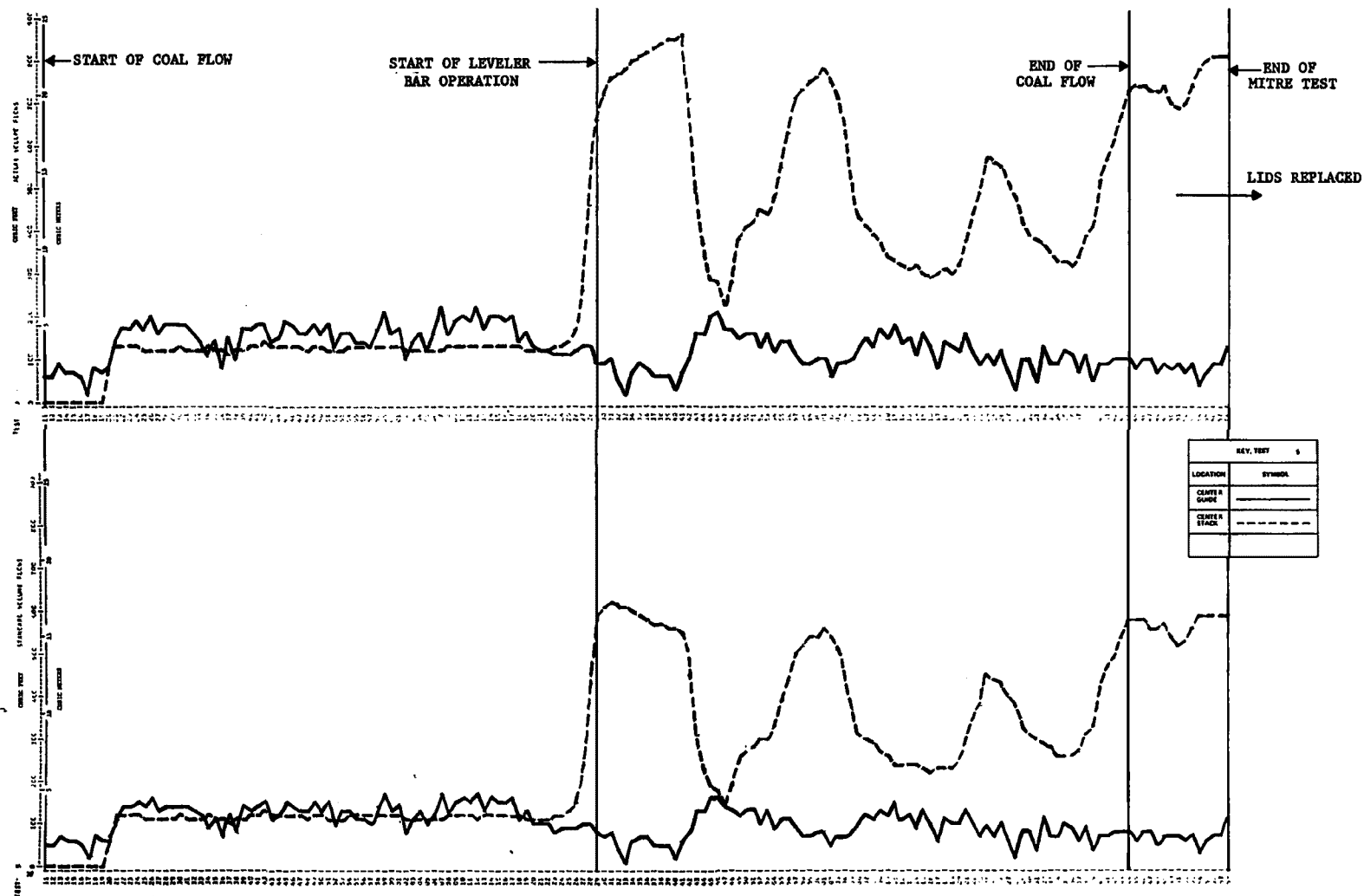


FIGURE 17  
TYPICAL VOLUME FLOW GRAPH VERSUS CHARGING PROCEDURES

to determine the volume flow,  $F_i(t)$ , at location  $i$  for a given test. Constants and variables required in this equation are listed in Table 4. Equation 2 was used to determine the in-stack real time volume flow (CFM) at each emission point and these values were then stored for use with the particulate sampling program.

A second real time volume flow adjusted to standard conditions (SCFM),  $F_i'(t)$ , (70°F @ 1 atm) was required for use with the continuous gas and manual gas calculations where:

$$F_i'(t) = \frac{F_i(t) P_i(t)}{[T_i(t) + 460]^{\circ}R} \cdot \frac{530^{\circ}R}{29.92'' \text{ Hg}} \quad (3)$$

Then the total volume (CF) emitted at location  $i$ ,  $E_{Ti}$ , under stack conditions is given by:

$$E_{Ti} = \sum_{t=t_1}^{\tau} \Delta t [F_i(t)] \quad (4)$$

and under standard conditions (SCF):

$$E_{Ti}' = \sum_{t=t_1}^{\tau} \Delta t [F_i'(t)] \quad (5)$$

The real time volume flow in standard and stack conditions  $F_i'(t)$  and  $F_i(t)$  was stored on magnetic tape, but the output format was in graphic form only. The total volume values  $E_i$  and  $E_i'$ , however, were both stored and output numerically. The average temperature ( $F^{\circ}$ ):

$$T_i = \sum_{t=t_1}^{\tau} T_i(t) / \tau \quad (6)$$

was also computed and printed during this operation, as well as the high and low temperatures.



TABLE 4

VARIABLES USED IN VOLUME FLOW

$\chi_p$	$\equiv$	Pitot tube factor, a value from .95 to .7
$A_i$	$\equiv$	.69 ft <sup>2</sup> for Wilputte Emissions Guide .85 ft <sup>2</sup> for Stacks and AISI/EPA Guides
$P_i(t)$	$\equiv$	Static pressure - Channel 14 (inches Hg)
$G_k$	$\equiv$	Specific gravity of the gas relative to air
$\tau$	$\equiv$	Total time of test, in most cases, will be described by Channel 48 (in seconds)
$t_1$	$\equiv$	Start of test, Channel 48 will read on (1 volt)
$\Delta P_i(t)$	$\equiv$	Differential pressure at time t and location i (inches H <sub>2</sub> O)
$T_i(t)$	$\equiv$	Temperature at time t location i (F°)
$\Delta t$	$\equiv$	Time interval (seconds)

### Continuous Gas Monitoring System Parameters

The gaseous concentrations are given for standard conditions and the concentrations,  $C_j(t)$ , of the gas constituents are assumed to include %  $H_2O$  in total volume. Gases measured after drying ( $H_2$ ,  $O_2$ ,  $CO$ ,  $CO_2$ : channels 06 to 09, respectively) were corrected to wet gas concentrations by:

$$C_j(t) = C_{j\text{dry}}(t) \left\{ \frac{100 - C_1(t)}{100} \right\} \quad (7)$$

where,  $C_{j\text{dry}}(t)$  = volume % in dry gas as measured by respective instruments.

To determine the volume flow (SCFM) of each gas constituent,  $j$ , that is measured in the stack under standard conditions (70°F, 1 atm) the equation:

$$\dot{E}_j(t) = C_j(t) \left\{ \sum_i^n F_i'(t) \right\} \quad (8)$$

was used for a preliminary calculation. A corrected constituent volume  $E_j'(t)$  was calculated by:

$$\dot{E}_j'(t) = C_j'(t) \left\{ \sum_i^n F_i'(t) \right\} \quad (9)$$

$C_j'(t)$  is a corrected concentration (% volume) of  $j$  to account for the sampling of ambient air at points where  $F_i'(t) < F_T$  and

$$C_j'(t) = \frac{C_j(t) - \gamma C_{Aj}}{1 - \gamma} \quad (10)$$

where

$C_{Aj} \equiv$  Concentration of  $j$  at ambient

$$\gamma \equiv \frac{\text{Number of Locations: } F_1(t) < F_T}{\text{Number of Locations}} .$$

$F_T$  is a constant which was determined after the first run of the volume flow data was analyzed.

Equation 9 (correction for ambient dilution) was only used for channels:

SO <sub>2</sub> - 01	THC - 05
H <sub>2</sub> S - 02	CO - 08
NO - 03	CO <sub>2</sub> - 09
NO <sub>x</sub> - 04	

Then the total volume (SCF) of constituent  $j$  measured directly was:

$$E_j = \sum_{t=t_1}^{\tau} \Delta t [\dot{E}_j(t)] \quad (11)$$

and the total volume corrected for continuous sampling is

$$E_j' = \sum_{t=t_1}^{\tau} \Delta t [\dot{E}_j'(t)] . \quad (12)$$

The real time volume per unit time  $[\dot{E}_j(t)$  and  $\dot{E}_j'(t)]$  for each constituent  $j$  was displayed in graphic form. The total volumes in correct and uncorrected form ( $E_j'$  and  $E_j$ ) was listed numerically. The average concentrations  $C_j(t)$  and  $C_j'(t)$  were computed by

$$\bar{C}_j = \sum_{t=t_1}^{\tau} C_j(t) / \tau \quad (13)$$

and

$$\bar{C}_j' = \sum_{t=t_1}^{\tau} C_j(t)/\tau \quad (14)$$

and output numerically. Table 5 indicates the channel-to-variable relation, and lists other variables necessary to complete the algorithm. Data reduction of the manual gas data was similar to the continuous data. Equations 8 through 12 were used, although the gas data were input on IBM cards. The variable  $C_j(t)$  is a concentration measured for a sample integrated over 30 to 60 seconds of test time.

Solutions to Equations 2 and 3 were output in a graphic form, and are displayed in Appendix B. The total volume under stack conditions,  $E_{Ti}$  (Equation 4), and the high, low, and average temperature for each location  $i$  of each test are displayed in the same appendices, along with the total volume emitted relative to standard conditions,  $E'_{Ti}$  (Equation 5).

Data produced by Equations 8 through 19 were used in the continuous gas analysis program. The resultant output of this program is provided in Appendix C.

Concentration Calculation - The calculations for quantification of the gas concentration are shown below. Briefly, the volume percent of each gas was calculated, as follows: the volume of the unknown gas was calculated from the instrument response in peak area or height and the response ratio of the instrument per volume of each standard gas. The volume of unknown gas was divided by the total volume of sample introduced into the chromatograph after both were corrected to atmospheric pressure. The response ratios were calculated from at least four different levels of each standard gas.

- (1) Volume of standard gas calculated to atmospheric pressure =

$$V_{sa} = (5) (P_s/P_a) (s), \text{ where}$$

$V_{sa}$  = Volume of standard gas at atm. pressure;

5 = Gas sample loop volume;

TABLE 5

## VARIABLES FOR GAS ANALYSIS

$F_i'(t)$  - from volume flow program (SCFM)

$C_1(t)$  - %  $H_2O$  - 00

$C_2(t)$  - ppm  $SO_2$  - 01

$C_3(t)$  - ppm  $H_2S$  - 02

$C_4(t)$  - ppm  $NO$  - 03

$C_j(t) \equiv C_5(t)$  - ppm  $NO_x$  - 04

$C_6(t)$  - %  $THC$  - 05

$C_7(t)$  - %  $H_2$  - 06

$C_8(t)$  - %  $O_2$  - 07

$C_9(t)$  - %  $CO$  - 08

$C_{10}(t)$  - %  $CO_2$  - 09

$\gamma \equiv \frac{\text{Number of } F_i'(t) < F_T}{\text{Number of Locations Monitored}}$

$F_T \equiv$  A constant to be determined after volume flow data has been reduced

$P_s$  = Standard pressure, mmHg;  
 $P_a$  = Atmospheric pressure, mmHg;  
 $S$  = Volume % of gas in standard.

- (2) Ratio of standard gas at atmospheric pressure per instrument response unit =

$R = V_{sa}/IRU_s$ , where

$R$  = Ratio, volume of standard gas per instrument response unit;

$IRU_s$  = Instrument response units (either peak area or height) for standard gas.

- (3) Volume of unknown gas at atmospheric pressure =

$V_{ua} = (R) (IRU_u)$ , where

$V_{ua}$  = Volume of unknown gas at atmospheric pressure;

$IRU_u$  = Instrument response units for unknown gas.

- (4) Total sample volume at atmospheric pressure =

$V_{ts} = (5) (P_v/P_a)$ , where

$V_{ts}$  = Total sample volume;

$P_u$  = Pressure of sample, mmHg.

- (5) Concentration of unknown gas, volume percent =

Volume percent of unknown =  $(V_{ua}/V_{ts}) 100$ .

Size Analyses - The primary methods used to determine a particle size distribution consisted of a combination of Andersen size distribution and optical sizing performed in samples taken from the MITRE Carrousel.

The Andersen samples were taken in the measurement ducts. At the completion of a test, the Andersen sampler was hand carried to the field laboratory and allowed to cool down to a stable temperature. The sampler was then disassembled. The plates and rings were then weighed on site. The sampler was cleaned and readied for the next test and the washings were stored and labeled for later reference.

The data from the field weighings were later analyzed at the MRI Kansas City facilities. Standard computer programs were used by MRI to produce size distribution information in ranges from about 20  $\mu$  to .5  $\mu$  and information on gross weight percent of the sample above and below these boundaries. The data are listed in Appendix C. They were then combined and reduced with MITRE data as described in another section. The original Andersen distribution was calculated assuming a 1 gm/cc density; however, the final distribution given was calculated assuming a 1.2 gm/cc density.

Samples collected by the MITRE Carrousel were analyzed by optical techniques. Representative slides were selected from each test and analyzed for particle size distribution and number density. The microscope reticle was calibrated with 39 $\mu$ m and 28 $\mu$ m pollen. Particles were grouped in one of seven size ranges using the calibrated reticle with the "Ferets diameter" method. The ranges are:

1 - 4.6 to 9.2 $\mu$ m	5 - 73.6 to 147.2 $\mu$ m
2 - 9.2 to 18.4 $\mu$ m	6 - 147.2 to 230 $\mu$ m
3 - 18.4 to 36.8 $\mu$ m	7 - 230 $\mu$ m .

The particles were sized optically with a B & L microscope at 300, and 150 powers. The magnified samples were displayed and counted on a closed circuit television system coupled optically to the microscope. Through the use of a polaroid camera attachment, pictures were periodically taken.

A particle count of about 500 (termed a "batch")\* was required at each of the powers. Areas scanned (fields-of-view) were selected at random to produce a representative sample, until the batch was complete. Each

---

\* Lodge, J. P. Production of Controlled Test Atmospheres In: Air Production, Volume II, Stern, A. C. (ed.) New York and London, Academic Press, 1968. p. 465-481

slide to be analyzed was chosen such that a field-of-view had less than 200 particles\*\* in the countable ranges for any given power. The areas of field-of-view at 150 power and 300 power are  $965 \mu\text{m}^2$  and  $241 \mu\text{m}^2$ , respectively.

A batch counted in the 300 power range includes particles between  $4.6 \mu\text{m}$  and  $147.2 \mu\text{m}$  (excluding ranges 6 and 7). The 150 power batches include particles greater than  $9.2 \mu\text{m}$  (excludes range 1). To combine the results for 300 power and 150 power batches sized for the same test, the number of particles in the omitted ranges were calculated from the ratios of the other batches. For example, the number of particles in range 1 of batch 2 would be calculated as the ratio:

$$N_{12} = \frac{N_{11} \cdot \sum_{i=2} N_{i2}}{\sum_{i=2} N_{i1}} \quad (15)$$

$N_{12}$  = the number of particles in (unmeasured) range 1 of batch 2,

$N_{11}$  = the number of particles in range 1 of batch 1,

$N_{i2}$  = the number of particles in range i of batch 2,

$N_{i1}$  = the number of particles in range i of batch 1.

The number of fields-of-view completing a batch were counted and recorded and the area calculated. The density of the slide was then calculated as a ratio between the number of particles counted to area scanned. The location of each field-of-view was recorded to the nearest tenth of a mm using the movable stage position scale. All slides were labeled and stored for later access.

---

\*\* Silverman, L., Billings, C. E., First, M. W. Particle Size Analysis in Industrial Hygiene. New York and London, Academic Press, 1971. p. 106-107



The theoretical collection efficiency of the microscope slides was investigated to determine system biases relative to particle size and emission velocity.

The collection efficiency corrections were applied to the respective size ranges. Though the optical sizing of the coke oven particles included ranges from 4.6  $\mu\text{m}$  and larger, the data analyzed will include the size ranges where the particles were larger than 18.4  $\mu\text{m}$ . Ranges 1 and 2 were excluded from final computations because:

- a) it was found that the collection efficiency drops off rapidly below 20  $\mu\text{m}$ ;
- b) the Andersen sampler adequately sized particles up to 20  $\mu\text{m}$ ; and
- c) it was difficult to confidently identify the smaller particles due to foreign materials and grease anomalies on the slides.

Each slide was also analyzed for particles larger than 1000  $\mu$  with a ten power magnifier. The number of particles larger than 1000  $\mu$  was counted on each slide and the density for particles >1000  $\mu$  was calculated and recorded.

All data obtained from optical sizing are presented in Appendix E which includes:

- a) Particulate counts for each test,
- b) Particle density for each slide for particles larger than 18  $\mu$ ,
- c) Particle density of particles larger than 1000  $\mu$ ,
- d) Calculated percentage of particles versus size range,
- e) Cumulative number and weight percents versus size range.

Secondary methods of size analyses are described in Appendices B and E.

The methods included:

Brink

Sieve and Sedigraph

Coulter counter

Optical of Andersen and cyclone cateles.

Mass Loading - Due to oven constraints and the unique features of emissions produced during a charging operation, particulate sampling was done anisokinetically, where the sampling velocity was held constant, independent of stack velocity. To bracket the error created by anisokinetic sampling and determine theoretical isokinetic values, modified procedures explained in detail in MTR-6288, "Manual Sampling System, Coke Oven Emissions Test Program," were used and are summarized here.

The theoretical isokinetic mass,  $EM_i$ , can be calculated by the algorithm:

$$EM_i = \frac{A_i}{a_i} M_i \sum_{l=1}^n Q_{il} \cdot (\%W_l) \quad (16)$$

where

$M_l$  = mass of sample collected at location  $i$ ,

$\%W_l$  = the weight percent of total mass at a given range,

$A_i$  = area of stack at duct  $i$ ,

$a_i$  = area of sampling nozzle at duct  $i$ ,

$Q_{il}$  = anisokinetic correction factor for particle size range  $l$  at location  $i$  from a given test.

The correction factor is found as a function of particle size, sampling velocity and stack velocity and is calculated from:

$$Q_{il} = \sum_{t=1}^{\tau} Q_{il}(t) / T \quad (17)$$

and

$$Q_{il}(t) = \frac{1}{[1 - \alpha_{il}(t)] V_{si} A_i / F_i(t) + \alpha_{il}(t)} \quad \text{for } F_i(t) \neq 0. \quad (18)$$

The inertial parameter  $\alpha_{i1}(t)$  can be determined from:

$$\alpha_{i1}(t) = \frac{1 - \exp[-4.5/\lambda_{i1}(t)]}{4.5} \left( \lambda_{i1}(t) \right) \quad (19)$$

where

$$\lambda_{i1}(t) = (.508)F_i(t)\gamma_1/(A_i g) \quad (20)$$

and

$A_i$  = Area of location i    .69 ft<sup>2</sup> for Wilputte Emissions Guide  
    .85 ft<sup>2</sup> for stacks and AISI/EPA Guide

$$a_i = \text{Area of sampling nozzle}$$

$\%W_{i1}$  = Weight percent of mass in size range  $i$  at location  $i$ . The values and ranges were calculated beforehand from Andersen and Optical sizings and assumed constants for all tests. Volume flow data are needed to determine  $\%W_{i1}$ .

$\tau$  = Total time of test measured by Channel 48

$V_{si}$  = Sampling velocity to be computed for each sampling location for each test

$F_1(t)$  = Volume flow at stack conditions computed and stored during volume flow calculations.  $\text{ft}^3/\text{minute}$

$g$  = Acceleration due to gravity.  $980 \text{ cm/second}^2$

$\gamma_1$  = Average free fall velocity of particles in size range 1 (in cm/second)

Ideally, when employing this sampling method in the stack velocity or volume flow,  $F_i(A)$  should never go to zero. Correction factors for  $F_i(t) = 0$  are inadequate. However, the condition did exist on a number of tests and was handled by setting  $Q_{i1} = 0$  for small particle ranges where  $F_i(t) = 0$  and  $Q_{i1} = 1$  for the larger particle ranges. The rationale behind this concept is simply small particles (those which act as gases) remain in the stack after the flow has gone to zero and are

sampled. Hence, they mistakenly add some amount of weight to the sample. The larger particles fell out rapidly and similarly are not sampled. The amount of mass produced by the large particles is correctly zero for  $F_i(t) = 0$  implying  $Q_{i1}(t) = 1$ .

The particle mass distribution is described by  $\%W_1$  where  $1 = 1, 2, \dots, 13$  (number of size ranges). It is calculated as a function of anisokinetic weight percents found for each test duct  $i$  and is found by:

$$\%W_{i1} = \frac{\%W_{i1} Q_{i1}}{\sum_{i=1}^{13} \%W_{i1} Q_{i1}} \quad (21)$$

and the average weight percent is ranged over all tests,  $n$ , for range  $1$  is:

$$\%W_1 = \sum_{i=1}^n \%W_{i1} / n \quad (22)$$

These values for weight percent were calculated and used for anisokinetic corrections, as well as to determine a representative mathematical frequency distribution model.

#### Optical Monitoring System Parameters

Data analysis for the optical monitoring system was divided into three phases. The first phase consisted of the necessary operations to convert data in the form of a photographic image to information about the source light transmission characteristics of discrete areas of the emission plume. The second phase included the calculation of mass loading estimations from the transmission values for discrete areas and the combination of these estimations to provide mass loading data across the entire light source image at some instant in time. The third phase involved the estimation of total mass emitted over time by multiplying the instantaneous mass loading estimations by the velocity at which the emission plume is passing upward across the light source. The calculations and quantities involved in each phase will be discussed below.

Quantitative data was obtained from the photographic record through the use of a microdensitometer having a digitized output. The machine measured the optical density of discrete areas on the source film image and produced a record on magnetic tape in the form of an eight-place binary number. The 256 integral values possible in an eight-place binary number are uniformly distributed between two bounding optical density values as part of the initial adjustment of the microdensitometer. The bounding values for the optical density range were selected so that the lower value fell below the observed optical density for the photographic image of the black portion of the light source in the absence of emissions. The upper bound of optical density was chosen so that it was above the maximum observed photographic image density of the lighted portion of the light source in the absence of emissions. Further, the photographic film was processed so that a close to linear relationship existed between light source image optical density values and the log exposure values which produced them.

The relationship between the exposure values was established for each film roll through a 21-step density versus exposure tablet placed on each roll prior to processing. Each step associated a relative exposure value with a resulting optical density. From the 21 tablet steps sequentially spaced at .15 log exposure units apart, a vendor-supplied computer program fitted a cubic curve of density versus exposure values. The program then continued to assign individual relative exposure values to each of the binary density values between 0 and 255 as represented on the magnetic tape.

The output values of this program were provided in the form of a punch card deck and the magnetic tape. The exposure values were positioned in the table matrix so that their sequential position number (address) corresponded to the binary number value associated with that particular density. Thus, using the binary value as an address in the matrix, the relative exposure value was found as the numerical contents of that address.

Transmittance "T" is defined as  $f/f_0$ , where  $f$  and  $f_0$  are the values for light intensity incident upon the system detector in the presence and absence of a plume, respectively. The relative exposure values are a product of light intensity and time:

$$EV = \text{Meter Candle Seconds.}$$

In this system, distance in meters, which determine apparent intensity and exposure time in seconds, was held constant. Thus, a change in EV can be considered to be a change in luminance (candles) caused by a change in plume transmission characteristics.

In order to facilitate the calculation of "T" from exposure values, a lower exposure value associated with zero source light was established. The density readings of the black area in the absence of emissions was taken to represent this value. This condition existed on the designated "base frame" of each test. There were, however, slight differences in individual density values in the scan record of this area. These could be caused by machine inconsistencies, anomalies in the photographic films, or small quantities of emission somewhere along the line of sight causing a plume-air light return. In order to obtain a representative zero value, all measured densities across the unobscured black portion of the bar were averaged as follows:

$$D^0 = \frac{\sum_{i=1}^P D^0_{1i}}{P} \quad (23)$$

where  $D^0_{1i}$  was the binary density number for a point; and  $P$  was the total number of points scanned across the black area on the base frame.

This value was established for each roll of film or test run. This density value is assumed to be the image density value of the light source if transmission were to go to zero and there were no other scattered light, which appeared to come from the light source position on the frame.

This density value was then located in the density versus exposure table and a corresponding exposure value was determined. This exposure value was then substituted in the equation for determination of the reciprocal of transmittance:

$$\frac{1}{T} = \frac{f_{oa} - f_{ob}}{f_a - f_b} \quad (24)$$

where  $f_{ob}$  is always the exposure value corresponding to  $\bar{D}_o$ ,  $f_{oa}$  is the exposure value corresponding to the unencumbered point density of the light source and  $f_a$  and  $f_b$  are equal to the exposure values corresponding to the point image density of adjacent light source and black areas respectively, in the presence of the emission plume.

The exposure values  $f_{o2}$ ,  $f_a$ , and  $f_b$  were obtained by using the binary optical density value of each record on the magnetic tape as an address in the exposure value matrix table. The contents of that address is the corresponding relative exposure value for direct substitution in the formula above.

As the reciprocal of transmittance was found for each point in the scan, the natural log of that value was determined and added to an accumulation. When transmission calculations on all the 539 points in a frame scan were completed, the contents of the log 1/T accumulator was multiplied by the constants representing particulate characteristics.

The equation for the calculation of the mass emission rate for each film data frame is:

$$M = \frac{4}{3} \phi K \Delta L \sum_{i=k}^P \ln \left[ \frac{f_{oA}(1_i) - f_{oB}(1_i)}{f_A(1_i) - f_B(1_i)} \right] \quad (25)$$

where  $\phi$  represents the mass density of the particles,  $K$  is defined as the specific particulate volume divided by the light extinction coefficient ratio and  $\Delta L$  is the lateral dimension of a small area of the light source (termed a point) which is represented by each of the measured

density values (539) across the light source. The values of  $1/T$  were calculated for each of the measured density points across the light source and summed as  $\ln(1/T)$  as described above.

The values of  $\phi$  directly determines the calculated mass volume from particulate volume determined by the opacity measurement. If the particles collected were made up of a single material or compound, the value of  $\phi$  would be simply the mass density of that single material. The particle population collected on the coke oven was not, however, composed of a single material. An analysis of particulate samples collected in particle sizing equipment shows that several different materials were present in the population. There is, however, a predominance of two materials. They are carbon (as it occurs in coal) and heavy hydrocarbons or coal tars. A further analysis shows that the larger particles are composed mostly of carbon with some tar causing considerable particle agglomeration. The smaller particle size ranges, on the other hand, are composed primarily of tar globules which are probably condensed from the existing gas as it reaches the ambient air. The particulate size distribution from the particle sizing equipment further explains the apportionment of the material between the two ranges. The combined weight of the stages shows that 53.4% of the total average sample mass is contained between  $9.4 \mu$  and  $\sim 1000 \mu$ , while 46.6% is contained in the ranges  $6.4 \mu$  and below. Using this information, a representative particle mass density value was estimated. The value used in mass rate calculations for the optical system is  $1.2 \text{ gm/cm}^3$ . It is quite simple, however, to determine mass rates for other assumed values of density since this factor is purely multiplicative in the mass rate equation.

The determination of an appropriate value for the constant  $K$  is complicated by the complex particle material makeup and the distribution of particle size. The value of  $K$  is mathematically evaluated using the equation:



$$K = \frac{4}{3} \frac{\int_{r_1}^{r_2} \exp - \left[ \frac{\ln^2 r/r_{gn}}{2\ln^2 \sigma_g} \right] dr}{\int_{r_1}^{r_2} r Q_E(d,m) \exp - \left[ \frac{\ln^2 r/r_{gn}}{2\ln^2 \sigma_g} \right] dr} \quad (26)$$

in which  $r$  is the radius of a particle,  $r_{gn}$  is the simple geometric mass mean radius and  $\sigma_g$  the standard deviation of a lognormal particle size distribution, and  $Q_E$  is the extinction coefficient assigned or calculated for size distribution. It was shown by Conner and Hodkinson\* and Pilat and Ensor\*\* that  $Q_E$  can reasonably be set equal to 2 for large particles (larger than 2-4  $\mu$ ) without serious error in calculations. This approach cannot, however, be used for small particles since their  $Q_E$  value is much more strongly influenced by their material makeup, their complex index of refraction, and the wavelength of the light source which they attenuate.

Measurements and analysis of the particle size distribution have shown that the size frequency curve is bi-populate in nature. It has also been demonstrated through graphic and chi-square tests that each half of the combined curve generally fits a lognormal distribution.

The upper portion of the combined curve representing the larger particles has a geometric mass mean radius of  $\sim 100 \mu$ . This portion of the particle population can be expected to have a value of  $Q_E$  approximately equal to two. The lower portion of the combined curve, however, has a geometric mass mean radius of  $.85 \mu$ . With this mean radius, it is improper to assign a value of  $z$  for  $Q_E$  of these particles.

---

\* Conner, W. D., Hodkinson, J. R. Optical Properties and Visual Effects of Smoke Stack Plumes. U. S. Department of Health, Education, and Welfare, Cincinnati, Ohio. Publication #PB 174-705. 1967.

\*\* Ensor, D. S., Pilat, M. J. Calculation of Smoke Plume Opacity from Particulate Air Pollutant Properties. Journal of Air Pollutant Control Association. Volume 21, Number 8, August 1971.

In order to develop a K value for the total particle population, K was determined for each of the two particulate mean values and the observed variance about that mean. The upper portion around 100  $\mu$  was assumed to be made up primarily of carbon with an index of refraction of 1.96-0.66 i. The lower portion of the population was assumed to be primarily coal tar with an estimated value for the complex index of refraction of  $1.54 - 1.9 \times 10^{-4} i$ . The values of K found for each half were combined using the particle number distribution as a weighing factor.

Particle number distribution showed 4% of the total particles to be in the upper distribution, while 46% was contained in the lower portion. The K value for the upper portion was found to be 28, while the lower K value was estimated to be .22. The combining of these two values using the associated population percent as a weighing factor yields a combined value of 1.33 for K. This value was used in the mass rate calculations. Since this factor is purely multiplicative, mass rate for other K values can be easily estimated.

The last constant,  $\Delta L$ , is the lateral width of a single sample point. The microdensitometer was set up to take 539 equal width samples across the 48' light source. The equation for  $\Delta L$  is therefore:

$$\Delta L = \frac{48' \times .3048 \text{ M/ft}}{539} = .027 \text{ M.} \quad (27)$$

This is the value for  $\Delta L$  used in the mass rate calculations across the horizontal bar. The same  $\Delta L$  can be used for rate calculations involving the vertical "wing" light sources.

In order to calculate a total mass emitted over any period of time during a charge, the instantaneous value of mass emission rate is multiplied by the plume vertical velocity or plume rise velocity. In the original system concept, the value or values for plume velocity was to be determined using motion pictures of the actual plumes. This approach was modified slightly to utilize the system sequence camera instead of a motion picture camera.

In order to measure the vertical progress of the plume, an illustrated scale was constructed and placed on one of the equipment towers approximately 30 feet above the top of the oven. The bar consisted of ten small light bulbs spaced one foot apart. As viewed from the coal bin balcony, the scale started about one foot below the light bar and extended upward about nine feet above it. This scale was used to calibrate the visible vertical area included in each frame which extended about 30 feet above the image of the bar.

In order to prevent special distortion, emission plumes were chosen which were rising near vertically (not being blown by wind) in the vicinity of the illuminated scale (about the same distance from the camera). An additional consideration in the selection of emission periods was the visibility of the illuminated scale during at least some portion of the period recorded on film. It was not necessary that the bar be visible the entire period since only two or three frames per period were required to calibrate the viewing screen.

The technique used in photographing the plume involved observing the emissions until a vertically rising plume developed with a number of distinguishable features such as puffs. The sequence camera was then operated at either one or five frames per second for some period of time - usually from 30 seconds to one minute. The record of the vertical motion was thus made at known time intervals.

The resulting film was processed and viewed using a standard 35mm projector and a square grid as a viewing screen. The projector was adjusted with respect to the screen until the distance between two adjacent bulbs on the scale image correspond to some convenient number of viewing screen grid dimensions. This allowed a direct estimation of the vertical rise distance of some observed feature on the plume.

A total of 60 observations were made on five different charges. The arithmetic mean value was calculated for those observations. This value was 6.63 feet/second free rise velocity for the plume in the vicinity of the light source. A one  $\sigma$  value for the population was also calculated. These values were used for mass emission calculations in the optical program.

## SECTION V

### RESULTS

This portion of the document summarizes the final results of the data analyses. A comparison is provided of gaseous emissions released by the AISI/EPA car and Wilputte car along with a comparison of gaseous emissions that were measured by both the continuous and manual sampling systems.

The results of the particulate analyses are provided in two parts. First, particle size information is given for a number of sizing methods used during the program. An overall frequency size distribution is also determined. Following this, a comparison is given between the total particulate mass emitted during a charging operation of the AISI/EPA car to that emitted by the Wilputte car.

The optical monitoring results are also presented. The results are evaluated and compared to the in-stack measurement system results. The feasibility of this system for general use in source monitoring is also discussed.

#### COMPARISON OF CONTINUOUS MEASUREMENT AND MANUAL GAS SAMPLING METHODS

The continuous monitoring system was used to obtain gas measurements on 27 charging operations, 25 of which produced useful data. The manual sampling system was in operation on 16 of the 27 tests, and data from 10 of the tests were analyzed.

Table 6 lists the constituents measured by the continuous and manual sampling systems. The data from manual and continuous gas analyses is presented in Appendices B and C, respectively. Of the 16 gases, eight gases were analyzed by both the continuous and manual systems. In the presentation of results, either the continuous or manual values were used, based on the comparison of the systems as described below. The results for both manual and continuous analyses are shown in Tables 7 through 14. In these tables, the columns labeled "Interval Average" refer to average values calculated over the period during which manual gas sampling was taking place. Under the "MITRE Values" heading, the "Interval Average"

TABLE 6

CONSTITUENTS MEASURED BY THE CONTINUOUS AND  
MANUAL SAMPLING SYSTEMS

<u>Constituent</u>	<u>Continuous</u>	<u>Manual</u>
CO	X	X
CO <sub>2</sub>	X	X
SO <sub>2</sub>	X	X
H <sub>2</sub> S	X	X
THC	X	X
CH <sub>4</sub>		X
NO	X	
NO <sub>x</sub>	X	X
N <sub>2</sub>		X
NH <sub>3</sub>		X
H <sub>2</sub> O	X	
HCN		X
H <sub>2</sub>	X	X
O <sub>2</sub>	X	X
pyridine		X
phenols		X

TABLE 7, SO<sub>2</sub>

MITRE # /MRI #	MITRE VALUES IN PPM				MRI VALUES IN PPM				
	TEST AVERAGE	INTERVAL AVERAGE	HIGH	LOW	INTERVAL AVERAGE	BAG A	BAG B	BAG C	BAG D
5/W4	427.9	<380 *	1088.1	0	7.033	<4.5 *	9.2	<7.4 *	
6/W5	76.1	< 69.35	293.6	0	159.99	87.51	232.47		
7/W6	496.9	450 **	857.5	256.2	28.69	< 4.5 *	< 19.16 *	69.1	< 22 *
10/W10	221.8	125 **	454.2	0		< 9.7 *			
11/W11	388	425 **	654.1	0	9.55	< 7.3 *	< 6.6 *	< 4.5 *	< 19.8 *
19/K1	120.1	19.22	381.6	4.7	22.33	25.4	24.75	21.32	17.84
21/K3	1453.4	450 **	3485.7	8.4	23.63	21.03	9.72	48.25	< 15.53*
23/W12	3.8	2.35	14.0	0	14.85	<23.2 *	< 6.5 *		
24/K4	188.9	250 **	833.3	18.8	28.34	< 6.3 *		<50.37 *	
* Detectable Limit - Minimum detectable quantity calculated for sample size									
** Approximated Values - Data not completely reduced due to obvious instrument operational problems									

TABLE 8, H<sub>2</sub>

MITRE # /MRI #	MITRE VALUES IN %				MRI VALUES IN %				
	TEST AVERAGE	INTERVAL AVERAGE	HIGH	LOW	INTERVAL AVERAGE	BAG A	BAG B	BAG C	BAG D
5/W4	.1	.0497	1.0	0	.0933	0	.28	0	
6/W5	0	0	0	0	.315	.17	.46		
7/W6	0	0	0	0	1.66	1.8	.01	.43	4.39
8/W7	0	.01	.2	.1	.54	.48	.13	1.23	.32
10/W10	0	0	0	0	.38	.21	.51	.42	
1/W11	0	0	0	0	.977	2.13	.3	.06	1.42
19/K1	0	0	0	0	.0175	.01	.03	.02	.01
21/K3	2.2	1.57	9.0	0	2.038	.41	.36	3.54	3.84
23/W12	.2	.175	2.3	0	.875	.19	1.56	1.56	
24/K4	.1	.081	.6	0	1.9	.48		3.32	

TABLE 9, CO

MITRE # /MRI #	MITRE VALUES IN %				MRI VALUES IN %				
	TEST AVERAGE	INTERVAL AVERAGE	HIGH	LOW	INTERVAL AVERAGE	BAG A	BAG B	BAG C	BAG D
5/W4	.68	.6	2.02	.02	.02	.01	.04	.01	
6/W5	1.08	1.0	2.15	.58	.99	.77	1.22		
7/W6	1.18	1.2	2.88	.13	1.15	1.53	.12	1.4	1.53
8/W7	1.22	1.2	3.34	.20	.63	.34	.17	1.34	.68
19/K1	.41	.1	2.36	.04	.02	.02	.02	.03	.01
21/K3	1.12	1.3	2.53	.08	.93	.5	.15	1.96	1.11
23/W12	.69	.7	2.95	.10	.27	.2	.33		
24/K4	.41	.6	1.63	.01	.26	.1	.43		



TABLE 10, CO<sub>2</sub>

MITRE # /MRI #	MITRE VALUES IN %				MRI VALUES IN %				
	TEST AVERAGE	INTERVAL AVERAGE	HIGH	LOW	INTERVAL AVERAGE	BAG A	BAG B	BAG C	BAG D
5/W4	.0	.1	.4	.0	.21	.06	.28	.29	
6/W5	3.2	3.1	8.1	.6	2.7	2.33	3.06		
7/W6	2.1	2.1	6.3	.0	1.9	.96	2.14	2.77	1.84
8/W7	1.2	1.3	4.5	.0	.9	.74	.27	1.4	1.3
10/W10	.7	.3	2.0	.0	.7	.29	.56	1.2	
11/W11	.8	.9	1.9	.0	.6	.86	.07	.15	1.39
19/K1	.2	.0	.9	.0	.1	.07	.14	.12	.11
21/K3	.4	.5	1.1	.0	.7	.22	.16	1.24	1.14
23/W12	.0	.0	.0	.0	.4	.42	.4		
24/K4	.3	.6	1.8	.0	.6	.15	.95		
9/W9	.0	.0	.0	.0	.2				

TABLE 11, THC

MITRE # /MRI #	MITRE VALUES IN %				MRI VALUES IN %				
	TEST AVERAGE	INTERVAL AVERAGE	HIGH	LOW	INTERVAL AVERAGE	BAG A	BAG B	BAG C	BAG D
6/W5	.73	.69	1.84	.00	.93	.68	1.18		
.7/W6	1.57	1.23	6.34	.00	1.44	.8	.15	2.08	2.72
19/K1	1.12	.14	7.00	.00	.09	.11	.09	.10	.06
21/K3	3.62	3.45	7.00	.00	5.77	7.41	.52	8.1	7.05
23/W12	3.00	2.50	13.96	.00	.87	.26	1.48		
24/K4	1.78	2.55	6.98	.00	1.51	.44	2.59		

TABLE 12, O<sub>2</sub>

MITRE # /MRI #	MITRE VALUES IN %				MRI VALUES IN %				
	TEST AVERAGE	INTERVAL AVERAGE	HIGH	LOW	INTERVAL AVERAGE	BAG A	BAG B	BAG C	BAG D
5/W4	18.1	18.19	18.7	15.0	16.29	16.56	15.71	16.6	
6/W5	16.7	16.96	21.6	5.8	13.52	15.75	11.29		
7/W6	15.1	15.22	19.0	9.7	14.72	15.23	16.59	12.99	14.06
8/W7	14.7	15.14	18.7	7.5	15.87	15.58	16.33	15.96	15.6
10/W10	14.4	15.4	16.9	11.0	15.69	16.1	16.27	14.7	
11/W11	16.5	16.25	18.9	13.9	15.64	15.33	16.01	16.22	15.0
19/K1	18.9	19.46	19.6	15.8	16.13	16.03	16.42	15.96	16.11
21/K3	17.5	17.72	19.6	15.3	15.075	14.85	16.41	14.20	14.84
23/W12	18.0	17.98	19.3	13.9	16.195	16.05	16.34		
24/K4	19.6	16.37	20.3	18.3	15.39	15.76		15.02	

TABLE 13, NO<sub>x</sub> PLUS NH<sub>3</sub>

MITRE # /MRI #	MITRE VALUES IN PPM				MRI VALUES IN PPM				
	TEST AVERAGE	INTERVAL AVERAGE	HIGH	LOW	INTERVAL AVERAGE	BAG A	BAG B	BAG C	BAG D
5/W4	22.2	22	47.9	0.0	< 4.89 *				
6/W5	42.2	40.9	103.8	1.4	< 37.07 *				
7/W6	124.9	95.7	483.8	6.0	<140. *				
8/W7	68.8	65.2	144.3	0.0	<208.0 *				
10/W10	57.9	50.6	120.5	0.0	< 4.4 *				
11/W11	82.7	91.2	365.4	0.0	< 37.3 *				
19/K1	3.4	.5	14.0	0.0	< 8.16 *				
21/K3	113.7	42.5	319.0	0.8	< 22.4 *				
23/W12	21.4	25.1	70.3	0.0	< 8.3 *				
24/K4	.6	1.6	11.3	0.0	< 31.1 *				
* Detectable Limit - Minimum detectable quantity calculated for sample size									

TABLE 14, NO<sub>x</sub>

MITRE # /MRI #	MITRE VALUES IN PPM				MRI VALUES IN PPM				
	TEST AVERAGE	INTERVAL AVERAGE	HIGH	LOW	INTERVAL AVERAGE	BAG A	BAG B	BAG C	BAG D
5/W4	22.2	22	47.9	0.0	< 3.5 *	< 2.16 *	6.20	< 2.17 *	
6/W5	42.2	40.9	103.8	1.4	34.5	< 12.48	56.59		
7/W6	124.9	95.7	483.8	6.0	< 124.7 *	< 2.19 *	6.3	< 2.19 *	488.4
8/W7	68.8	65.2	144.3	0.0	< 151.7 *	< 2.17 *	< 2.18 *	301.28	301.28
10/W10	57.9	50.6	120.5	0.0	< 2.18 *	< 2.17 *	< 2.18 *	< 2.18 *	
11/W11	82.7	91.2	365.4	0.0	< 29.6 *	< 2.16 *	< 2.15 *	3.09	110.95
19/K1	3.4	.5	14	0.0	< 1.96 *	< 1.96 *	< 1.97 *	< 1.94 *	< 1.96 *
21/K3	113.7	42.5	319.0	0.8	< 4.7 *	< 1.96 *	11.26	2.8	2.78
23/W12	21.4	25.1	70.3	0.0	< 2.38 *	2.79	< 1.97 *		
24/K4	.6	1.6	11.3	0.0	< 1.94 *	< 1.95 *	< 1.93 *		
* Detectable Limit - Minimum detectable quantity calculated for sample size									

values are an average of five second averages (see Appendix C, page C-123) during the manual sampling period. "Test Average" values are averages of five second averages over the total test period. Under the "MRI Values" heading, the "Interval Average" is a simple average of the measured concentrations in the sample bags. Thus, only the "interval" values are comparable, whereas the "test" value represents an average over a longer period of time.

Also included in these tables are values of detectable limits for individual samples. This value is a function of sample size and is included to indicate that concentrations of the particular constituent below this level may have been present, but would not have been detected by the analytical techniques utilized. Thus, this value does not indicate the absolute absence or verified presence of the constituent.

In general, good agreement was observed between manual and continuous data for CO, CO<sub>2</sub>, THC, and O<sub>2</sub>. For these four gases, it was felt both systems were producing results that agreed within the constraints of the system. Generally, large disagreement for these gases on specific tests could be traced to some specific problem occurring during the test. Good comparisons were also found between the results of each test and the general qualitative descriptions of the emissions recorded on the voice tapes. The emission volumes determined for each of these gases were calculated using the continuous results. This was done because more continuous measurements were performed than manual, and hence, offered a large statistical sample.

The continuous SO<sub>2</sub> and H<sub>2</sub>S data when compared with the manual data were found to be orders of magnitude higher. As a result, a number of laboratory tests were performed. These tests established the fact that certain aromatic hydrocarbons, probably present in coke oven emissions (especially phenol), interfere with the UV bands used to measure H<sub>2</sub>S and SO<sub>2</sub>; (215 m and 280 mμ, respectively). Therefore, even with the constraint of a smaller statistical sample, it was necessary to use the manual results to determine the typical SO<sub>2</sub> and H<sub>2</sub>S emission volumes per charge.

Similarly, interference problems, as well as calibration problems, for the  $H_2$  analyzer resulted in considerable disagreement between manual and continuous data, and it was concluded that manual data should be used for any computation requiring hydrogen.

Comparison of  $NO_x$  data shows values for certain tests in agreement, while others differ by as much as an order of magnitude. The data from both systems were compared to qualitative descriptions of each test, and it was determined that there were inconsistencies in the manual sampling results. As a result, it was concluded that the continuous measurements would be used for  $NO_x$ .

In summary, of the eight gases measured by both systems, the continuous results were used in the data reduction procedures for  $CO$ ,  $CO_2$ ,  $THC$ ,  $O_2$ , and  $NO_x$ ; and the manual data were used for  $H_2S$ ,  $SO_2$  and  $H_2$ .

#### COMPARISON OF GASEOUS EMISSIONS FOR WILPUTTE AND AISI/EPA CAR

During the field measurement program, it was not possible to monitor all emission points simultaneously. Therefore, the estimate of total gaseous emissions released by the car was prepared using aggregate data on measured gaseous concentrations from the series of individual tests. The average volume flow for each emission point was calculated for each test and summed to determine the average total volume flow of gases emitted during a charge. These values were multiplied by the average concentration of the individual gases and by the test times to calculate the volume of gaseous constituents emitted per charge. All volume calculations are based on average test times of 2.61 minutes and 3.48 minutes for the AISI/EPA and Wilputte car, respectively. A charge or test is defined as the period of time beginning when the larry car starts to unload its coal and ending when the lids are replaced by the automatic lid lifters (for the AISI/EPA car) or 15 seconds after all the coal is dumped (for the Wilputte car). Since the Wilputte car had to move away from the ports before the lids were replaced, and since monitoring could be performed only when the car was in place, the Wilputte test time was extended to allow for the emissions that would normally occur before the lidman replaced the lids. Fifteen seconds was considered the very minimum time

in which a man could replace the lids and only under the very best conditions. Table 15 lists the average volumes for gases monitored by the continuous measurement system for the Wilputte car and Table 16 lists them for the AISI/EPA car. The measured and corrected values represent flows and volumes calculated using measured and corrected (Equation 10) concentrations, respectively. The measured value can be interpreted in most cases as a lower limit value, while the corrected would indicate the upper limit of the emission levels. It can be assumed that the volume of emission escaping through the measurement points would lie in a range somewhere between the measured and corrected values. Hence, the closer the measured value is to the corrected value, the more confidence can be placed in the results. When the measured value is very close to the corrected value, this is an indication that the error caused by dilution of the sample with ambient air was minimized.

During testing of the AISI/EPA car, a combination of conditions caused number 3 drop sleeve during Test 21 fail to seal. The emission guide surrounding the drop sleeve presented detection of the faulty seal until the charge had begun. Hence, no alternative measures could be taken to correct this condition. Therefore, this test was not considered a fair representation of normal AISI/EPA emissions, and Table 17 lists AISI/EPA volumes excluding Test 21 values from the averages. The results are presented with and without Test 21 included, so as to give a representation of average emissions under poor conditions and under a more typical set of conditions which might require a reasonable amount of care to obtain.

Table 18 is based on corrected values and compares the Wilputte car to the AISI/EPA car for  $\text{NO}_x$ , NO,  $\text{CO}_2$ , CO and THC. As noted on Table 18, the volume of  $\text{NO}_x$ , NO,  $\text{CO}_2$ , CO and THC was shown to decrease significantly with the new car. Emission reduction ranged from 14 to 99%, with the greatest reduction being in NO emissions. The smallest reduction of these five constituents was still very significant, THC average emission volume for the new car averaged between 14% and 40% less than the other car.



TABLE 15

EMISSION VOLUMES FOR WILPUTTE CHARGING

Constituent	Average Volume Emitted/Charge (SCF)	
	Measured	Corrected
NO <sub>x</sub>	.1107	.1144
NO	.0783	.0802
CO <sub>2</sub>	29.00	29.36
CO	16.94	17.49
THC	33.28	33.77

TABLE 16

EMISSION VOLUMES FOR AISI/EPA CHARGING INCLUDING TEST 21

Constituent	Average Volume Emitted/Charge (SCF)	
	Measured	Corrected
NO <sub>x</sub>	.0456	.0492
NO	.0059	.0061
CO <sub>2</sub>	4.05	4.71
CO	8.18	9.04
THC	26.69	29.12

TABLE 17

EMISSION VOLUMES FOR AISI/EPA CHARGING EXCLUDING TEST 21

Constituent	Average Volume Emitted/Charge (SCF)	
	Measured	Corrected
NO <sub>x</sub>	.0169	.0211
NO	.0008	.0011
CO <sub>2</sub>	3.08	3.83
CO	5.30	6.28
THC	17.09	20.43

30.56 ft<sup>3</sup> v 25 ppm = 7.600 ft<sup>3</sup>  
 1.36 x 10<sup>-4</sup> lb/24.9

TABLE 18

PERCENT REDUCTION OF GASEOUS EMISSIONS

Constituent	(Wilputte Volume-AISI/EPA Volume)/Wilputte Volume x 100	
	% Reduction	% Reduction w/o Test 21
NO <sub>x</sub>	56.8	81.6
NO	92.4	98.6
CO <sub>2</sub>	83.9	86.9
CO	48.3	64.1
THC	13.7	39.5

Table 19 lists the average, maximum and minimum concentration for all the gaseous pollutants measured. The first five constituents were measured by the continuous monitoring system. The remaining seven constituents were measured by the manual sampling system. It should be noted that the averages of gases measured by the manual sampling system was based on 10 tests for the Wilputte car and three tests for the AISI/EPA, while the continuous system was operational on 18 Wilputte tests and 10 AISI/EPA tests.

Data for  $\text{SO}_2$ ,  $\text{H}_2\text{S}$ ,  $\text{CH}_4$ ,  $\text{NH}_3$ , phenol, CN and pyridine are presented in Appendix C. For a substantial number of tests, measurement of these seven constituents produced concentrations below the detectable limit. It was felt, due to the small number of tests on which these constituents were measured and the large number of times they were below detectable limits, that no calculation of volume would be truly representative of their emissions. Instead, the comparison of cars was made on a measured concentration basis. Table 19 shows that the maximum concentration measured, excluding Test 21, was larger for the Wilputte car in every case. When Test 21 is involved in the comparison, the concentrations were reduced for the AISI/EPA car in every case except for the constituents of  $\text{H}_2\text{S}$  and  $\text{CH}_4$ .

In general, gaseous emissions from the AISI/EPA car were significantly reduced between 14% and 99% for  $\text{NO}_x$ , NO,  $\text{CO}_2$ , CO and THC, while for the other seven pollutants measured, a qualitative evaluation indicates reductions of better than 15% in all cases.

#### RESULTS OF PARTICLE SIZE ANALYSES

Along with the obvious health reasons for interest in the size distribution of coke oven particulate matter, its characterization is required to predict the physical behavior of particles relative to aerodynamics and optical characteristics.

TABLE 19

CONSTITUENT CONCENTRATIONS (MEASURED)

CONSTITUENT	WILPUTTE			AISI/EPA				
	Average	Maximum	Minimum	Without Test #21			With Test #21	
				Average	Maximum	Minimum	Maximum	Minimum
NO <sub>x</sub> (ppm)	38.9	484	0.0	9.6	70.2	0.0	319	0.0
NO (ppm)	15.6	336	0.0	.13	20.3	0.0	52.8	0.0
CO <sub>2</sub> (%)	.5	8.1	0.0	.11	1.5	0.0	1.5	0.0
CO (%)	.69	3.76	0.0	.21	2.2	0.0	2.53	0.0
THC (%)	1.6	13.98	0.0	.59	11.4	0.0	11.4	0.0
SO <sub>2</sub> (ppm)	*	232.5	BDL	*	25.4	BDL	48.3	BDL
H <sub>2</sub> S (ppm)	*	42.5	BDL	*	BDL	BDL	72.27	BDL
CH <sub>4</sub> (%)	.62	4.3	.01	.53	1.77	.01	7.79	.01
NH <sub>3</sub> (ppm)	*	130.6	BDL	*	BDL	BDL	12.37	BDL
Phenol (ppm)	*	31.1	BDL	*	BDL	BDL	17.72	BDL
CN (ppm)	*	16.5	BDL	*	BDL	BDL	5.48	BDL
Pyridine (ppm)	*	BDL	BDL	*	BDL	BDL	BDL	BDL

\* A large number of tests were below detectable limits (BDL) and no average could be computed.

The particle size distribution determined is also required for use with anisokinetic mass loading and volume flow data to produce a set of calculated isokinetic mass values, and with optical data (opacity measurements) to calculate theoretical mass emissions.

In the calculation of theoretical isokinetic mass data from anisokinetic mass values, the size distribution of the sample is a critical factor. Anisokinetic sampling will result in correct particulate concentrations if the particles are aerodynamically small. For most conditions, particles  $<5 \mu$  may be considered as small particles. The mass of large particles (those which move independently to gas stream) will produce the correct concentration values if sample volume calculations are made using stack velocity instead of sampling velocity. For the average particle density of coke oven emissions, particles  $<200 \mu$  can be considered large particles which move independent of the gas stream. However, for particles between 5 and  $200 \mu$ , anisokinetic sampling can produce results far different from isokinetic sampling. Hence, to approximate isokinetic results, corrections are required and are partly dependent on the particle size distribution. The relations and calculations are discussed in the Analytical Methods section of this report.

A particle number distribution is also required to relate absorption and scattering effects measured by the optical measurement system to the mass of particulate matter in the plume.

Five methods of particle analysis were used during this test program:

<u>Method</u>	<u>Range Measured</u>	<u>Number of Tests*</u>
Anderson	$\sim 20\mu \sim .5\mu$	10
Brink	$\sim 3\mu \sim .3\mu$	2
Sieve & Sedegraph	325 mesh to $.6\mu$	2
Coulter	$\sim 100\mu$ to $1\mu$	1
Optical	$500\mu$ to $4\mu$	9

Though data from all the methods were compared and considered, the Andersen data and optical analysis data of samples taken by the MITRE Carrousel were the primary methods used for development of the particle distribution. The following paragraphs explain the rationale for this decision, as well as discuss the methods and sample handling techniques.

Both the Andersen and the Brink samplers use aerodynamic sizing methods. The sample is simultaneously collected and sized. Weighing of the collection stages is performed within a few hours of the tests, and no redispersion of the sample is needed. The Andersen sampler was used on a total of ten tests (all were performed in the stacks or guides). Due to underloading or overloading or anomalies in stack velocities, five of the tests produced suspected data and were not used in the final compilation of the data. The Brink sampler was used a number of times, producing data from six tests. Three of the six tests concerned samples taken from emission plumes 20 feet above the car; two were of leaking door tests and only one test concerned sampling from the emission guides. The emission guides and stack areas are of most importance, since the mass loading samples were taken from these areas.

Sieve, sedigraph, Coulter and some optical analyses were performed on samples redispersed after various forms of collection. It is intuitively felt that dissolving the particulate matter could seriously alter the particle size distribution by reducing aggregation and floccing, and hence produce biased results.

---

\* This number indicates the total number of both "good" and suspect samples taken at emission guides and stacks. Test of leaking doors of free plumes, etc., are not listed here.

A number of the optical sizings were performed on samples collected on field constructed equipment (MITRE Carrousel) specially designed to collect the particles and retain them in a form that could be directly used for optical size analyses. The resulting optical size distribution was used to develop a weight distribution and combined with the Andersen results to produce a typical particle size distribution.

Data from the Andersen and MITRE Carrousel optical analyses are listed respectively in Appendices B and E. The Andersen sampler was used on ten tests. Only five of the ten were acceptable for determining a distribution function. Table 20 lists all ten tests, location of samplers and reasons why certain tests were suspect and, hence, not included in the average. The values of the remaining "good" tests were combined with the optical results and corrections applied to the anisokinetic distribution to determine an average calculated isokinetic distribution shown in Table 21. The cumulative distribution of Table 21 is plotted in Figure 18. Inspection of the figure implies that the distribution could fit a bi-populate lognormal distribution. To check this, the distribution was broken into two separate distributions - one between Range 1 and Range 7 (containing ~46.6% of sample by wt.) and the other Range 8 to Range 12 (containing ~53.4% of sample by wt.). These were then normalized (Table 21) and plotted on log probit paper (Figures 19 and 20). As expected, a straight line can be drawn through the data points implying that both curves can be approximated by log-normal distributions. The lower range curve has a mass mean diameter of about 8.5  $\mu\text{m}$  and a sigma of about 2.5, whereas the larger range curve has a mass mean diameter around 235  $\mu\text{m}$  and a sigma of about 3.9. The overall mass frequency distribution can be described by:

TABLE 20

ANDERSEN ANALYSIS

<u>Test Number and Location</u>	<u>Status and Reason</u>
7 - 1	Test was acceptable.
8 - 2	Test was acceptable.
8A - 3	Test was suspect due to stage overloading (the 2/3 stage had more than 120 mg on it).
9 - 1	Test was suspect, load on stage was very light (<.2 mg) and emission velocity was zero during much of the test making calculation of theoretical correction factors difficult.
10 - 6	Test was acceptable, loading was light.
11 - 5	Test was acceptable, loading was lighter than ideal.
23 - 2	Test was acceptable, one stage suffered minor overloading.
20 - K2	Test was acceptable.
21 - K3	Test was suspect, stages were over-loaded (as much as 590 mg).
24 - K1	Test was suspect, stages under-loaded (some as light as .02 mg).



TABLE 21  
SIZE DISTRIBUTION DUE TO COKE OVEN CHARGING

Assigned Range Numbers	1	2	3	4	5	6	7	8	9	10	11	12	13	
Range Mean Particle Diameter $\mu^*$	Filter	.584	.883	1.387	2.631	4.313	6.412	9.433	14.791	45	112	273	700	
Weight % in Size Range	14.7	4.3	6.2	11.8	6.5	1.9	1.2	1.7	4.5	3.3	11.0	18.7	14.1	
Cumulative Weight % < Upper Range Bound	14.7	19.0	25.2	37.	43.5	45.4	46.6	48.3	52.8	56.1	67.1	85.8	99.9	

102

NORMALIZED SEPARATE POPULATIONS OF BIPOPULATE DISTRIBUTION

Lower Mode Weight % < Upper Range Bound	31.5	40.7	54.0	80.6	93.3	97.4	100.0							46.6% of Sample
Upper Mode Weight % < Upper Range Bound								3.2	11.6	17.8	38.4	73.5	99.9	53.4% of Sample

\* Assumed 1.2 gm/ml density. Some overlap of ranges occurs in sampling/sizing equipment. As a result, the mean value must be derived from theoretical range bounds.

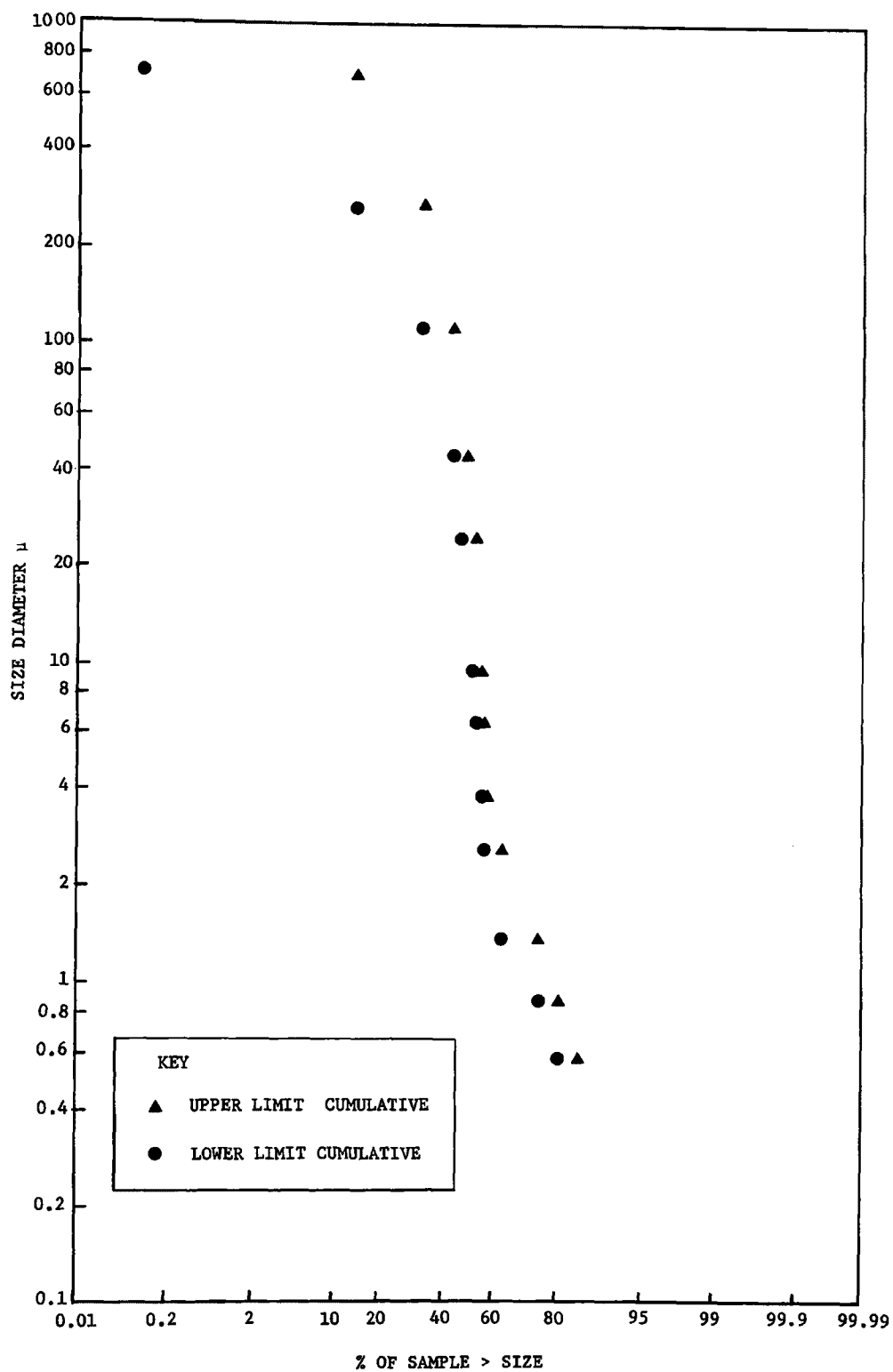


FIGURE 18  
COKE OVEN PARTICULATE DISTRIBUTION

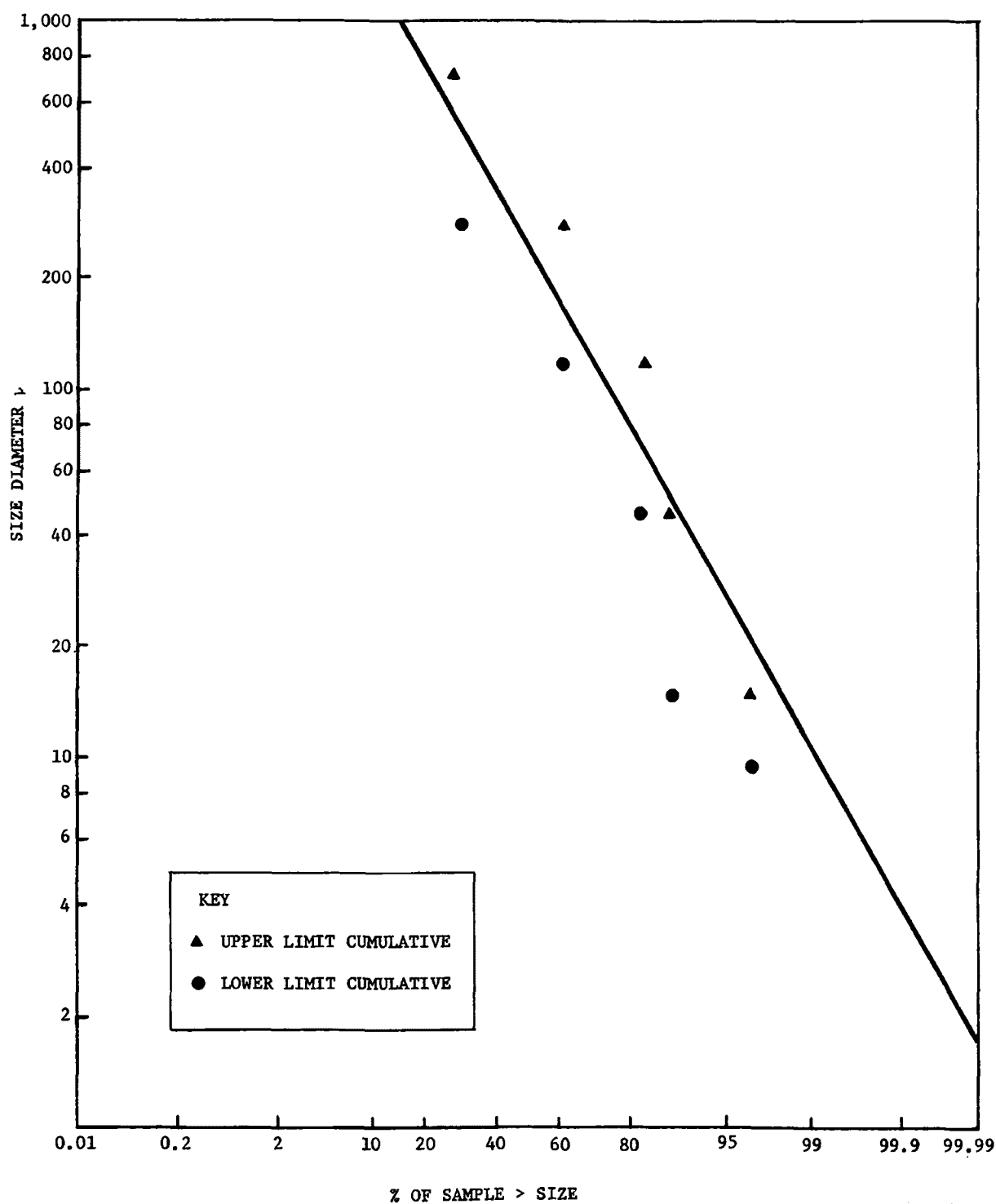


FIGURE 19  
LOG NORMAL PLOT OF RANGES 1 THRU 7

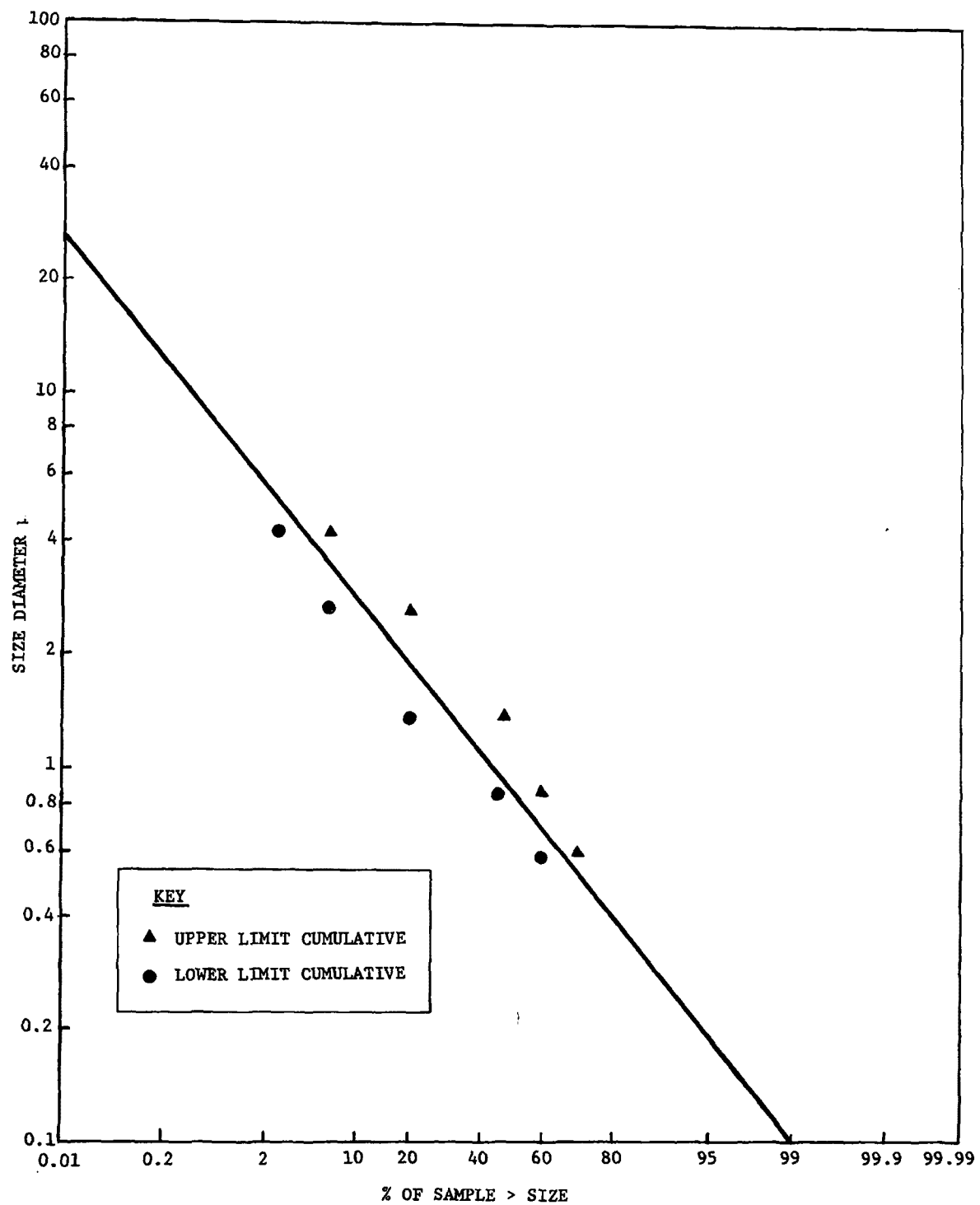


FIGURE 20  
LOG NORMAL PLOT OF SIZE RANGES 8 THRU 13

$$\begin{aligned}
f(D) &= W_1 f_L(D) + W_2 f_u(D) \\
&= \frac{W_1}{D \cdot 2\pi \ln \sigma_1} \exp - \left( \frac{\ln^2(D/\mu_1)}{2 \ln \sigma_1} \right) \\
&\quad + \frac{W_2}{D \cdot 2\pi \ln \sigma_2} \exp - \left( \frac{\ln^2(D/\mu_2)}{2 \ln \sigma_2} \right)
\end{aligned} \tag{28}$$

where it is assumed  $f_L(D)$  is independent of  $f_u(D)$

$f(D)$  = mass frequency distribution of bi-populate lognormal e

$f_L(D)$  = mass frequency distribution lower lognormal curve

$f_u(D)$  = mass frequency distribution of upper lognormal curves

$D$  = diameter of range

$W_1$  = weight % of lognormal portion of bi-populate centered about .85  $\mu$  (46.6%)

$W_2$  = weight % of lognormal portion of bi-populate centered about .235  $\mu$  (53.4%)

$\mu_1$  = mean of lower curve (.85  $\mu$ )

$\mu_2$  = mean of upper curve (235  $\mu$ )

$\sigma_1$  = sigma of lower mode, 2.5

$\sigma_2$  = sigma of upper mode, 3.9

This distribution function would seem to give the best possible general description of the coke oven charging particulate emissions based on the collected data. However, it should be noted that this distribution is based on an average density of 1.2 gm/ml. Though the measured distribution fits the bi-populate lognormal form reasonably well, it is based on only five tests which cannot be considered the most ideal statistical example. Therefore, the bi-populate lognormal frequency distribution is not

presented as the absolute particle distribution, but rather as a simplified mathematical model to be used as a representation of coke oven charging particulate distribution.

Appendix E gives the particle distributions from Brink samplers for emission guide, boom, and leaking door tests. Due to the limited range of the Brink sampler, the data concerns only the lower lognormal portion of the bi-populate distribution and, hence, can only be compared against this portion of the curve. Furthermore, only Brink Test #4 can be used as a comparison because it was the only test performed at the emission points of the charging operation. Figure 21 is a plot of the cumulative weighted percent of Test 4. Assuming a lognormal distribution, a straight line drawn through the points produce a mean of about  $1.2 \mu$  and a sigma of 2.2. This is in good agreement with the calculated lower distribution of a mean  $\sim .85 \mu$  and sigma  $\sim 2.5$ . In addition, the Brink data are all based on an assumed density of .8 gm/ml and the Andersen data are based on 1.2 gm/ml. Equating the densities of both methods would tend to bring them into closer agreement.

The Coulter counter produced a volume mean of  $\sim 27 \mu$ . The sample was taken by scraping particulate matter off a 1/4" wire screen which had been exposed to the emission plume of the Wilputte stack.

Optical analyses were performed on portions of the samples removed from the cyclone and Andersen sampler. These samples were suspended in benzene when removed from the sampler and were later suspended in isopropyl alcohol just prior to sizing. The number mean diameter was found to be between 5.5 and  $3 \mu$  or around  $30 \mu$  mass mean diameter.

The sieve and sedigraph analyses were performed on particulate matter trapped in the case of the MITRE Carrousel Sampler (not on the collection slides of the sampler). The size distribution of these samples was found to be bi-populate. Seventy percent of the sample mass was greater than  $43 \mu$  (325 mesh by sieve) and 30 percent less than  $3 \mu$  with a mean of about  $1.3 \mu$  for the portion of the sample less than  $3 \mu$ . The sedigraph analysis was performed using water as the medium. This is in fair agreement with the

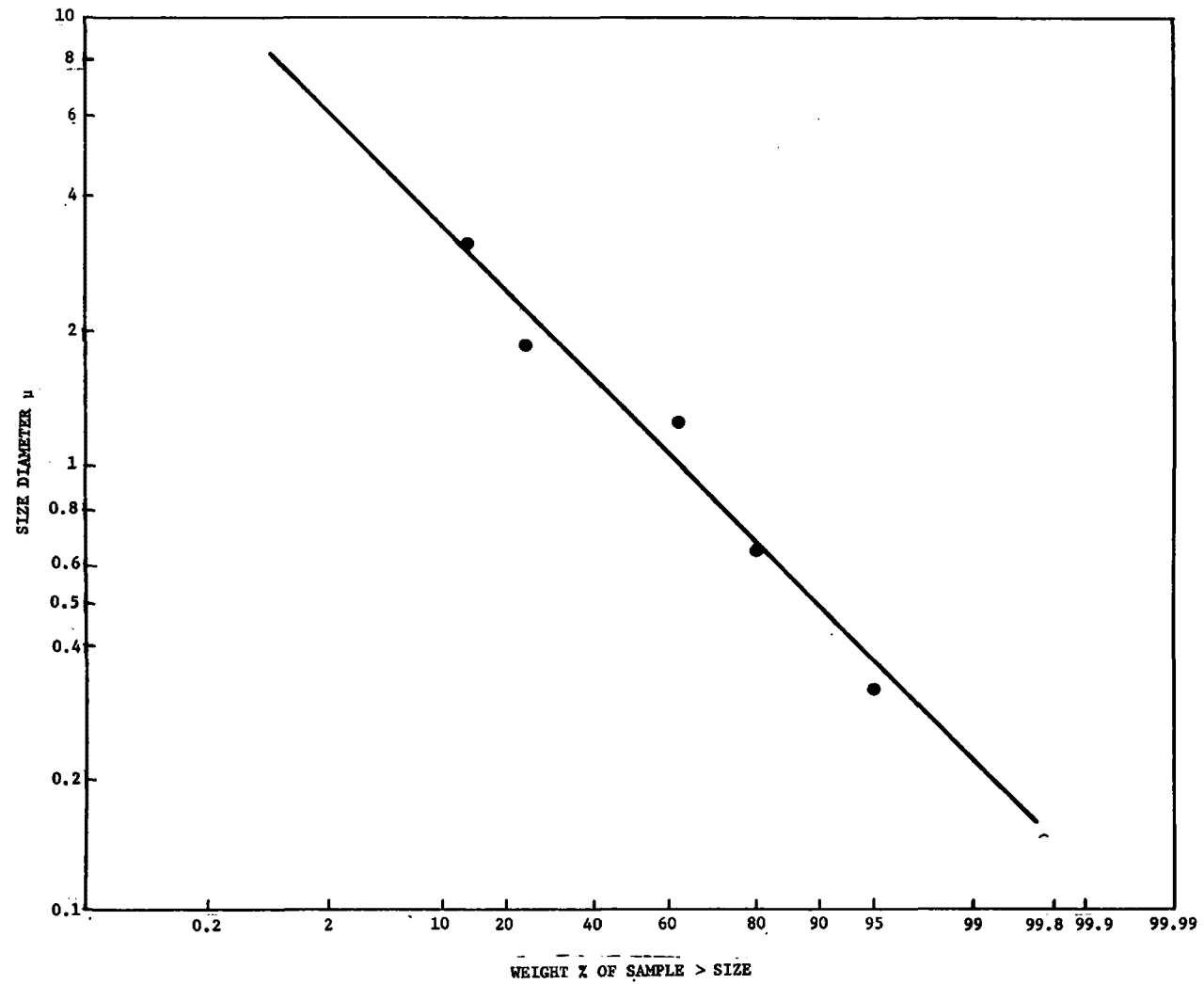


FIGURE 21 —  
BRINK DATA

Andersen, Brink, and MITRE Carousel analysis.

#### STATISTICAL EVALUATION OF SIZE DISTRIBUTION DATA

The arithmetic averages for the acceptable tests including anisokinetic and calculated isokinetic values are shown in Table 22. Chi-square ( $\chi^2$ ) tests were performed on both anisokinetic and theoretical isokinetic averages against the respective values for individual tests. As shown in the table, the theoretical isokinetic values produced equal or lower  $\chi^2$  values, hence, higher confidence levels. All  $\chi^2$  tests on the corrected data pass the goodness of fit test while only two of the anisokinetic tests pass the test. To pass the  $\chi^2$  test implies only that there is no reason to doubt the distribution fits by the hypothetical distribution.

The bi-populate lognormal distribution was determined from the values of the arithmetic average of all the corrected isokinetic values and passes the  $\chi^2$  goodness of fit test.\* However, the data do suggest the distribution varies between guide and stack. The distributions from the emission guide tend to shift the mean of the lower mode toward a lower mean and higher standard deviation, while the stacks tend to the other extreme. Though these differences were noted, there was statistically insufficient data to produce separate distribution for the guides and stacks. Therefore, the bi-populate distribution previously described was used to approximate particulate emissions in all cases.

#### COMPARISON OF PARTICULATE EMISSIONS FROM WILPUTTE AND AISI/EPA CAR

A number of analyses were performed on the particulate mass samples. The primary analyses (for mass emitted) was performed on all samples and corrections (Equation 16) for errors due to anisokinetic sampling were applied. Secondary investigations include analyses for:

---

\* Herdan, G. H., Smith, M. L., Hardwick, W. H., Conner, P. Small Particle Statistics. London, Butterworths, 1960. p. 122-125



TABLE 22

## SIZE RANGE

Assigned Range Numbers	1	2	3	4	5	6	7	8	9	10	11	12	13
Range Mean Part. Diam. Filt.		.58	.88	1.39	2.63	4.31	6.41	9.43	14.79	45	112	275	700
Average Anisokinetic Distribution*	14.65	4.57	7.12	14.2	6.73	2.1	1.29	1.89	5.13	3.53	11.8	17.0	11.34
Average Calculated Isokinetic Distribution**	14.7	4.3	6.2	12.4	5.9	1.9	1.2	1.7	4.5	3.3	11	18.7	14.1
Bipopulate Lognormal Approximation at Mean Upper=235 $\mu$ , $\sigma_U$ =3.9, Mean Lower=.85, $\sigma_L$ =2.5	12.58	8.39	8.85	8.85	5.22	1.93	.84	.73	2.74	6.62	12.28	13.99	16.92

Test	Chi-Square Test For***	
	Average Anisokinetic	Average Isokinetic
07	17.12	11.04
08	29.52	20.80
10	23.69	16.37
11	21.16	12.96
23	11.25	11.31
Bipopulate Lognormal	---	---

\* Actual particulate sampling was conducted at a constant sampling velocity independent of variations in stack velocity.

\*\* Theoretical corrections were applied based on instantaneous emission velocity measurements to yield a calculated isokinetic distribution

\*\*\* For 12 degrees of freedom if  $\chi^2$  is larger than 21.03 the probability becomes significant that the test does not fit the distribution.

% tar content  
benzpyrene content  
density  
elemental

The major objectives of the secondary analysis were to develop baseline data on coke oven emissions with emphasis on the detection of potentially hazardous substances such as carcinogens and heavy metals, and an assessment of the state of the art in techniques for making such measurements and determinations. This analysis is necessary in any assessment of the importance and potential effects of coke oven emissions. These analyses were performed on only a portion of the total number of samples.

#### MASS EMISSIONS

The average calculated isokinetic mass emitted by the Wilputte car was 814.7 gm per charge, while the like value for the AISI/EPA car was 120 gm per charge. This is a reduction of about 85.2% from Wilputte to AISI/EPA emissions. These calculated isokinetic mass values were obtained by applying a theoretical correction process to the anisokinetic data.

All particulate samples were collected under anisokinetic conditions. Tables 23 and 24 present this particulate emissions data for the Wilputte and AISI/EPA car, respectively. The values in these tables were calculated by the following equation which assumes isokinetic conditions:

$$EM_i = \frac{A_i}{U_i} M_i \quad (29)$$

where  $EM_i$  = total mass emitted at location I during the charge,  
 $A_i$  = area of measurement duct,  
 $U_i$  = area of sampling nozzle,  
 $M_i$  = mass of sample collected at location I.

The tables show the average mass emission assuming isokinetic conditions to be 808.9 gm/charge for the Wilputte car and 245.5 gm/charge for the AISI/EPA car. These results are incorrect, however, since isokinetic conditions did not exist.

TABLE 23  
ANISOKINETIC MASS EMISSIONS  
WILPUTTE

TEST NO.		STACK 1	STACK 2	STACK 3	GUIDE 1	GUIDE 2	GUIDE 3	TOTAL
2						36.8	38.3	
5			250.6			28.7		
6				134.5			26.2	
7		201.5	182.0	132.4				
8		144.7	123.6	269.3				
9		42.0	294.2	355.3				
10					41.7	67.9	50.6	
11					37.6	34.0	48.7	
23			257.3					
8A		65.0	82.4	975.9				
Average		113.3	198.4	374.7	39.65	41.9	40.9	808.9

TABLE 24  
ANISOKINETIC MASS EMISSIONS  
AISI/EPA

TEST NO.		STACK 1	STACK 2	STACK 3	GUIDE 1	GUIDE 2	GUIDE 3	TOTAL
19		N/A*	N/A*	N/A*	30.8	108.1		
20		↓	↓	↓		49.7	138.7	
21		↓	↓	↓	9.52	62.6	2652.5**	
24		↓	↓	↓	3.3	12.2	206.9	
Average		↓	↓	↓	14.54	58.15	172.8	245.5

\* The AISI/EPA car does not have coking stacks, and as a result these columns are not applicable

\*\* Test 21 not included in average

A theoretical approximation of isokinetic mass values may, however, be obtained by applying Equation 16 to the anisokinetic data. Tables 25 and 26 present the calculated isokinetic values of mass emitted for the AISI/EPA and Wilputte cars, respectively, and from the basis for the 85.2% reduction figure.

A failure of the number 3 drop sleeve to seal during Test 21 may have been caused by a cocked emission guide. However, detection and hence, resealing of the drop sleeve was prevented by the emission guide. Therefore, Location 3 on Test 21 for the AISI/EPA car was omitted from all the average mass emission calculation. The magnitude of the mass, measured at 21-3, is another indication that it is not representative of a normal charge. It is almost two orders of magnitude higher than the next largest mass value for the AISI/EPA car.

Out of the 10 tests performed on the AISI/EPA car, no charge other than Test 21 demonstrated emissions of this magnitude.

The accuracy of the calculated isokinetic values in Tables 25 and 26 is difficult to assess. However, a comparison of the anisokinetic mass value to the calculated isokinetic values can be used to give an evaluation of the relative errors induced by anisokinetic sampling. It can be assumed that if the calculated value is close to the measured value, the error is minimized and the mass is representative of the emissions. As the difference between the calculated mass and measured mass increases, the values become less reliable. But they are still quite useful, for the difference between the values is a measure of the direction and magnitude of the error due to anisokinetic sampling. For example, in Test 10, Guide 1, the anisokinetic value was 41.7 gm; the isokinetic value was 42.9 gm; the masses are very close. One might, therefore, assume sampling was near isokinetic and if the sampling velocity (193.4/min) and the average stack velocity (204.3 ft/min) are considered, it is obvious conditions are near isokinetic.

TABLE 25

## CALCULATED ISOKINETIC MASS

MASS IN GRAMS FOR WILPUTTE CAR

TEST NO.		STACK 1	STACK 2	STACK 3	GUIDE 1	GUIDE 2	GUIDE 3	TOTAL
2						19.0	30.1	
5			410.6			28.4		
6				221.9			29.3	
7		117.8	125.8	94.1				
8		132.7	77.4	182.0				
9		20.2	234.3	213.6				
10					42.9	71.2	56.9	
11					48.4	42.0	58.0	
23			141.9					
8A		35.9	52.5	1028.2				
Average		76.65	173.62	434.95	45.65	40.15	43.58	814.7

TABLE 26

## CALCULATED ISOKINETIC MASS

MASS IN GRAMS AISI/EPA LARRY CAR

TEST NO.		STACK 1	STACK 2	STACK 3	GUIDE 1	GUIDE 2	GUIDE 3	TOTAL
19		N/A*	N/A*	N/A*	14.38	50.92	-----	
20					-----	23.20	74.26	
21					8.3	45.1	1736.78**	
24					1.3	5.68	86.78	
Average		↓	↓	↓	8.0	31.5	80.5	120.0

\* The AISI/EPA car does not have coking stacks, and as a result these columns are not applicable

\*\* Test 21 not included in average

Conversely, there is a large difference between sampling velocity (470.5 ft/min) and stack velocity (209.9 ft/min) for Test 7, Stack 1. As expected, there is a large difference between the mass values (~41.6%).

If this rationale is extended by comparing the anisokinetic and isokinetic values for average mass/charge, the Wilputte anisokinetic and isokinetic averages differ by less than 1%, while the AISI/EPA values differ by about 50%. This would imply the Wilputte data offers a somewhat higher confidence level than the AISI/EPA.

However, the 50% difference found with the AISI/EPA data is still relatively good, considering the sampling problems encountered with coke oven charging emission monitoring. The data indicates the constant sampling velocity method employed at the coke oven is more precise than originally expected.

#### SUPPLEMENTARY ANALYSES

Supplemental analysis was performed on particulate material collected from coke oven emission streams as well as prepared coal prior to oven charging. The intent was to establish the quality and quantity of trace constituents in the material and access the technique for these determinations. The body of data presented below represents the results of this analysis. The difficulties or limitations applicable to each area are discussed.

Tar roughly defined as the particle fraction soluble in benzene was found to be a major constituent of the collected material. The average tar concentration for a particulate sample was 57.1%. No separation was made between the Wilputte and AISI/EPA emissions due to the small number of samples analyzed for tar.

Tar analysis was performed on 20 samples which were primarily Andersen catches. In most cases, the analysis was done on the entire sample collected excluding impinger catches. However, a few samples were separated into parts (i.e., in Test 21-3). The Andersen plates were done separately from probe tip and the Andersen front. Table 27 lists the test number and % Tar as measured in the entire sample.



TABLE 27  
TAR CONCENTRATIONS

<u>Test Number</u>	<u>Location</u>	<u>Tar Percentage</u>
7	1	29.2
8	2	56.1
8A	3	25.9
9	1	75.0
10	6	86.2
11	4	42.1
19	1	64.8
21	3	<u>54.5</u>
Average		57.1

Polycyclic organic matter present in coke oven emissions will be found chiefly in the particulate fraction which has been defined as tar. Several of the more widely accepted carcinogens are species of benzpyrene. In order to establish and characterize the presence of this general group, Benzpyrene Analysis was performed on the tar portion of a group of samples. These tests indicate that benzpyrene is present in amounts ranging from 18,000 ppm to less than 260 ppm. (1ppm equivalent to 1  $\mu$  gram benzpyrene/gram of tar).

Sample sizes and lack of available analytical techniques precluded a more detailed examination of these samples. The data obtained is presented in Table 28 and gives the benzpyrene content for samples analyzed prior to and including the filter. A few analyses were performed on the impinger catches and are presented in Appendix B, but all measurements of impinger tests were below the detectable limits. The maximum concentration was 18,000 ppm found on the Andersen plates of Test 21-3. The Andersen front and probe tip also produced measurable values. The results indicate the general presence in the emissions of a species containing widely accepted carcinogenic substances in relatively heavy concentrations. Further conclusions are impossible because of the limited data.

An elemental analysis was undertaken to identify the trace constituents of the coal charged and the resulting emissions. The intended emphasis was the identification and quantification of hazardous elements, particularly heavy metals. The emissions analysis was performed on particulate sizing equipment catches, and was thus limited by the sample size, as well as available analytic techniques. These limitations resulted in a large number of instances where constituent concentrations, if they did exist, were below detectable limits. The emission constituent concentrations which were successfully measured and are reported in Table 29 are consistent with the constituents identified in the elemental analysis of the charging coal. The sample numbers can be cross-referenced with Table 30 to determine the portion of the sample that was analyzed.

TABLE 28  
BENZPYRENE ANALYSIS

Test Number	Location	Sample Number	Description	Total Benzpyrene ( $\mu$ g)	Benzpyrene Concentration* (ppm)
7	1	1045	Andersen Front Probe Tip	30	510
8	2	1060	Andersen Front Probe Tip	70	1,000
8A	3	1066	Andersen Plates	100	560
8A	3	1067	Andersen Front	B.D.L.	<260
9	1	1095	Andersen Front Probe Tip	B.D.L.	<630
10	6	1102	Andersen Front Probe Tip	30	560
10	4	1105	Probe Tip Cyclone	B.D.L.	<1,300
11	4	1111	Probe Tip Cyclone	B.D.L.	<1,000
11	5	1114	Andersen Front Probe Tip	B.D.L.	<590
19	1	1208	Probe Tip Filter	B.D.L.	<980
20	2	1213	Andersen Plates	B.D.L.	<1,400
21	3	1222	Andersen Plates	22,000	18,000
21	3	1223	Andersen Front	520	3,000
21	3	1229	Andersen Back	B.D.L.	<610
23	2	1241	Andersen Plates	220	1,700

\*  $\mu$ g of Benzpyrene/gram of Tar

**TABLE 29**  
**ELEMENTAL ANALYSES AND SUPPORTING COAL ANALYSES**  
**AISI/EPA DATA**

Test Number	Sample Number	Al %	Ba ppm	Be ppm	Ca ppm	Cd ppm	Co ppm	Cr ppm	Cu ppm	Fe %	Ga ppm	Ge ppm	Hg ppm	K %	Mg ppm	Mn ppm	Mo ppm	Na ppm	Ni ppm	Pb ppm	Sb ppm	Se ppm	Sn ppm	Sr ppm	Ti ppm	Te ppm	V ppm	Zn ppm
19-1	1208		5.1%	<.96		<11		.12%	90							140			770	250		<680	<710				<480	
20-2	1213		<.17%	<.83		110		750	750				83			410			.15%	.39%		<520	<560				<370	3.3%
21-3	1222		<380	<.16		<1.9		15	<6.9				.27			<2.8			11	35		<210	<84				<36	19
	1223		<290	.42		260		160	80				3.4			26			110	.37%		<160	<63				<28	.11%
	1224		<670	<.40		25		180	.31%				80			97			270	.330		<260	<280				<190	.22%
	1229		11%	<2.4		400		170	180				61			170			.18%	.59%		<3300	<.13%				<540	
	1230		<.95%	<4.2		28		860	.57%				28			260			1.30%	<830		<2900	<.31%				<2100	.19%

WILPUTTE DATA

7-1	1045	2.27	4.1%	<7.4	.65	<9.4	<59	.14%	280	.84	<360	<140	46	1.1	690	360	<360	2.5%	.12%	140	<540	<180	<.18%	400	540	<74	<74	1.1%
8-2	1060	0.39	4.7%	<8.8	1.14	<12	<73	.11%	110	.51	<460	<180	96	8	480	96	<460	.8%	.10%	6.4	<680	<230	<.22%	560	390	<88	<88	.64%
8A-3	1067	1.06	<1.7%	<3.5	.75	<4.7	<28	.11%	50	.87	<180	<69	12	.35	.38%	69	<180	1.57%	880	27	<260	<88	<880	31	820	<35	<35	940
	1066	.54	<0.3%	<6	<60	<7.8	<48	.36	<18	.22	<300	<120	20	.06	.30	36	<300	<300	61	<24	<450	<150	<.15%	<30	392	<60	<60	30.0
9-1	1095	3.74	15%	<31	1.56	<40	<240	450	130	.36	<.15%	<610	59	4.0	31%	190	<.15%	9.5%	500	500	<.23%	<780	<.78%	.17%	950	<310	<310	3.3%
10-6	1102	1.73	11%	<19	1.16	<25	<150	.13%	62	.96	<990	<400	150	1.6	.13%	250	990	3.2%	.10%	190	.19%	<490	<.49%	640	590	<190	<190	1.3%
	1105		<.32%	<.14		45		.16%	730				19			300			.17	490		<970	<.10%				<700	1.5%
11-5	1114	280	15%	<29	1.40	<38	<230	.29%	120	1.64	<.15%	<590	36		480	450	.15%	4.8%	.21%		<.22%	<740	<.74%	480	880	290	<290	1.9%
	1111		4.5%	<.86		470		.49%	390							1100			.88%	3.40		<560	580				<390	.86%
23-2	1241		.41%	.35		16		240	380				13			41			350	410		<350	<130				<57	

COAL ANALYSES

8A (W8)	1.06	<362	1.1	<99	<1.9	<79	49	9.2	.50	<490	<200	.06	.12%	180	9.2	<490	<490	66	<32	<740	<250	<81	<49	890	<99	<36	1
10 (W10)	.94	<320	<.14	240	<1.7	<56	42	<5.8	.49	<350	<140	.24	.09%	210	6.6	<350	<350	12	<28	<520	<170	<71	<35	690	<69	<32	8.4
23 (W12)		<360	<.16		<1.9		65	8				.27			3.8			57	44		<210	<80				<36	16
24 (K4)		<360	.54		<1.9		47	<6.7				.54			12			20	<32		<210	<82				<36	8.6

TABLE 30

COAL ANALYSIS (ULTIMATE AND PROXIMATE)

Test	As Received				Dry			
	8A	10	23	24	8A	10	23	24
% Carbon	72.94	73.23	73.89	72.91	78.28	79.01	78.16	77.77
% Hydrogen	5.34	5.29	5.13	5.11	4.92	4.83	4.78	4.71
% Nitrogen	1.16	1.13	1.27	1.35	1.25	1.22	1.34	1.44
% Sulfur	1.12	1.13	1.13	1.27	1.20	1.22	1.19	1.35
% Ash	6.90	6.56	7.36	7.40	7.40	7.08	7.78	7.89
% Oxygen	12.54	12.66	11.22	11.96	6.95	6.64	6.75	6.84
% Moisture	6.82	7.32	5.46	6.25	--	--	--	--
% Volatile Matter	30.34	30.50	31.90	30.59	32.56	32.91	33.74	32.63
% Fixed Carbon	55.94	55.62	55.28	55.76	60.04	60.01	58.48	59.48
(BTU/lb) Heat of Combustion	13.142	13.121	13.140	13.162	14.103	14.157	13.905	14.039

Some of the more important elements identified in detectable concentrations in the emitted particulate material were Cu, Fe, Pb, and Zn. Due to the variances in particulate sample sizes, it is not possible to make a generalized statement concerning constituent concentrations in the emissions. It should be pointed out, however, that no constituent concentrations in excess of what can be reasonably explained by coal constituents also reported in Table 29, was identified in the particulate material. In order to obtain more definitive information on particulate constituents, much larger samples distributed as a function of particle size must be obtained and analyzed. The particle size information is important in assessing the results, since this property will determine whether the particles fall or settle out quickly (i.e., particles  $>200\ \mu$ ), or behave similar to a gas in the atmosphere (i.e.,  $<3\ \mu$ ).

Further coal analysis was performed as support for the particulate analysis. Table 30 reports the ultimate and proximate analyses of the coal as received and dry. The size analysis is listed in Appendix B. One hundred percent of all four samples passed the 1" round sieve size and always less than 6% of the sample passed the number 200 square sieve size. The average size was between square #8 and square #30 sieve size.

The density of the particulate matter was investigated at the MITRE lab where float tests indicated the specific gravity of the solid portion of the sample ranged between 1.6 and .9 relative to water. Generally, better than 50% of the solid particles were greater than 1.3. The tar portion of the sample was assumed to have a specific gravity similar to that of coal tar between 1 and .85. To simplify calculations using density throughout this document, 1.2 g/ml was used as the approximate density. This is probably on the high side of the average. However, there was not enough data concerning the density of the tar portion of the sample to justify any other value.

As a part of the supporting analyses, a sample of the collected particulate was provided by EPA to the Columbus Laboratories of Battelle. The sample consisted of a number of black granules, and a loaded 5 cm

diameter filter. Several of the granules were placed in a probe tube and inserted into the MS9 mass spectrometer. Eight high-resolution mass spectra were obtained starting at 60°C and terminating at 350°C. The spectra were dominated by hydrocarbon fragments and a strong phthalate ester peak at mass 149.024. This latter peak was thought to be attributable to a contaminant from the plastic bottle top of the container. No evidence of carcinogens was found in this analysis. However, ions with mass 228.094 ( $C_{18}H_{12}$ ) and 252.094 ( $C_{20}H_{12}$ ) were detected. These peaks correspond to the molecular ions for benzphenanthrenes and benz-( $\alpha$ )pyrene, or their structural isomers. It is, of course, impossible to determine from high resolution spectra whether the carcinogens are actually present or whether the peaks are due to their noncarcinogenic isomers. Detailed chromatographic studies would be required to confirm the presence or absence of the carcinogenic PNA's. Unfortunately, extraction of the few remaining black granules with methylene chloride yielded insufficient soluble material to permit gas chromatographic-mass spectrometric analysis.

The sample filter was Soxhlet extracted with methylene chloride for 30 hours, and the extract concentrated to approximately 0.25 ml. A portion of this extract was injected into a MS9 probe sample tube, and the sample was thermally volatilized. Six high resolution mass spectra were obtained, starting at a probe temperature of 60°C and terminating at 300°C. Despite repetition of these high resolution runs, the exceedingly complex mixture and high number of compounds present precluded detection of the most important reference calibration peaks. Consequently, no useful high resolution data was obtained from this sample.

The filter extract was subsequently subjected to gas chromatographic-mass spectrometric analysis, using both OV-17 and Dexil 300 columns, in an attempt to detect OSHA carcinogens and carcinogenic polynuclear aromatic hydrocarbons, respectively. The total mass chromatogram, obtained using OV-17 (150 to 280°, programmed at 6° min<sup>-1</sup>), exhibits a large number of quite well resolved peaks. In only one instance was there a possibility of the presence of a carcinogen, benzidine. Three

lower polynuclear hydrocarbon, anthracene, pyrene, and fluoranthene, were readily identified from their mass spectra and chromatographic data.

In order to examine the possibility of the loaded filter extract containing known polynuclear aromatic hydrocarbon carcinogens, gas chromatographic-chemical ionization mass spectrometry was carried out using a 10-foot 2-1/2 percent Dexil 300 at 260°C, programmed at 1°C min<sup>-1</sup> to 300°C. The combination of mass spectra and chromatographic data clearly indicated the presence of benz(c) phenanthrene (potent carcinogen), benz(a) anthracene (carcinogen), a benzfluoranthene isomer (possible carcinogen), a benzfluoranthrene isomer (possible carcinogen), benz(a)pyrene (potent carcinogen) and/or benz(e) pyrene, and cholanthrene (carcinogen).



## OPTICAL SYSTEM PROGRAM RESULTS

The primary objective of the optical measurement program is to determine the feasibility of a compliance monitoring system for charging emissions based on the technique of plume optical transmittance measurements. This assessment of feasibility is logically divided into three areas; technical feasibility, implementation feasibility, and operational feasibility. The technical feasibility of the optical system concerns the demonstrated ability to measure plume transmittance with conventional light sources and photographic recording techniques. The basic measurement concept has been established under laboratory conditions by several other investigators. MITRE's optical measurement program extended this work to establishment of feasibility under field conditions for polydisperse emission plumes with high dynamic characteristics. The second area, implementation feasibility, concerns the availability and practicality of equipment and materials needed to implement and operate the system in the environment of an operational coke oven. The feasibility of this approach for other extended emission sources should be investigated independently, however, the coke oven environment is sufficiently severe and demanding so as to provide a basis for a valid implementation feasibility test. The last area, operational feasibility, concerns the cost of fabricating, installing and operating a number of such systems on typical coke ovens, where operating costs cover the upkeep and maintenance of the equipment, as well as the cost of film densitometry and data analysis. Other factors to be included in a feasibility assessment are the accuracy and dependability of the system, how information from this system might be used in a compliance system, and what equipment configurations might be applicable for such a system.

### Technical Feasibility

In order to provide a theoretical background for the proposed measurement, the basic theory of particle and light interaction had to be shown to be compatible with the expected polydisperse characteristics of the coke oven emissions. Such a compatibility can be shown mathematically and was developed in the preliminary optical system report, MTR-6546. In

addition to the basic transmission measurement theory, a theoretical technique for the detection of non-source light interference (plume air-light) was developed and explained. The theory showed how the system could be self-compensating for long term variations in light source conditions and ambient lighting conditions.

The objective of most optically oriented systems has been to estimate mass loading value by dealing with a known volume of intervening space between light source and detector. The intent of this system is to estimate total mass emitted. With such an intent, the geometry of the system is relaxed and variability in size of the emission plume is diminished in importance. The theory of this system has been to estimate the mass in a cross-sectional area in the path of the light source. In order to produce an estimation of total mass emitted, a measurement of the vertical rise speed of the plume must be made. The mass rate indicated on a single photographic frame multiplied by the rise velocity was shown theoretically to be a reasonable estimation of total mass emitted over time. The characteristics of plume dynamics for the charging cycle were studied and reasonableness of plume consistency over a period of a few seconds established. In addition, it was found that a characteristic velocity for plume rise rather than a continuously measured value did not seriously affect the validity of the measurement system.

A study of photographic material characteristics was conducted to establish the availability of a suitable film for the proposed measurements. The study showed that the material having the widest exposure range and longest linear portion of the exposure curve was one of the most common photographic films. This fact simplified the selection of film for use in this system. The choice of film was then considered in the determination of the required intensity for the system light source. This investigation showed that there were several common light sources available which could produce the required intensity.

A limitation basic to the proposed system configuration was the probable undependability of mass calculations in situations where the transmission fell below 10%. This is because in such a situation, multiple scattering

has an increased likelihood of occurrence. A lower limiting value for transmittance was selected after consideration of the distance between the light source and detection, the acceptance angle of the detector, and the expected nature of the emissions. Based on this limitation, the system will calculate a maximum mass value for the point corresponding to the lower limit and indicate that the calculated value is  $\geq$  the actual mass rate.

It is now felt at the conclusion of our test period that all theoretical aspects of the system have proved to be feasible within the constraints expressed at the outset of the project. Some questions have arisen stemming from the highly variable nature both in size and composition of the particulate as to the ability of developing average characteristics. However, such a limitation would have equal impact on other mass measurement approaches and is not considered a detriment unique to this optical system concept.

#### Implementation Feasibility

During the selection, fabrication, and assembly of system components, one criteria which was stressed was off-the-shelf availability. The major components of this system meet this criteria. The selection of components also considered the adaptability of components to other locations or environments. This objective was accomplished to a lesser degree.

The test system utilized a standard sequence camera which was modified to provide a secondary exposure of a digital clock. This system proved to be a virtually trouble free recording device. Although the camera was not run in an unattended mode, its performance was such that the feasibility of unattended operation was established to a great extent. All tests performed on the camera to establish its reliability yielded positive results. Specifically, the test for accuracy and repeatability of shutter timing shows a repeatability of better than  $\pm 4\%$  of the marked values at 1/1000 and 1/50 second speeds. On continuous runs of 12 and 24 hours at one frame per second exposure rate, no malfunctions occurred in the camera system. Modification which might be desirable to increase

the film capacity of the camera should not affect the basic reliability and operability of the unit.

For extended periods of operation (one month) camera equipment would require a minimum of a "dust proof" housing with a suitable transparent window which can be cleaned regularly without optical damage. Such an enclosure could be constructed using a NEMA water tight box with a hard plate glass window installed. A cleaning and maintenance routine similar to those used for pen-type pressure and temperature recording instruments in use in the oven environment should be sufficient for reliable operation.

The camera was operated using an AC power supply during the field test period. The basic camera, however, was designed to operate from a 12 volt DC power source, such as a battery. The camera was tested in the laboratory using a 12 volt battery and found to operate in essentially the same manner with no detectable degradation in performance. Such a capability provides operational flexibility needed in situations where temporary operation in a remote or difficult to reach location is required.

Additional details of tests performed on the camera system can be found in Appendix C of this report.

The camera control used in the test configuration was somewhat more complex than would be required for an operational system. This complexity was the result of control flexibility needed in performing the tests. The test, however, demonstrated the feasibility of the control concept. Specifically, a control circuit based on a clock locked to the AC line provides a satisfactory time base for the system. This clock consists of integrated circuit counting modules which drive both the digital display recorded on each film frame and exposure control. A fixed exposure rate (one frame per one or five seconds) would be wired into the system.

During the test period, occasional electrical noise would cause the clock counter to advance. The environment of the coke oven contains much high power electrical equipment which can generate electrical spikes on the

AC power line. For this reason, additional attention should be given to the power supply of the control unit to eliminate this interference. This problem is not, however, considered serious and should be relatively easy to solve.

The camera control unit is designed to operate from either 110 volt AC commercial power or 12 volt DC power. In the DC operational mode, the camera exposure rate is continuously adjustable using an RC circuit. The digital display then becomes a counter operating on the frequency of the exposure pulse. Should a realtime clock display be desired on DC operation, a time standard oscillator operating at radio frequency must be added. Such an oscillator would provide a standard with accuracy of better than  $\pm 5$  seconds in 24 hours. All other functions of the control remain the same.

The system light source is the one component which must be considered "custom made" for the specific observation site. The unit fabricated for this test utilized all off-the-shelf electrical lighting components with the exception of the reflector surface. The intent of the special reflector was to obtain maximum apparent source width with uniform light output across this width. The parabolic reflector proved to be very efficient in the achievement of this objective. Densitometry traces across the width of test frames showed excellent uniformity. It was originally expected that a 10 inch width might be required to provide for densitometry alignment error. Experience has shown, however, that the densitometry trace can accurately follow an image of a source having a width of less than 200  $\mu$ . For this reason, it is felt that the special reflector could be replaced by 4 or 5 parallel fluorescent tubes, each having a diameter of 1-1/2 inches.

The stroboscopic effect of fluorescent tubes was discussed in the document containing initial design considerations. It was decided that the simplest method to eliminate this problem was to use a shutter speed that would capture one complete cycle of light source supply current. Test exposures using this method showed minimal variation in image density less than  $\pm 5\%$  exposure change for the overall system. It is felt, however,

that this might be improved by using a DC supply voltage for the fluorescent tubes. Discussions with tube manufacturers indicate that such operation is possible and can be implemented with few changes. These consist primarily of isolating a filament supply source and provision for periodic polarity reversal to prevent breakdown of the tube through the plating effects present in DC operation. It should also be noted that the light output of the unit would be increased for a given supply voltage and any shutter speed could then be used without stroboscopic related problems.

The system light source is physically the largest system component. In addition to this fact, its configuration is affected more by the physical details of the observation site than any other unit. The light source for the test system was designed and fabricated to provide maximum flexibility both at the test location and for possible reuse at some other site. Even with this in mind, major structural components would probably require considerable modification for reuse. It is difficult to imagine a suitable "portable" unit which would be designed for quick assembly and disassembly. It is expected, therefore, that each site to be observed would require a unit designed for that location and permanently installed on suitable support structures.

All other details of the light source configuration are considered feasible and desirable and would be recommended for inclusion in specifications for new units.

The environment of a coke oven is quite severe on all types of equipment. The pervasive heat, corrosive gases, and dust/grit, act upon all equipment in the area. It was necessary to select or develop system components which could function continuously in this environment. During the course of the tests, no significant problems were encountered in maintaining the various system components selected for system implementation. The system light source was left in place and is still operating as a lighting facility for the P4 battery.

The densitometry analysis of film from this system was the area where the most difficulty in performance was encountered. It is well within the capability of standard densitometers to measure density with the required accuracy for small image areas. There are also many machines which produce a computer compatible magnetic tape output. The primary difficulty with such machines is that they are not normally used to selectively scan a small portion of the image area, but rather to scan the complete area and allow computer processing to locate and reconstruct the area of interest. Although such an approach might be applicable to our system data, it was decided that the necessary computer programming for image recognition was excessive in terms of the desired test results. A rather specialized machine with the ability to provide usual image alignment, selectability of small scanning areas and computer compatible magnetic tape output was selected for film analysis. The resolution, accuracy, and stability of the machine were somewhat greater than would be required for our analysis. As a result of its unique features and versatility, the machine availability was less than desirable and the operational cost higher than expected. Film analysis using this machine and associated operational practices is not considered to be feasible for any large scale operation of the system.

Film processing and calibration is an important phase of system operations. Although the actual processing of the film is not complex, very few service facilities were found which would guarantee the control necessary in the processing operation. This is explained by the fact that such control is not normally necessary in processing for standard image photography and the amount of processing which we projected for the conduct of the test was not sufficient to persuade a supplier to change his operations to accommodate our needs. It was determined, however, that the facility providing densitometry analysis could provide the required processing on a custom basis. They were also equipped to provide the sensitometric exposure calibration. It was decided that total film analysis service at one location was more desirable than a possible reduction in film processing costs.

Although not feasible for large scale implementation under the cost structure applied during this test period, the basic processing techniques are considered feasible. It is reasonable to assume that given some amount of assured business, a service organization would be willing to establish a facility where the required processing could be done on a routine basis.

### Operational Feasibility

The operational feasibility of this system for coke oven monitoring is difficult to assess for two reasons. First, the standards for emission compliance are not accurately defined or generally expressed in direct quantitative terms. Second, there are few, if any, alternative systems against which to compare the technique on a cost and operability basis.

The camera equipment required for such a system is available as an off-the-shelf item. The cost of this type of equipment ranges from \$1500 to \$8000 per unit. The primary difference in the various units is the level of versatility and ruggedness. The less expensive units provide acceptable performance and are suggested for system implementation. Since it is feasible to use one type of camera for a wide variety of site configurations, the modification required to place the secondary exposure of the digital clock display on the frame might be offered as a standard option on that type. The cost and availability of the equipment discussed above is considered reasonable and feasible for such a system.

The camera control system was a custom designed unit but could be greatly simplified when a routine is established for system operation. Reliability of the system is such that no change in the basic components is necessary. An improvement in line noise interference is needed but this should not affect the complexity, reliability or cost of the unit. It is estimated that a control suitable for system operation could be constructed in quantities of 10 or more for under \$300. Because of the limited quantity, they would be produced by a custom or small run fabrication facility. The basic concept and design is considered practical and feasible for



system application with a per-unit cost of up to \$500. If the cost should exceed this figure, it might be advisable to utilize a commercially available digital clock and display and an electromechanical exposure control.

The physical arrangement of the light source for the system is highly dependent on the characteristics of the monitoring site. The support structure for the source must be designed to allow normal operation of the coking plant. This involves minimization of interference to the oven top so as to provide the access necessary in the maintenance and operation of the battery. The structure must span the battery and extend over each end by several feet. The side sections must extend downward as close as possible to the oven surface. The support structure can be expected to represent at least half of the total light source cost.

The test activity showed that fluorescent lamps of the "very high output" type provide suitable light sources for this system. Placing four such bulbs side by side should provide suitable source width and eliminate the need for the rear reflecting surface. If these lights are operated from an A.C. source, the required case, lens, electrical components and fabrication are estimated to cost \$250 per 8 foot section. To operate these lamps on D.C. current would add approximately \$50 per 8 foot section to the cost. The costs would be the same for the side or "wing" sections of the source.

In general, coke ovens runs 45 to 55 feet wide. The light source should be placed above the larry car height which runs between 15 and 20 feet. With these assumptions, the typical installation would consist of 10 to 12 eight foot light sections. The total cost including a supporting structure, is estimated at between \$3500 and \$6000.

The light source should require a minimum of maintenance which can be performed by regular plant electrical maintenance personnel. Assuming a continuing requirement for emission surveillance and compliance monitoring and the costs of continuous equipment or trained personnel for visual observation, the cost of the light source and supporting structure is considered economically feasible. This assessment also takes into

account the direct operating cost of electricity supplied to the unit.

Processing of the film from this system must now be accomplished on a "custom" basis. The processing cost currently runs 29 cents per foot of film processed. At approximately 750 frames of data per 100 foot of film, the processing cost would be approximately 3.9 cents per data frame. At an exposure rate of one frame per second for approximately 2.5 minutes needed to charge a coke oven, 150 frames of data would be taken. The processing cost per average charge observed would then be approximately \$5.85.

If some volume of business could be guaranteed to a service organization, the cost could probably be reduced from 20% to 40%. However, the current cost of 3.9 cents per frame is not considered prohibitive for a system which would operate only during charges or during periods of high emission detected by some secondary system.

Densitometry analysis of the film output from the measurement system presents the greatest problem in current system operational feasibility. Because of the unique nature of the scanning requirement, the use of a highly flexible and sophisticated microdensitometer is required. As a result, the cost of analysis is high and the response time for this service is relatively slow because of the large demand for the instrument in question to perform other work. The standard rate set by the particulate supplier used in the test program is \$30 per hour for the instrument and \$16 per hour for the instrument operator. The machine must be set up for the particular scanning job which requires 15 to 30 minutes. This time is charged as operating time at the regular rate.

At these rates, the data frames scanned during the course of the tests cost between \$10 per frame including all test frames, calibration, special uniformity checks and set up, or \$15 per frame counting only test data frames scanned as production runs.

The use of a microdensitometer can only be considered feasible if the machine can be dedicated to this particular type of film analysis. This would allow the machine to be modified to facilitate quick and accurate

mounting of the system film size. It would also eliminate the "set up" operation since it is reasonable to assume that film from different observation sites would be very similar in terms of light source image size and density range. The utilization of such a machine would also lower the required skills of the operator. Since the machine could be made automatic once a scan is initiated, the operator would only be required to initially position the film in the machine and monitor the operation for obvious malfunctions. Output from the machine would be placed in computer compatible form on magnetic tape.

A machine capable of performing the required analysis is estimated to cost between \$5,000 and \$8,000. The machine could probably scan one complete frame of data in three to five minutes. If film was taken or analyzed at one frame every five seconds, the typical coke oven charging operation extending over three minutes would involve 36 frames. The optimal analysis time of the data frames would then be about two hours. To completely cover all oven charges on one battery during a typical eight hour shift (40 charges), the scanning time would be about 80 hours of machine time. Such coverage and analysis is not considered operationally feasible. Both time and money are considered to be excessive for such coverage. Should complete surveillance be considered necessary, a comparison would have to be made between this system and other systems with similar capabilities with particular emphasis placed on the data retrieval aspects of system operation.

If one hypothesizes the use of analysis by exception, the system analysis feasibility is greatly enhanced. As an example, if the camera is only activated during periods of excessive visible emissions, the amount of analysis required could be greatly reduced. The analysis load could be still further reduced if some specific number of film frames were to be established as a basis for non-compliance [i.e., visible emissions in three consecutive frames (15 second period) exceeding some set level]. Then analysis could be reduced to 20 to 30 minutes machine time for any charge during which violation is suspected.

The job of initial emission detection could be accomplished by several long path transmissometers crisscrossing the oven surface above the level of the larry car top. When one or more of these units detected some lower level of opacity, they would cause activation of the camera unit which in turn would take some predetermined number of data frames. This record could be correlated with over activities through the operation time logs.

Under the above assumptions, the use of a microdensitometer is considered feasible for use in data acquisition in the optical monitoring system.

Data processing of the densitometer output is a fairly straightforward task. The algorithm involves simple arithmetic and a relatively small amount of core memory is required to execute the program. The input to the program can be totally on tape and the output can be a single line giving the mass rate for a particular frame or a more detailed report displaying the quantities involved for each scanned point across the bar. During the course of the test data analysis, the latter option was chosen to allow a more detailed examination of the data and the results of the computations. Although helpful in gaining an understanding and confidence in system operation, the additional printed information is not necessary to the operational output of the system.

Computer compatible data (in a form which can be directly input to the computer) is feasible and indeed necessary to the efficient operation of any such system. The amount of raw data obtained from this system would be unmanageable in printed or strip chart form for any operational extension of the concept.

#### System Accuracy

Because of the multiple steps involved in system operation, opportunity for error is increased substantially over any single step measurement. In addition, some assumptions must be made to allow the application of this technique to a practical situation. The most important assumption is that the size of the emission particles can be accurately represented by some size distribution and that that distribution remains relatively

constant over the test period and to a lesser extent constant from one test to another.

Based on the information originally available on particulate sizing for coke oven emissions, a much larger particle size was anticipated. Under varying size distributions for larger particles, the effective light removal capabilities of a particle remain essentially constant at a value equal to about two times its cross-sectional area. For small particles, however, the effective light removal capability of a given particle varies between one and four as a function of particle material, wavelength of source light, and size of particle.

Coke oven emissions were found to be very dynamic in nature. The quantity of emissions varied widely over the total charging period, between source points in the charging system, and between the old and new charging cars. In addition, the visual characteristics of the emission varied widely from a puffy black smoke generally associated with visible flames around the car, to thick brown or mustard colored plumes which appeared to be the raw gases driven off the coal with little or no combustion taking place. Any investigation as to how each type of emission behaved in terms of optical system considerations was beyond the scope of this investigation. A further complication in the measurement process was the bi-populate nature of the particle size distribution. This fact negated the simple analysis of a single distribution and the establishment of a single mean diameter value to use in volume calculations.

In order to facilitate measurement calculations, the two distributions were considered separately. Through analysis of the particulate material, it was determined that the larger particles were made up primarily of carbon or coal particles, while the smaller particles were composed primarily of tar. Using this information, curves of K values versus particle size were selected for these materials, and the geometric mass mean radius of each separate distribution established. The representative value for K was determined from the curves using the mean radius. The two values were combined to produce a single value for computation by weighing each value as a function of the particle sample mass distribution.

The above discussion is included as an example of how difficult the accurate determination of particle size distributions can be, and what assumptions must be made if the distribution is found not to fit some standard form such as a single normal or lognormal curve. In addition, if the particle size tends toward values below 10  $\mu$  in diameter, the mass values calculated for assuming one mean diameter can vary by a factor of four with very small changes in the particle distribution and thus in the actual effective mean diameter.

Actual experience with some particular source or type of source can greatly improve the accuracy of the system through increased knowledge of the typical optical properties of the emission. The system could only approach 100% accuracy if the emissions were all of the same material with similar optical properties (surface conditions) and all particles were of the same size. With minimal knowledge of the particulate characteristics, only order-of-magnitude accuracy can be expected for total mass measurements. However, relative measurements performed on some small source which exhibits reasonably constant particle characteristics (either observed or measured) can be expected to have an accuracy factor on the order of 2-5. It is this range of accuracy which appears reasonable for measurements made with the experimental system.

To make the operation of this system feasible, two other assumptions must be made which are multiplicative in terms of mass measurement errors. The basic assumptions are that a representative value can be determined for particle density and emission rise velocity, and that these values once determined, remain relatively constant. In both situations, it is difficult to conceive of a case where the selected value for either quantity would introduce an error greater than 25% and indeed, the error actually experienced would probably be <10%.

Analysis of particle samples show that the primary constituents are tars and carbon or coal. The densities have ranged between  $\sim 0.9 \text{ Gm/cm}^3$  and  $1.4 \text{ Gm/cm}^3$ . The apportionment between the two materials has shown reasonable consistency. Based on these observations, a representative density of  $1.2 \text{ Gm/cm}^3$  was established. In the presence of very low emissions, we

would expect the material make-up to tend towards a predominance of tar and the selected value would tend to be high. If emissions were particularly heavy indicating considerable combustion and turbulence in the oven, the emissions would probably tend toward carbon and the selected value would tend to be low.

The selected value for emission rise velocity was based on a large number of photographic observations of plume behavior. Few inconsistencies in behavior were rated. This is probably because the position of the plume, when observed by the system, is removed from the larry car stacks and hopper structure, and its behavior is primarily determined by ambient air conditions which remain relatively constant.

The exception to this is when a relatively strong crosswind is blowing. The plume in this situation can have a horizontal velocity  $\geq$  the vertical velocity. In such a situation, the plume will probably pass across one of the light source vertical wing using units rather than the horizontal light source. In such situations, it might be necessary to make some wind measurements to obtain a reliable value for emission velocity pass the vertical bar units. In any case, the representative vertical velocity, when applied to the horizontal bar under minimal wind conditions, should cause minimal error in system measurements.

A second area of system error apart from the necessary quantitative assumptions, is the inability of the system to see or detect all emissions occurring on the oven battery during charging. This deficiency is a result of the geometry of a feasible system installation on a typical coke oven. In Figure 22 the field of view of the camera with respect to the light bar and the oven surface is shown. As the field of view narrows toward the camera, additional portions of the oven surface and space above that surface are excluded from detection by the system. The drawing shows what are considered ideal locations in terms of image size and detection locations. The camera could be moved further away from the source to provide an enlarged field of view, but this would have the effect of increasing the differences in plume behavior caused by the variations in distance from emission source for different positions on the

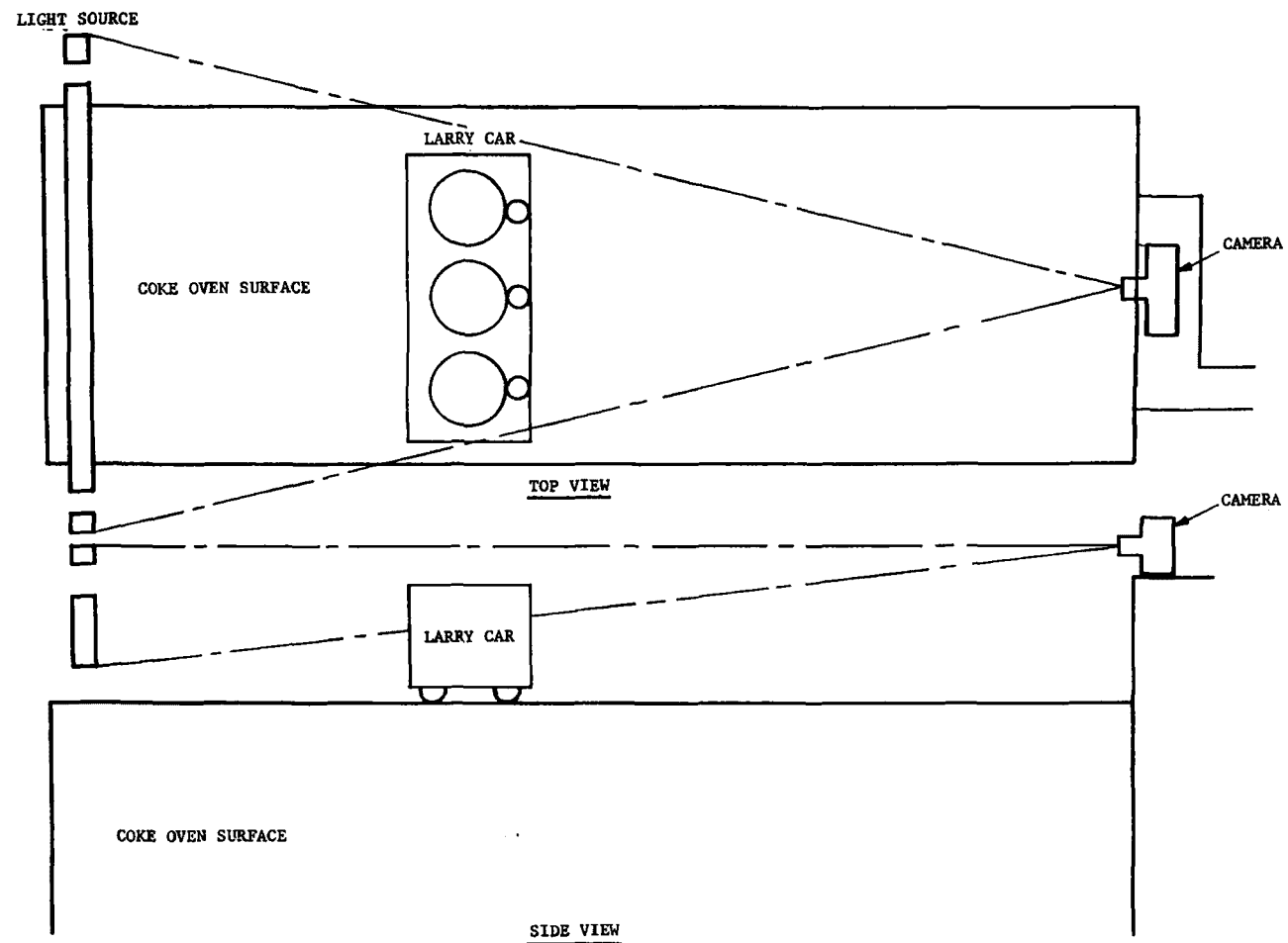


FIGURE 22  
TYPICAL SYSTEM GEOMETRY



oven. It would also tend to decrease the photographic image size which in turn makes densitometry more difficult. The light source might be increased in size, but this quickly approaches the practical limitations of available support for the structure. Additional cameras could be added, but the costs of implementation and operation would be increased proportionately.

It also appears possible, based on test experience, that light emissions occurring around the base of the car could become so diffused before rising to a detectable point above the car that the system would have considerable difficulty distinguishing them from heavy background or ambient.

In general, the conclusion must be drawn that this monitoring concept in configurations similar to the experimental system cannot be expected to provide 100% coverage or positive detection of any light emissions. Change to the system configuration can be made, but this would result in substantial increases in both cost of experiment and operation.

#### System Configuration, Operation, and Data Analysis

The configuration of system components in the implementation of this measurement concept does not provide a large latitude of possibilities. The detector (camera) must be positioned on one side of the emission plume and a light source must be positioned on the opposite side. The use of a reflector in place of the light source considerably complicates the system implementation, as well as data interpretation, and is not felt to be a practical alternative. As we stated previously, some secondary system for initial emission detection should be considered. This would allow the optical system to operate on an exception basis rather than continuously or on every charging sequence. Such a system might include relatively simple transmissometers operating over long paths over the oven top. These paths might use a single reflector at one end in order to minimize the number of units required. A simple path configuration is shown in Figure 23.

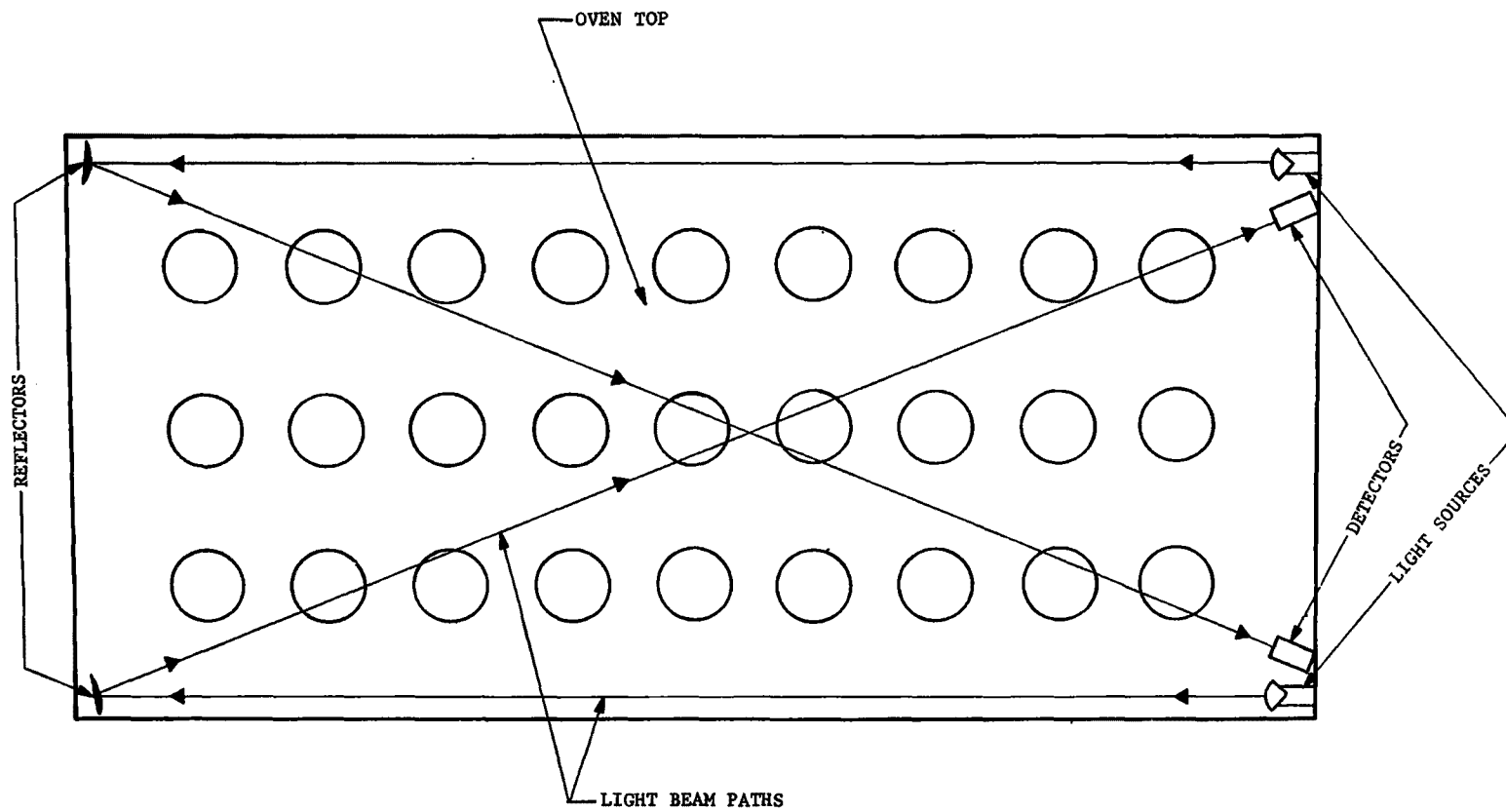


FIGURE 23  
SECONDARY EMISSION DETECTOR ARRANGEMENT

The system operating in this mode could function unattended for periods of days or weeks, assuming an 80% or greater compliance record and large capacity film magazines. The primary attention need by the system would be the occasional cleaning of the light source and camera/associated optics, the changing of film magazines, and checks of data clocks and secondary detection system operation.

In comparison to a Ringelmann assessment of emissions, the experimental optical system can provide additional data with higher quality. As applied to coke oven observations, the Ringelmann technique cannot account for the quantity or size of the emission plume. This is important in determining the total emission because of the wide variation in point source characteristics on and around the larry car. The coke stacks for instance, release large quantities of dense opaque emissions while small leaks around the drop sleeve may release equally dense emissions, but of a much lower volume. The situation where a large number of small leaks release a large quantity of diffused emissions as contrasted to a small dense emission from a stack is also not adequately differentiated. As understood for current compliance monitoring, the Ringelmann observer would time the period over which he observed a certain opacity, not noting the quantity (plume size) of emission at that opacity. This could obviously give a distorted picture of the actual emission volume in comparison to observations made on other charges. The optical system should be able to provide information that more truly reflects the actual quantity of emission and allows a better basis for comparison of this quantity between individual charging activities. The system has also been shown to adjust for conditions beyond the control of the Ringelmann observer, such as light conditions and color of the emission.

As previously stated, the optical system, although not providing a highly accurate value of absolute mass emitted, should provide a reliable basis for relative mass measurements within the system. If, however, the quantitative aspects of mass measurement are not sufficiently accurate or reliable for use in a compliance system, the basic transmission (the reciprocal of opacity) measurement capability of the system provides an

improvement over Ringelmann in terms of accounting for emission volume. By dividing up the light source into many point sources, the system makes the equivalent of many instantaneous Ringelmann assessments over a wide area with the advantage that variables, such as emission color or ambient lighting, have been eliminated or compensated for.

An example can be given to demonstrate this capability. Assume a light source whose photographic image can be divided into 500 equal sections for purposes of density measurement. If the bar is 50 feet long, then each of the 500 spots would represent a .1 foot wide area of the light source. Suppose that transmission values were determined for each of the 500 points along the bar, and that corresponding Ringelmann numbers were assigned to each of the points. These numbers could then be summed to provide a composite value (referred to here as a Ringelmann "Quotient" - RQ) which would take into account the size or extent of the emission plume or condition. A perfectly clear bar would produce a sum of zero, corresponding to a Ringelmann of "zero." Assuming a Ringelmann 1 condition across the entire bar, the sum would be 500. If a Ringelmann 2 condition existed across the bar, the sum would be 1000. The other Ringelmann sums would be proportional for constant Ringelmann numbers. The system upper cut-off limit at 90% opacity would yield a Ringelmann sum of 2000, which would also be obtained for an 80% opacity condition.

Since conditions can be expected to vary from point to point on the bar, the Ringelmann sum would be expected to vary as a function of emission quantity between 0 and 2000. Since a value for one photographic frame represents an instantaneous rate, the sum values for several frames might be totaled and divided by the number of frames to provide a rate average over time. As an example of how a Ringelmann Quotient would work for actual data, two optical system data frames of contrasting emission conditions along with their assigned Ringelmann Quotient (RQ) and calculated mass emission rates are presented in Figure 24. Additionally, the values used to compute the RQ from transmission data are presented in Table 31. For the test system, 539 spot transmission measurements were made yielding a possible maximum RQ value of 2156. This value would

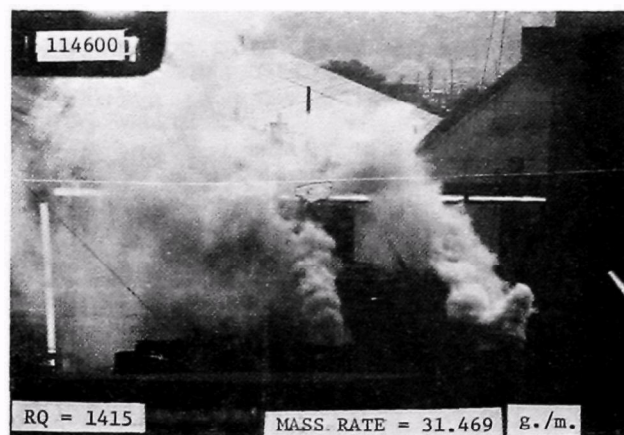
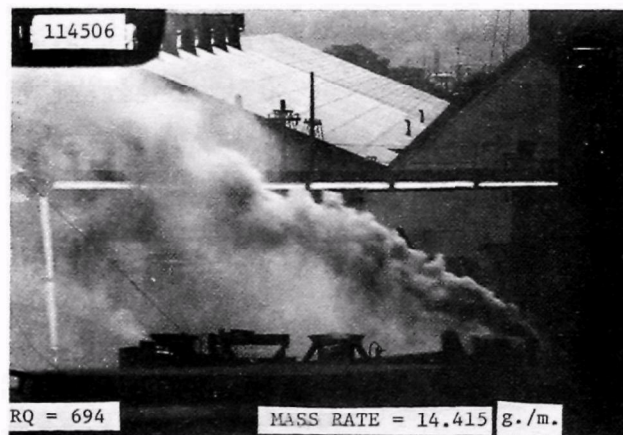
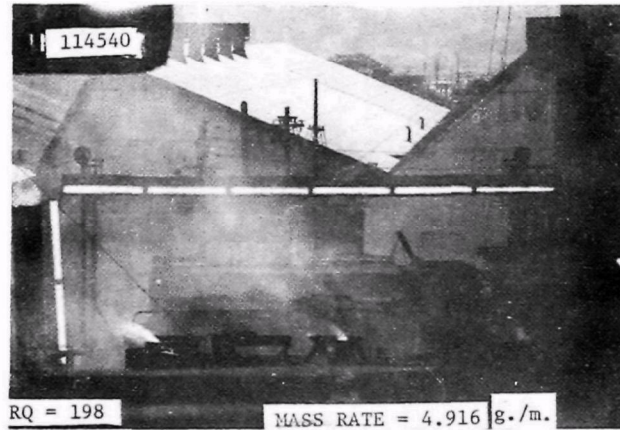


**FIGURE 24**  
**EMISSION CONDITIONS AND CALCULATED RQ VALUES**

TABLE 31

CONVERSION OF TRANSMISSION VALUESTO RINGELMANN VALUES

<u>% Transmission</u>	<u>% Opacity</u>	<u>1/T</u>	<u>Corresponding Ringelmann Value Assigned</u>
100	0	1	0
90	10	1.11	
80	20	1.25	
70	30	1.43	1
60	40	1.66	
50	50	2.00	
40	60	2.50	2
30	70	3.33	
20	80	5.00	
10	90	10.00	3

correspond to a Ringelmann condition 4 measured at all 539 points along the light source. The test system cannot, however, reach this absolute value since about 30 points fall on gaps in the light source and are assigned 0 mass values. It is easy, however, to see the difference between the two RQ values in comparison to the emission conditions pictured. It can be seen that such a technique might offer an improved capability in assessing the amount of emissions actually released to the air during a charging operation.

#### Data Processing Output

The basic output of the data analysis for the optical monitoring system is a total mass rate value per unit vertical height of the emission plume. This value is in turn made up of 539 individual mass rate values calculated for corresponding spots along the length of the light source. In an operational situation, the only number of interest is the mass rate associated with a particular frame. For purposes of system performance assessment, however, additional information was included on the data analysis print-out for the selected tests. Figure 25 presents one page of a typical analysis print out.

The header information contains frame identification consisting of test number and frame time in hours, minutes, and seconds. The base and scan numbers used in "housekeeping" refer to the base frame number on the data tape and the scan number performed against that particular base. Each of the seven line groups on a page present data from fifteen consecutive points in the left to right scan of the light source. A total of six pages are required to present the 539 points from one complete scan of the light bar. A seven space column associated with a single point contains the base exposure value (no emission) for that point on the light source labeled "BASE L". The base exposure value for the corresponding spot on the black portion of the bar is obtained by averaging black area readings over some specific number of points at the end of the light source and designating this average as a constant to be used in all calculations involving that base frame. This value is presented as part of the header information and is labeled "ZERO PAL",

TEST 7 ZERO PAL = 1.077															
* LIGHT BAR GAP	* PAL > BL	* DL > BL	* DL < DD (NOISE)	* DL < DD (NOISE)	* DL < DD (NOISE)	* DL < DD (NOISE)	* DL < DD (NOISE)	* DL < DD (NOISE)	* DL < DD (NOISE)	* DL < DD (NOISE)	* DL < DD (NOISE)	* DL < DD (NOISE)	* DL < DD (NOISE)	* DL < DD (NOISE)	* DL < DD (NOISE)
DATA D	1.906	1.962	2.020	2.020	1.962	1.962	1.906	1.962	1.906	1.906	1.906	1.906	1.906	1.906	1.906
BASE L	9.903	9.903	10.048	10.055	10.055	10.055	10.499	10.346	10.346	10.346	10.195	9.903	9.903	9.903	9.903
DATA L	4.712	4.477	4.477	4.633	4.633	4.633	4.400	4.555	4.477	4.477	4.477	4.477	4.477	4.477	4.477
1/T	3.146	3.539	3.709	3.666	3.666	3.666	3.778	3.575	3.606	3.606	3.567	4.433	3.539	3.539	3.539
LN(1/T)	1.14612	1.25542	1.32680	1.29909	1.27710	1.29363	1.32915	1.27401	1.29247	1.28247	1.26612	1.23355	1.26386	1.25311	1.24500
EL MASS	0.950	0.954	0.957	0.956	0.955	0.956	0.958	0.955	0.956	0.956	0.955	0.953	0.955	0.954	0.954
FLAGS	106														
DATA D	1.951	1.951	1.976	1.976	1.962	1.962	1.962	1.962	1.962	1.962	1.962	1.962	1.962	1.962	1.962
BASE L	9.984	9.955	10.005	10.004	10.004	10.004	10.402	10.702	10.335	10.335	10.195	9.903	9.903	9.903	9.903
DATA L	4.477	4.325	4.325	4.500	4.477	4.555	4.633	4.477	4.477	4.477	4.477	4.477	4.477	4.477	4.477
1/T	3.292	3.185	3.258	3.024	2.934	2.990	2.855	3.032	3.030	2.774	2.714	2.597	3.004	3.150	3.150
LN(1/T)	1.16365	1.15858	1.18110	1.10645	1.07634	1.09513	1.04907	1.10914	1.10849	1.02026	0.99847	0.95439	0.87721	0.76636	0.76636
EL MASS	0.950	0.950	0.951	0.948	0.947	0.947	0.945	0.948	0.948	0.944	0.943	0.941	0.938	0.933	0.933
FLAGS	91														
DATA D	1.906	1.977	2.020	1.962	1.976	1.962	1.906	1.906	1.962	1.962	1.962	1.962	1.962	1.962	1.962
BASE L	1.421	1.348	1.797	3.529	5.929	7.284	7.982	8.456	8.335	8.335	8.827	8.578	8.456	8.456	8.456
DATA L	2.463	2.398	2.529	3.324	4.249	4.712	4.955	5.121	5.121	5.121	5.292	5.379	5.379	5.379	5.379
1/T	1.900	1.000	1.000	1.801	2.071	2.257	2.265	2.295	2.297	2.297	2.328	2.323	2.160	2.064	1.901
LN(1/T)	0.64154	0.00000	0.00000	0.58831	0.72795	0.81694	0.81769	0.83083	0.83181	0.83181	0.84486	0.84354	0.76907	0.73677	0.64154
EL MASS	0.950	0.950	0.950	0.950	0.950	0.950	0.950	0.950	0.950	0.950	0.950	0.950	0.950	0.950	0.950
FLAGS	70	95	18	95	12										
DATA D	1.976	1.962	2.020	2.020	1.962	1.962	1.962	1.962	1.962	1.962	1.962	1.962	1.962	1.962	1.962
BASE L	1.044	0.215	0.456	8.578	8.456	9.084	8.702	8.335	8.578	8.827	8.827	8.456	8.216	8.216	8.216
DATA L	6.123	5.739	5.833	6.033	5.379	5.946	5.929	5.666	5.666	5.739	5.576	5.666	5.666	5.666	5.666
1/T	1.475	1.100	1.000	1.000	1.000	1.000	1.000	1.000	1.000	1.000	1.000	1.000	1.000	1.000	1.000
LN(1/T)	0.34125	0.07601	0.00000	0.00000	0.00000	0.00000	0.00000	0.00000	0.00000	0.00000	0.00000	0.00000	0.00000	0.00000	0.00000
EL MASS	0.979	0.952	0.952	0.952	0.952	0.952	0.952	0.952	0.952	0.952	0.952	0.952	0.952	0.952	0.952
FLAGS	61														
DATA D	1.797	1.851	1.851	1.797	1.851	1.797	1.851	1.851	1.851	1.851	1.851	1.851	1.851	1.851	1.851
BASE L	3.215	0.335	0.335	8.955	9.215	9.094	9.348	9.484	8.827	9.215	9.215	9.094	8.792	8.955	8.955
DATA L	6.556	5.833	5.833	6.123	6.323	6.424	6.631	6.737	6.952	6.777	6.777	6.631	6.777	6.777	6.777
1/T	1.819	1.823	1.823	1.821	1.820	1.730	1.730	1.759	1.586	1.547	1.547	1.547	1.577	1.544	1.544
LN(1/T)	0.64154	0.60639	0.60639	0.59935	0.59888	0.54834	0.54837	0.56660	0.46152	0.43604	0.43604	0.43604	0.43604	0.43604	0.43604
EL MASS	0.978	0.978	0.978	0.978	0.978	0.978	0.978	0.978	0.978	0.978	0.978	0.978	0.978	0.978	0.978
FLAGS	40														
DATA D	1.689	1.689	1.689	1.689	1.689	1.689	1.689	1.689	1.689	1.689	1.689	1.689	1.689	1.689	1.689
BASE L	3.355	0.335	0.335	8.955	9.215	9.094	9.348	9.484	8.827	9.215	9.215	9.094	8.792	8.955	8.955
DATA L	6.952	6.342	7.172	7.284	6.952	6.952	6.631	6.737	6.952	6.777	6.777	6.631	6.777	6.777	6.777
1/T	1.462	1.915	1.419	1.335	1.449	1.379	1.262	1.312	1.292	1.312	1.292	1.312	1.292	1.312	1.312
LN(1/T)	0.39363	0.64397	0.34376	0.32635	0.37091	0.32163	0.23237	0.27118	0.27118	0.27118	0.27118	0.27118	0.27118	0.27118	0.27118
EL MASS	0.917	0.918	0.915	0.914	0.916	0.914	0.910	0.910	0.910	0.911	0.911	0.911	0.911	0.911	0.911
FLAGS	31														
DATA D	1.689	1.742	1.743	1.689	1.743	1.743	1.636	1.636	1.636	1.743	1.689	1.689	1.689	1.689	1.689
BASE L	7.397	7.964	8.099	7.864	8.335	8.216	7.982	7.628	7.512	7.597	7.172	6.777	6.631	6.624	6.624
DATA L	6.952	7.172	7.204	7.284	7.172	7.284	6.952	6.737	7.172	7.172	6.952	6.631	6.527	6.624	6.624
1/T	1.231	1.250	1.267	1.213	1.257	1.239	1.294	1.284	1.162	1.164	1.164	1.164	1.164	1.164	1.164
LN(1/T)	0.13319	0.22333	0.23691	0.19327	0.29050	0.25252	0.26166	0.25018	0.15191	0.15206	0.14677	0.13767	0.13319	0.12165	0.12165
EL MASS	0.908	0.910	0.910	0.908	0.913	0.911	0.911	0.911	0.907	0.907	0.907	0.906	0.906	0.905	0.905
FLAGS	16														

ZERO PAL = 1.077

TOTAL FRAME MASS RATE 22.750

#### FLAG SUMMARIES

\* 44  
+ 22  
13  
\$ 37  
# 0  
? 0  
% 22  
@ 0

ALIGNMENT SHIFT = 0  
NUMBER OF HOLES MATCHED 0

FIGURE 25  
SAMPLE OPTICAL DATA ANALYSIS PRINTOUT



meaning a value for zero plume air light.

Exposure value information for the point obtained in the scan of that particular data frame is labeled "DATA D" for the value of the black area and "DATA L" for the value of the lighted area. The three exposure values plus the value for "ZERO PAL" are used to calculate a reciprocal value for transmittance which is printed and labeled "1/T". The value labeled  $\ln(1/T)$  is the natural log of the 1/T value and is presented as an interim quantity to be saved for possible re-run of the data. The quantity labeled "EL MASS" is the calculated mass rate in grams per meter vertical plume size for that particular point. This value is obtained using constants whose values are assigned and listed at the start of each data reduction run. In order to obtain a total mass rate for a complete frame, "EL MASS" values for each of the 539 points are summed. This value is presented on the last page associated with the particular scan as "TOTAL FRAME MASS RATE." The last line of each group summarizes special situations which may occur on a particular frame. An abbreviated explanation of the "FLAGS" is presented as part of the header information for each page. The "\*" signifies a point at which the value for "BASE L" falls below some pre-set value. This situation occurs for points falling on the gaps between bulbs of the light source and is generally 5-8 points long. In general, no mass rate is calculated for these points and the value of "EL MASS" is set to zero.

The "+" denotes a situation in which the frame plume-air light value, "DATA D", is high when compared to a corresponding base light value (BASE L). This situation can logically occur under two different conditions. The first occurs when a gap value for "BASE L" is compared to a slightly high value of "DATA D", caused by light smoke over the black area. The second occurs when very heavy smoke of a bright or highly reflective color occurs and the smoke image density appears brighter than the light source in the base frame. Few situations of the latter type were detected and in general, indicated that the light source remained dominant for most conditions of plume air light. A "\$" signifies that a value for "DATA L" was found to be larger than a corresponding

value for "BASE L." This occurs in the presence of heavy emissions where the light source is still visible, giving rise to an addition of plume air light to the apparent light source brightness. It may also occur to a lesser degree in a no emission situation due to system inaccuracies. To differentiate, the difference between the two values is compared to a threshold value. If it is less than that value, a "ç" flag is raised and the computation continues. If it occurred during a high emission condition, the calculation will force the value of "EL MASS" to its maximum value. If it occurred during a light or no emission situation, the calculations will generally produce a zero or very low value for "EL MASS." If the difference is greater than the threshold value, a "\$" is printed and the calculation continues. This situation, when valid, usually occurs in a high emission condition and the calculation will generally enter a high value for "EL MASS." The situation "ç" can also occur at gaps in the light source and is handled in the same way. The "#" flag signifies that a comparison between "DATA L" and "DATA D" values showed the dark area to be brighter than the light area. Again, this situation occurs in conditions of very heavy emissions and if the difference is small, is probably caused by system inaccuracies. To check, the difference is compared to a threshold value. If it is less, the maximum value is set for "EL MASS." If it is greater than the difference threshold value, a "?" flag is entered and the "EL MASS" value is set to zero since no valid calculation can be made under these conditions. The "%" flag indicates that the calculated transmission has dropped below 10%. In this situation, the maximum value of "EL MASS" is entered for that spot. The exposure and transmission data is retained for examination. The last flag, "@", signifies that a "BASE L" value is below the "ZERO PAL" value and can only occur in a light source gap (already signified by "\*" flag) or in an invalid measurement. In the presence of this flag, a zero value for "EL MASS" is entered.

Using the flag summary at the end of a frame scan, a quick assessment of possible processing problems can be made and a judgement formed as to the quality and potential validity of the results. Printed below the flag summary are data shift values. This shift is performed on the data

frame if its start point does not coincide with that of the base frame. The alignment is based on the position of the gaps in the base and data frames and in general, require little or no shifts. The total print-out provides a convenient method for scanning individual data frames for areas of interest such as observed areas of high or low transmission or suspected interferences. In short, it provides a valuable tool in the understanding and assessment of optical system performance.

### Test Data

During the course of the overall test program, 21 tests were photographed by the optical system which were also observed using the continuous monitoring system. In addition to the 21 tests in common, a number of other charges were photographed using the optical system to provide test data for that system. The original intent at the outset of testing was to process and analyze all optical system output for comparison with the continuous monitoring results. This became impractical in the light of higher than expected processing and analysis costs and unexpected but necessary alterations in the original test schedule. As a result, the selection of a sub-set of optical film was made and analysis accomplished prior to the processing and analysis of the continuous monitoring system data.

The original test concept involved monitoring all emission source points simultaneously (six points on the Wilputte car and three points on the AISI/EPA car). The combination of volume flow from all points on a test would have provided a reasonably good second-by-second picture of visible emission volume against which the optical system data could be compared. Problems encountered during the course of testing precluded the measurement of all points on the Wilputte car simultaneously and made necessary the use of aspirating fans on the three AISI/EPA car test points with the result that the absolute volume flow was a function of the fans rather than the volume of emission.

An alternative selection of tests where all three stacks on the Wilputte car were monitored for volume flow or all three guides of the AISI/EPA car were monitored for gas concentrations was made. The rationale was

that during the charging period for the Wilputte car, a high percentage of the total emissions escaped through the stack. Also, that on the AISI/EPA car, the concentrations of selected emission constituents such as total hydrocarbons could be used as an indicator of visible emissions volume at that instant in time. A further selection of specific frames was made by visual observation of the test film to include periods of highly contrasting emissions (high versus low volume visible) and transients. The results of this comparison are presented in the following material.

Presented in Figures 26 through 30 are graphs of actual volume flow, in cubic feet per second, combined for all three stacks on the Wilputte larry car or measured concentrations in % total hydrocarbons for the three combined guides on the AISI/EPA car. The second trace on each graph presents calculated mass emission rates as measured by the optical monitoring system. These values expressed in grams per meter vertical plume size, are plotted on the same time base to show event correlation. After inspection of the film, and comparison of photographed events with the data acquisition system record, it was obvious that some loss in synchronization between the optical system clock and data acquisition system had occurred. This was probably caused by noise pulses causing the optical system clock to jump ahead in time a few seconds. The events displayed were graphed using the time displayed by the clock rather than arbitrarily correcting this time. In general, however, it appears from several observations that in the absence of wind, events in the Wilputte stacks are seen by the optical system with about a five second delay and events in the AISI/EPA guides are seen by the optical system with a five to ten second delay.

Also, since the continuous monitoring system volume flow measurements are taken in a confined stack on a one second basis, abrupt changes in flow can be detected and represented in a very precise fashion. The optical system, however, detects the emission after it has had an opportunity to diffuse and, in general, become more spread out over both time and space. The analysis interval for the optics system was selected

at five seconds as opposed to the one second frame rate so abrupt changes cannot be detected with the same resolution as the volume flow measurement system. Association of event records displaced by an abnormally long period in time according to the two clock values, will be noted in the text discussing that test. Also, trend arrows showing the smoke conditions before, after, and between optical data points are included on the graphs. These were placed on the basis of visual observations of the subject data frames and are not intended to be quantitative, but instead to aid in the correlation of the two sets of results.

Shown in Figure 26 is data obtained during Test 7. The trace of volume flow represents a typical example of conditions during a Wilputte car test. The optical system data is divided into two parts, each of which cover an observed transient condition during the charge. The large volume flow peak occurring just after the start of observations was detected as a less abrupt peak in mass rate by the optical system with some time delay. Visual inspection of the optical system film showed a smoke condition corresponding to approximately the next to last calculated point of the first trace persisting until the first part of the second optical system trace. In the second trace, the actual shape of the volume flow curve was more closely matched by the optical system results. This is probably because the changes in trend of volume flow were less abrupt and of a more consistent nature. It is also interesting to note the optical system saturation point ("optical-system maximum value") with respect to the measurements displayed here. Roughly speaking, a 10% transmission or 90% opacity condition covering the complete length of the bar would correspond to a mass rate of 53 grams/meter, allowing for the gaps between bulbs in the light source and not including the "wing" light source units. One can easily see that the smoke densities typically experienced during a Wilputte car charge could approach or exceed the measurement capability of the optical system. In such cases, the rate would have to be expressed as 53 grams/meter or greater. It would appear, however, that this condition would lie well outside any standard for visible emissions which might be established. The volume flow data

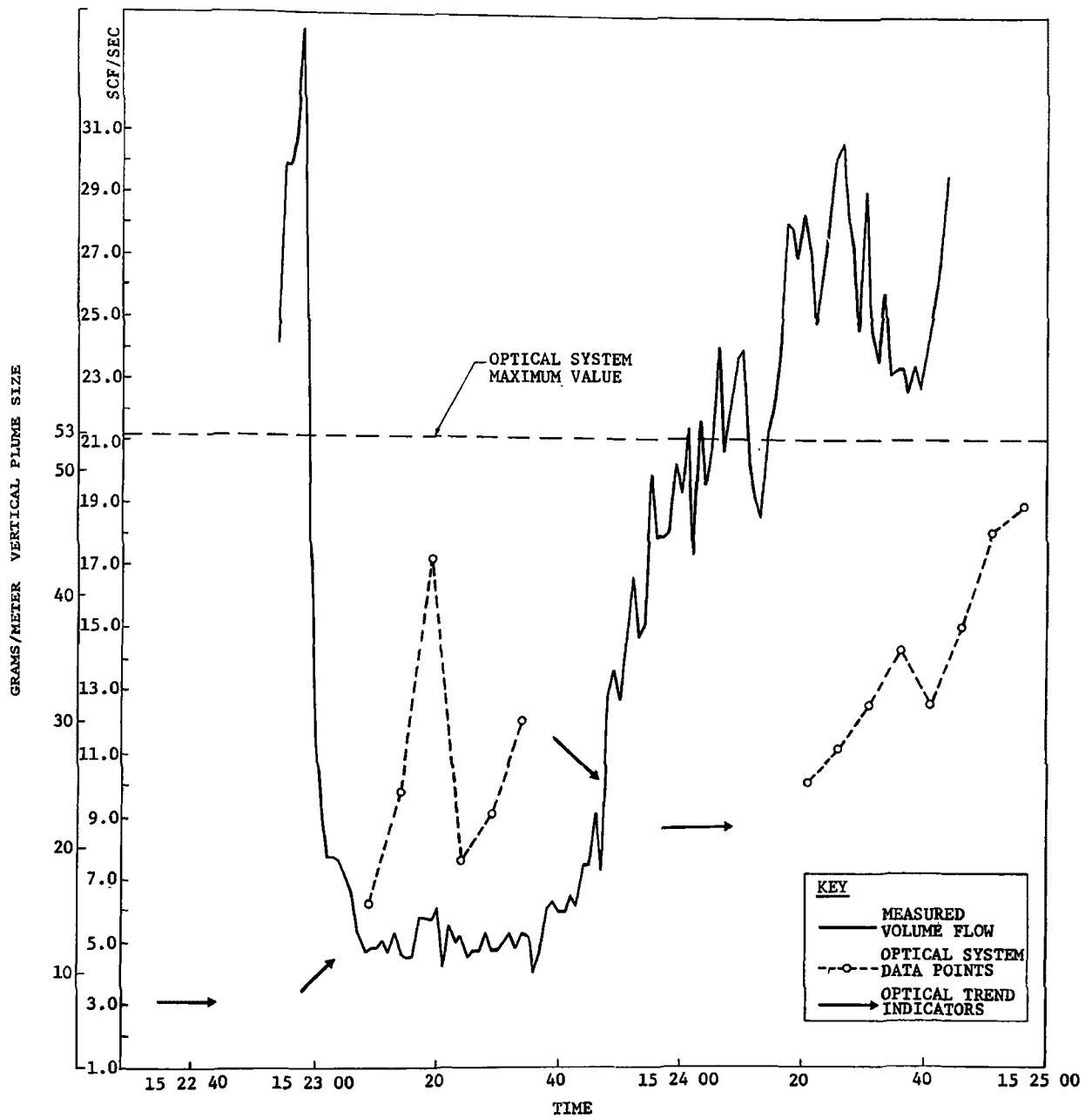


FIGURE 26  
TEST 7 DATA

available from the continuous monitoring system ends with an increasing flow rate. This trend is also observed in the optical system data as an almost totally obscured light source after the last measured point. This condition corresponds to the maximum measureable value for the optical system.

Presented in Figure 27 is data obtained during Test 9. Again, the optical data is divided into two sections covering obvious transient flow conditions. During the first part of this test, a strong cross wind caused a large portion of the emission to pass undetected below the light source. The data frames displayed in Figure 24 are from Test 9 and show the effects of the wind conditions. The arrow shown on the second data point indicates that the measured value was much lower than the actual emission because of the cross wind condition. During the second portion of the optical data trace, the wind subsided allowing a truer measure of the actual emission condition. Lower peak values were recorded because of the wind condition and the resulting emission dispersion. The flow characteristics are similar to Test 7 showing an initial abrupt high flow rate, decreasing toward the middle of the test and then building up again toward the end.

Figure 28 shows data collected during Test 17. This test was performed on the AISI/EPA car and shows total hydrocarbon concentrations rather than volume flow data plotted against optical system data points. The optical data is divided into three parts on this test. The first and the last parts have been identified as quench steam interference using the photographic film record and voice tape commentary. The center optical system trace shows the detection of the heavy emission flow near the center point of the test. The peak values are much lower than those noted for the Wilputte tests because of the lower quantity of emission and the fact that the smoke source is at the oven surface under the car. As a result, the emission has been diffused to a greater extent by the time it rises to the light source detection area. The trend of the data recorded by the optical system closely follows the density of emission as indicated by the concentration of total hydrocarbons. The values

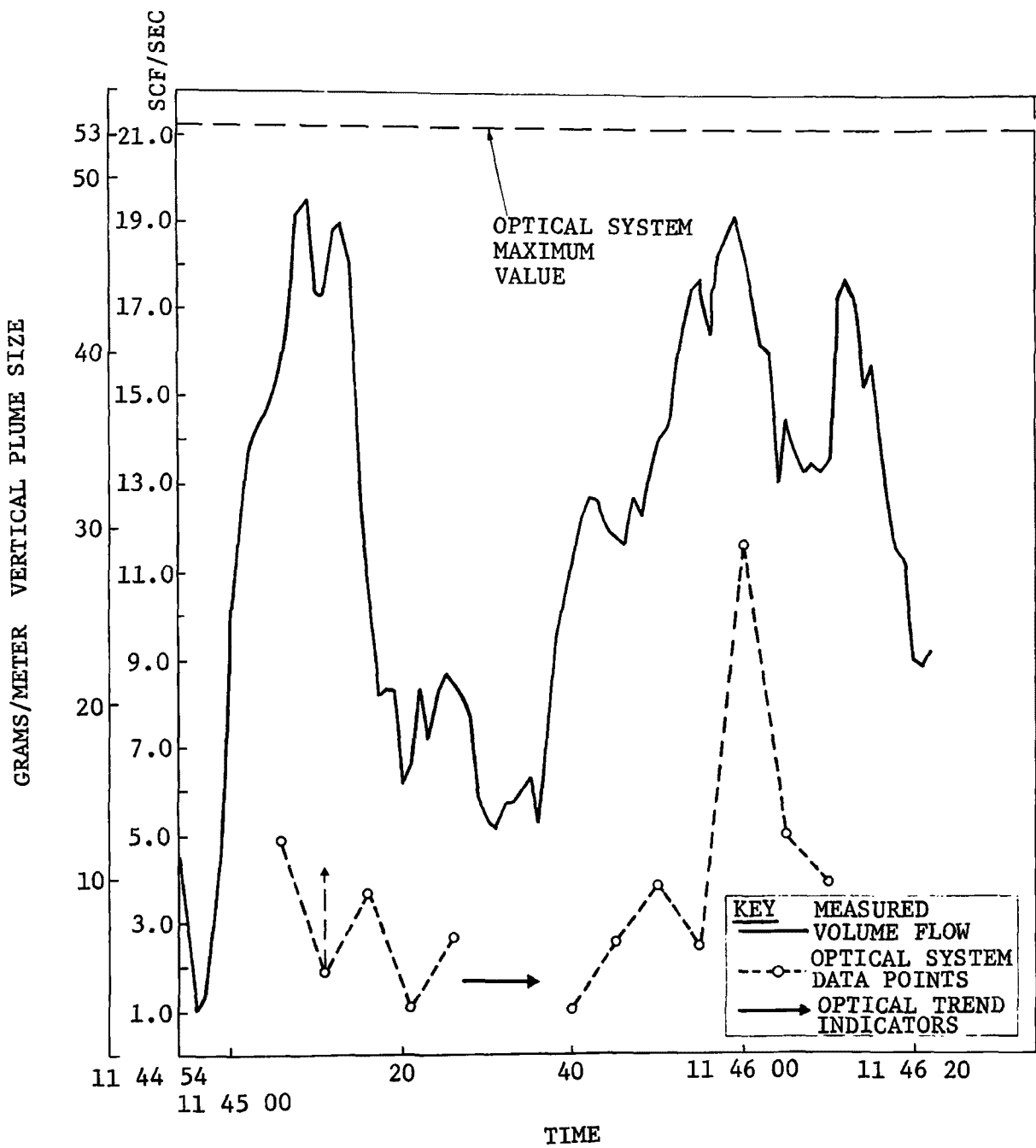


FIGURE 27  
TEST 9 DATA



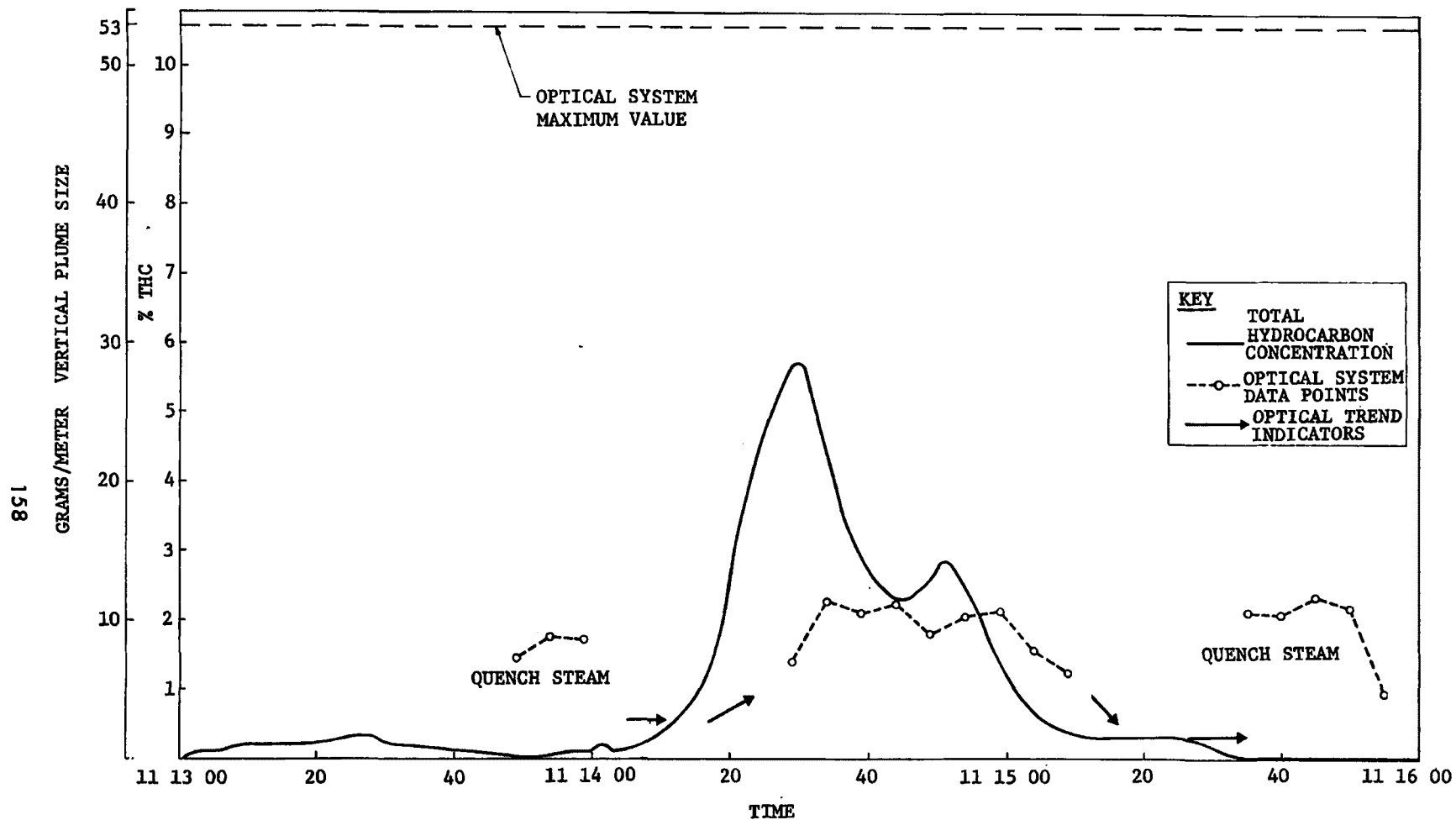


FIGURE 28  
TEST 17 DATA

detected are well below the saturation point for the optical system.

Figure 29 presents data taken during Test 20. During the first part of this test, a large quantity of emissions escaped through an open "chuck door" and ascension pipe cap. This smoke rose past the light source and in preliminary selection of optical data to be analyzed was mistaken as emissions from the drop sleeve area. The optical data frames selected showed a rapid rise in density during the first part of the trace followed by a rapid decrease in density during the second part of the optical data trace. This condition correlates with a slight increase in recorded THC concentration, but since the emission occurred through unmonitored points, was not recorded directly by the continuous monitoring system. The primary emission around the drop sleeve occurred later in the test but was of fairly low volume. The sequence of events and the source of emissions was determined by examination of the optical system film data. The data is presented to show the ability of the optical system to track rapidly changing emission conditions but also points out a deficiency in the system in that it has no way of differentiating between emission sources. Emissions originating from an ascension pipe or oven door will appear as part of the total emission detected if they pass between the light source and the camera. It might be necessary to develop some rather arbitrary rules to cover this situation since it may not always be possible to identify the exact source of the detected emission.

Figure 30 presents data obtained during Test 25 performed on the AISI/EPA car. During the first part of this test, an unusually heavy emission release occurred around the drop sleeve area. This event was easily identified on the optical system film record, but the optical system digital clock time associated with the event was approximately one minute later than the data acquisition time. The only reasonable explanation was a missetting of the optical system data clock in the minute position. A rather remote possibility exists that a line noise pulse caused the optical system clock to jump ahead one minute as opposed to one second. A check of the two observed emission periods on the optical

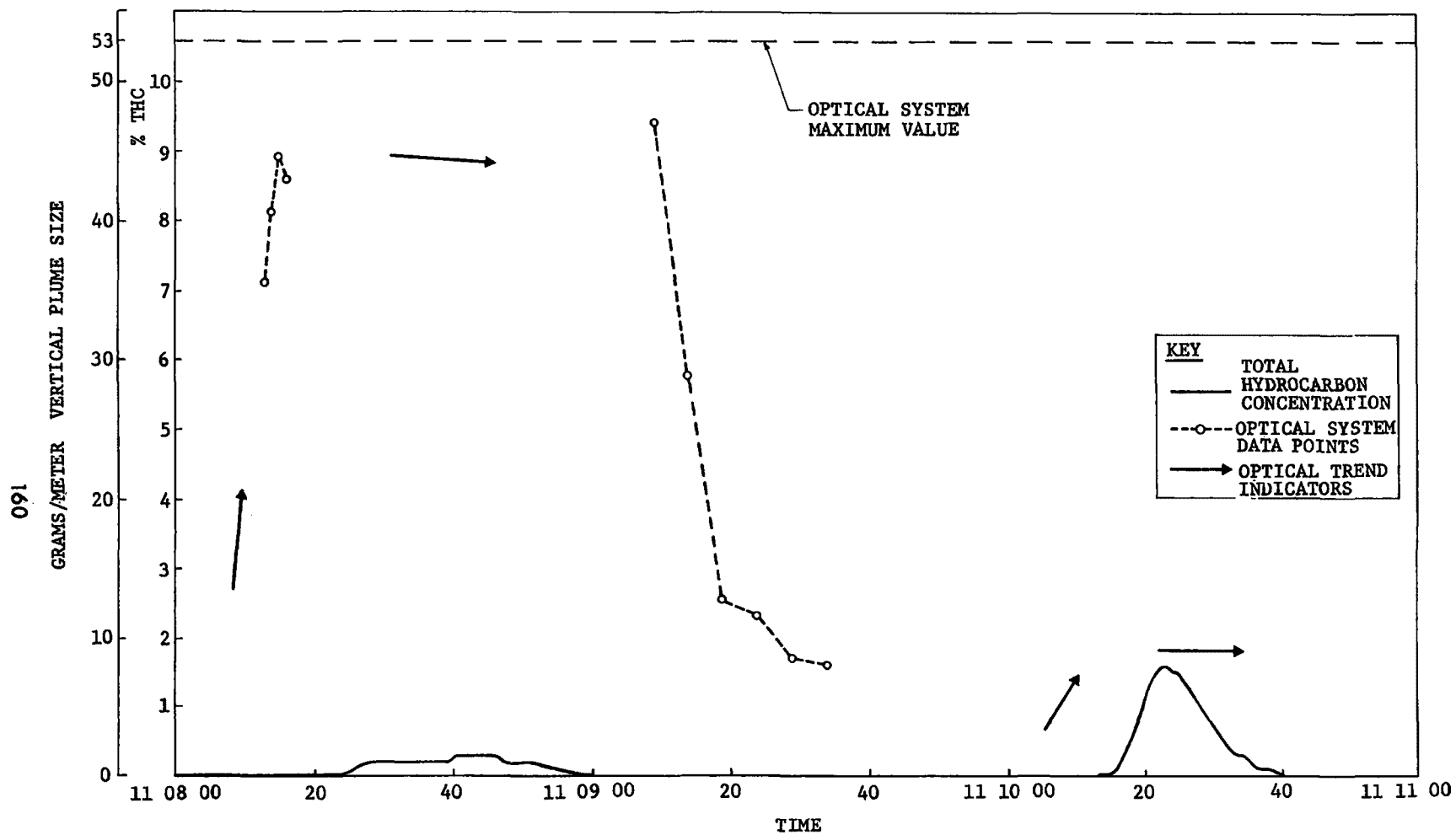


FIGURE 29  
TEST 20 DATA

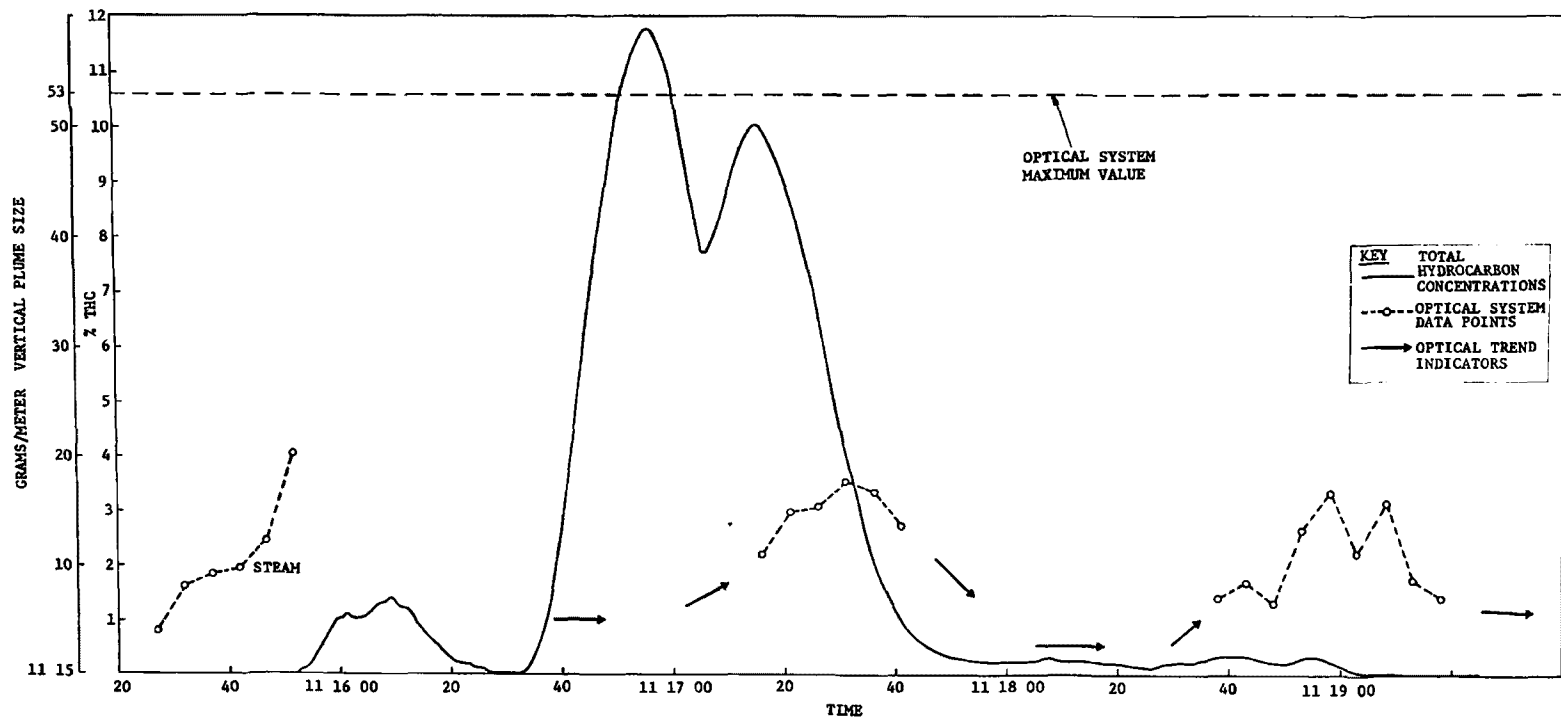


FIGURE 36  
TEST 25 DATA

data films show good agreement in spacing when compared to the continuous monitoring system record. The steam condition also detected by the optical system was identified as occurring about one minute before the test providing a further basis for a time adjustment. Assuming that the second portion of the optical trace should be associated with the first peak in THC concentration and that the third portion of the trace should be associated with the high THC concentration peak, good agreement is observed in the data comparison. The third portion of the optical system trace does not exhibit as high a value as might be expected from the THC trace, but examination of the data film showed only a highly diffused emission condition existing in the area of the light source at that time. It is possible, however, that a mild wind condition at that time might have blown the bulk of the diffused emission out of the camera view. It is difficult to identify sharp emission peaks in a diffused smoke condition, but the general concentration conditions are indicated by a number of frames selected over an extended period of time.

Several conclusions can be drawn based on the optical data completely analyzed and the large amount of optical data film manually examined. First, the system is capable of detecting trends in total emissions using opacity measurements. Second, the mass concentrations appear reasonable in light of the data available for comparison. Third, the system has obvious limitations in measuring very heavy emission concentrations or very high concentrations which are highly dispersed or which may be blown laterally beneath the light source and thus pass undetected. In contrast, the minimal interference caused to plant operations and the system potential for unattended operation offer positive reasons for consideration of this concept for application to compliance monitoring.

# SELECT PROJECT DOCUMENTATION LIST

MTR 6055	November 1971	Management Plan
MTR 6182	May 1972	Overview of Measurements
MTR 6215	July 1972	Continuous Monitoring System (Specifications COK-1 through 23)
WP 8788	15 July 1972	Important Considerations Concerning Sampling
MTR 6260	October 1972	Emissions Guide Systems
WP 10149	14 Dec. 1972	Design of an Optical Emissions Measurement System for Coke Oven Monitoring
MTR 6288	December 1972	Manual Sampling System
WP 10179	16 Feb. 1973	Manual Sampling and Analytical Re- quirements for the Coke Oven Charg- ing Emissions Test Program
WP 10427	25 Oct. 1973	Coke Oven Data Analysis Workbook
WP 7905 Vol. XXI	19 Nov. 1973	Test Plan for Coke Oven Emissions
MTR 6546	November 1973	Optical Emissions Measurement Pro- gram for the Smokeless Coke Oven Charging Demonstration
WP 10459	15 Jan. 1974	Monitoring Emissions from Leaking Coke Oven Doors
WP 10480	31 Jan. 1974	Direct Impaction Particulate Collec- tion Carousel
WP 10445	15 Feb. 1974	Correction and Conversion Factors of Coke Oven Emissions Data
MTR 6566	28 Feb. 1974	A Continuous Monitoring System for Coke Oven Emissions Due to Charging

**TECHNICAL REPORT DATA**  
(Please read instructions on the reverse before completing)

1. REPORT NO. <b>PA-650/2-74-062</b>		2.		3. RECIPIENT'S ACCESSION NO.	
4. TITLE AND SUBTITLE <b>Coke Oven Charging Emission Control Test Program--Volume I</b>				5. REPORT DATE <b>July 1974</b>	
				6. PERFORMING ORGANIZATION CODE	
7. AUTHOR(S) <b>R. W. Bee, G. Erskine, R. B. Shaller, R. W. Spewak, A. Wallo III, and W. L. Wheaton</b>				8. PERFORMING ORGANIZATION REPORT NO. <b>M74-45</b>	
9. PERFORMING ORGANIZATION NAME AND ADDRESS <b>The Mitre Corporation Westgate Research Park McLean, Virginia 22101</b>				10. PROGRAM ELEMENT NO. <b>LAB013; ROAP 21AFF-004</b>	
				11. CONTRACT/GRANT NO. <b>EPA-IAG- F192628-71-C-002 and Contract 68-02-0650</b>	
12. SPONSORING AGENCY NAME AND ADDRESS <b>EPA, Office of Research and Development NERC-RTP, Control Systems Laboratory Research Triangle Park, NC 27711</b>				13. TYPE OF REPORT AND PERIOD COVERED <b>Final: 4/71 Through 5/74</b>	
				14. SPONSORING AGENCY CODE	
15. SUPPLEMENTARY NOTES <b>Although Volume II (Supporting Appendices) of this report was not made available to NTIS, it is available through the Sponsoring Agency.</b>					
16. ABSTRACT  The report summarizes results of a coke oven charging emission control test program conducted at the P4 Battery of the Jones and Laughlin Pittsburgh Works between April 1971 and May 1974; actual field testing was between May and August 1973. Objectives of the test program were: to quantify atmospheric pollutants resulting from the coking process charging operation; to provide a comparative evaluation of a pollution abatement system (an improved design larry car versus an existing larry car); and to determine the feasibility of a compliance monitoring system concept based on optical measurement. All program objectives were accomplished: emission characteristics of the charging operation have been defined in terms of both gases and particulates released to the atmosphere. Emissions were also defined from leaking seals on the pusher side doors of the oven. Several pertinent conclusions were also developed relating to coke oven emissions measurement technology.					
17. KEY WORDS AND DOCUMENT ANALYSIS					
a. DESCRIPTORS		b. IDENTIFIERS/OPEN ENDED TERMS		c. COSATI Field/Group	
<b>Air Pollution                  Emission Iron and Steel Industry Coke                                  Measurement Metallurgical Fuels      Optical Measurement Coking                              Monitors Charging                          Sampling</b>		<b>Air Pollution Control Stationary Sources Manual Sampling Larry Car</b>		<b>13B 11F 21D, 14B 20F 13H</b>	
18. DISTRIBUTION STATEMENT <b>Unlimited</b>		19. SECURITY CLASS (This Report) <b>Unclassified</b>		21. NO. OF PAGES	
		20. SECURITY CLASS (This page) <b>Unclassified</b>		22. PRICE	